Skolkovo Institute of Science and Technology

OPTIMIZATION OF FREQUENCY CONTROL IN POWER SYSTEMS

Doctoral Thesis

by

Oleg Olegovich Khamisov

DOCTORAL PROGRAM IN ENGINEERING SYSTEMS

Supervisor:

Assistant Professort Anatoly Dymarsky

Co-adviser:

Professor Janusz Witold Bialek

Moscow - 2020

Abstract

The presented work addresses two important control aspects of power systems: frequency control and congestion management. In contrast to the other types of transportation networks (e.g. pipeline systems), in power networks it is not possible to store electrical energy in amounts sufficiently large for reliable network operation. As a result, generation in power networks must always be equal to demand. Frequency oscillations are indicators of power imbalance. Frequency control is aimed to keep power balance and consequently to reduce frequency oscillations. Traditional frequency control is divided into primary and secondary parts represented by proportional and integral controllers respectively. Control operates regulator valves on the generator unit's turbines. Therefore, there always exists control lag caused by turbine governor dynamics that may threaten system's stability, should control coefficients (proportional and integral gains) become too high. Thus, effectiveness of this traditional control is limited.

Such issue becomes more significant if system's inertia is reduced due to introduction of renewable generation. Improvement of control performance can be achieved via the following two approaches:

1. Addition of load-side control in order to avoid delay in the turbine governor dynamics;
2. Change of the control scheme to a new one less susceptible to the control lag.

Within this work both approaches are utilized. Load-side control implies controllability of some loads e.g. air conditioning units that may form up to 35% of total power consumption. Their short-term shut down does not lead to significant problems on the consumer side; however, it allows system operator to reduce consumption almost instantly. Such approach leads to significant increase of controllable buses (generators or loads) number. As a result, centralized control, as it is implemented in the present days, may not be feasible. Therefore, within this work it is assumed that buses have limited communication range and can only exchange information with adjacent buses of the network. Such reduction of communication complexity allows us to introduce plug-and-play approach, when a bus can be added to or removed from the network without alteration of the control operation.

There exists a large number of works that address frequency control and congestion

management problems. Majority of them utilizes improvement possibilities discussed above. However, in this work we derive globally asymptotically stable control that provides both frequency control and congestion management for the system model that includes second order turbine-governor dynamics. The latter introduces cascade type structure to the system of differential algebraic equations that define system's behavior. The usage of second order dynamics is necessary to ensure model correctness. However, cascade structure of the system makes it complicated to derive general form of Lyapunov function for such system. In order to counter this effect, the following approach is used. Firstly, optimization problem based on the imbalance size is formulated. Its solution gives control values that restore power balance with minimal deviation of power generation from the reference point. After that, control system is derived as a set of integral algebraic equations (IAE) that converges to the solution of the optimization problem. Special form of the control equations allows their decentralized implementation when communication is required only between neighboring buses.

Task of congestion management is to keep line power flows within the acceptable limits. Currently this task is done within the tertiary frequency control, when (N-x) secure constraint optimal power flow problem is solved, meaning that failure on any x elements of a power system does not render this system inoperable. However, if, congestion management is applied not only at tertiary control, but continuously at the timeframe of secondary frequency control, the system would become more robust. Moreover, such approach may relax (N-x) requirement; thus, reducing cost of the generation. In order to implement congestion management into the frequency control scheme the following algorithm is used. Firstly optimization problem is complemented with inequality constraints corresponding to the line limits. Then, differential equations with piece-wise linear right-hand sides are formulated based on Karush-Kuhn-Tucker (KKT) condition complementary slackens equations for the line limits. These equations are added to the IAE control system. This way the algorithm restores power balance in the system, thus performing frequency control, while keeping all line flows within the acceptable limits.

This thesis starts with the description of frequency and power flows dynamics. Then, power system model is chosen so that it provides realistic representation of the system's behavior. After that control scheme is derived step by step starting from simplest case of only frequency control with no decentralization and finishing with the decentralized full frequency control and congestion management problem. Global asymptotic stability proofs of the developed control are provided for every step of the control derivation together with the results of the numerical experiments.

List of publications and conferences

Published papers:

1. O. O. Khamisov, *Distributed Frequency Control in Power Systems with Limited Information.* Proceedings of the International Conference "Stability, Control, Differential Games" (SCDG2019), 2019.
2. O. O. Khamisov, *Frequency Control in Power Systems based on disturbance approximation*, Proceedings of MIPT, vol. 11, №2, 2019.
3. O. O. Khamisov, T. Chernova, J. W. Bialek, *Comparison of two schemes for closed-loop decentralized frequency control and overload alleviation.* Proceedings of IEEE PES Powertech 2019 Conference.
4. O. O. Khamisov, *Direct Disturbance Based Decentralized Frequency Control for Power Systems.* Proceedings of 56th IEEE Annual Conference on Decision and Control, pp:3271-3276, 2017.
5. O. O. Khamisov, T. S. Chernova, J. W. Bialek, S. H. Low, *Corrective power system control:stability analysis of Unified Controller combining frequency control and congestion management.* Proceedings of IEEE Conference on Sustainable Energy Supply and Energy Storage Systems, 2018.
6. O. O. Khamisov, V. A. Stennikov, *Interior Point and Newton Methods in Solving High Dimensional Flow Distribution Problems for Pipe Networks.* Lecture Notes in Computer Science, Springer, Vol.10556 LNCS. pp:139-149, 2017.

Presentations on conferences:

1. O. O. Khamisov, *Distributed Frequency Control in Power Systems with Limited Information.* International Conference "Stability, Control, Differential Games" (SCDG2019), 2019.
2. IEEE PES Powertech 2019 Conference, 22-28 June 2019, Milan, Italy. O. O. Khamisov, T. Chernova, J. W. Bialek, *Comparison of two schemes for closed-loop decentralized frequency control and overload alleviation.*
3. 56th IEEE International Annual Conference on Decision and Control, 12-15 December 2017, Melbourne, Australia. O. O. Khamisov. *Direct Disturbance Based Decentralized Frequency Control for Power Systems.*

4. 17th Bailkal International Triennual School-Seminar Methods of Optimization and Their Application, 31 July - 6 August 2017, Maksimikha, Russia. Oleg O. Khamisov. *Estimation of Frequency Deviations in Power Network with Primary Frequency Control.*

5. The 11th International Learning and Intelligent Optimization Conference LION 2017, 19-21 June 2017, Nizhny Novgorod, Russia. O. O. Khamisov, V. A. Stennikov. *Interior Point and Newton Methods in Solving High Dimensional Flow Distribution Problems for Pipe Networks.*

Seminars:

1. Distributed Frequency Control and Congestion Management. N.N. Krasovskii Institute of Mathematics and Mechanics of the Ural Branch of the Russian Academy of Sciences, Ekaterinburg, Russia, October 2019.

2. Distributed Frequency Control in Power Systems. Melentiev Energy Systems Institute, Siberian Branch of the Russian Academy of Sciences, Irkutsk, Russia, September 2018.

3. Distributed Frequency Control and Congestion Management in Power Systems. Matrosov Institute for System Dynamics and Control Theory, Siberian Branch of Russian Academy of Science, Irkutsk, Russia, September 2018.

4. Disturbance Based Decentralized Frequency Control for Power Systems. California Institute of Technology, Pasadena, California, USA, February 22, 2018.

5. Estimation of frequency deviations in power systems under continuous control. Institute of control Sciences, Russian Academy of Science, Moscow, Russia, March 2017.

6. Estimation of frequency deviations in power system under primary frequency control. Matrosov Institute for System Dynamics and Control Theory, Siberian Branch of Russian Academy of Science, Irkutsk, Russia, January 2017.

Contents

List of Figures

List of Tables

1 Introduction

Relevance of the problem. The subject of research is frequency control and congestion management in power systems. Power systems proved to be effective and secure method of long distance power transportation. However, power systems have a set of unique properties. First difference from other transportation networks is lack of energy storage capacity sufficient to provide power system's reliable operation. Energy storages are used for price arbitrage [4], additionally, they can be used as equipment for power systems control [5]. However, an installation and maintenance cost of the energy storage capacity necessary to cover power consumption for even short period of time is unacceptably high. As a result, generation must always be equal to demand in order to keep power balance. Second difference is lack of direct control over lines power flows. Power flows act according to the second Kirchhoff law and their regulation can only be done through changes in generation or demand. As a result, simultaneous control of power flows and power balance is a nontrivial task that requires advanced dynamical control system.

Frequency control is designed to keep power balance in the system. Frequency oscillations are indicator of deviations from power balance. If power generation is insufficient, electrical power drawn from the generators is higher, than the mechanical power injected in the generators by the turbines. As a result, generators slow down and frequency drops. Opposite situation happens in case of an energy surplus. Acceleration of generators leads to frequency increase. Such oscillations happen regularly due to deviations in power consumption or in rare cases due to power outage. Frequency oscillations lead to equipment wear, and big frequency deviations (above 2 Hz) may lead to generator units destruction. As a result, generator unit control decouples it from the network, which may lead to power deficit and cascade blackout.

Congestion management is also one of the important control aspects of power systems. It is responsible for the keeping lines power flows within acceptable limits dictated by thermal limitations or voltage stability requirements. In case of the thermal limits their short-term violations do not lead to line failure.

Currently implemented solution. Frequency control and congestion management are conducted via primary, secondary, and tertiary controls [6].

Primary frequency control (droop control) is aimed to limit maximal frequency deviations from the nominal value. This control is distributed (its operation requires only local frequency measurements and does not need any information from the rest of the network) and operates during first 10-30 seconds after imbalance appearance. Originally primary frequency control was implemented via centrifugal governor. Nowadays control values are calculated digitally through proportional controller with proportional gain (droop constant) varying between 2-6% based on the generator type.

Secondary frequency control (or Automatic Generation Control, AGC) is aimed to restore frequency to its nominal value. It is presented by proportional integral controller using frequency deviation as an argument of the controller. This control is implemented in centralized way. Frequency measurements are taken from several reference buses and sent to the system operator. Then, the system operator calculates control values and broadcasts them to all controllable buses.

Another function of secondary frequency control is control of inter-area flows. Usually, large networks are divided into areas for a set of reasons for example, country borders or different system operators. Inter-area flow is a sum of power flows that go into or leave the area. They should be equal to the nominal values. This allows us to restore balance of an area using only generators of the power reserves of this area. Moreover, power reserves distributed evenly throughout the system and avoid long distance power transfers that may result in big power losses.

Tertiary control is conducted once per every 15-120 minutes or in response to credible contingencies (i.e. those that are reasonably possible to occur or have the potential for a significant impact on the power system [7]), depending on the power system type. Similarly to the secondary control it is done in a centralized way, (N-x) Security Constrained Optimal Power Flow (SCOPF) aimed towards cost minimization is solved during its operation. The (N-x) condition is introduced in order to increase robustness of the system. It means that power system remains operational if x or less elements of the system (buses and lines) fail. Congestion management is done within tertiary control as a part of SCOPF.

Improvement possibilities. In case of power imbalance appearance frequency does not change instantly. Frequency in power systems is proportional to the rotational speed of generators which have big inertia; therefore, change of rotational speed as well as frequency takes 5-10 seconds [8]. Power plants using renewable energy generation (wind and solar plants) have low or zero inertia. As a result, frequency behavior becomes volatile in systems with high amount of renewable penetration. Thus, existing control scheme cannot stabilize frequency in such networks and system operator limits the amount of power generated by renewable sources (e.g. in 2016 averaged amount of available but not used wind power in Ireland is equal to 2.7% of the installed capacity [9]). Smart grids and systems with distributed generation are also susceptible to this problem.

Control nowadays is done via adjusting generators' power output [10]. Load disabling is done only in emergency situations. Nevertheless, it is possible to utilize load-side control during normal operation of power system. Short term disabling of some loads (e.g. air conditioning units that form up to 35% of total power consumption [11,12]), does not lead to any difficulties on the consumer side, therefore, it can be utilized along with generator side control.

If control signal change happens, it takes some time (5-20 seconds) for the generator unit to adjust its power output due to the delay in turbine-governor dynamics. This makes frequency drop during first several seconds after disturbance almost uncontrollable even if control response is instant. Load-side control can be performed much faster. As a result, load-side control allows us to control system during the first seconds after the disturbance, thus improving frequency behavior.

Centralized control scheme requires synchronization of communications (communication delays do not exceed discretization time of the control) with all buses participating in the control. As a result, signal broadcast cannot happen often (e.g. SCADA does one signal broadcast every 5 seconds). Thus, control gains have upper bound defined by the system's stability. Thus, speed of the secondary frequency control is limited to 5-10 minutes after power imbalance appearance. Moreover, communication synchronization implies limitation on the number of the controllable units. Therefore, load-side control with big number of controllable loads in the network might become problematic for the existing control scheme.

Congestion management is performed in preventive-corrective mode according to schedule and in response to credible contingencies. Such approach implies introduction of (N-x) criteria. As a result, majority of the lines is not fully loaded because from the mathematical perspective (N-x) criteria is an introduction of additional constraints to the cost minimization problem. Thus, it increases generation costs and requires overbuilt line capacity. Normally $x = 1$ and system remains stable after a single failure. This requirement is sufficient in majority of the cases because simultaneously appearance of two failures is highly unlikely. However, in the cases when $x \geq 2$ (i.e. in England $x = 2$) number of possible failure scenarios is equal to the number of x-combinations from N elements ($C_n^x = \frac{N!}{x!(N-x)!}$). This number is large for $x \geq 2$, which makes analysis of the system with such requirement computationally expensive and may not be a reliable approach for safe operation of power systems.

Even if computational complexity issues are solved and corrective SCOPF is used if the system suffered from a failure [13], there is still a possibility to improve congestion management as corrective SCOPF responds to only credible contingencies. Thus corrective SCOPF does not respond to small fluctuations of power consumption and System Operator must keep lines under-loaded in order to counter overheat issues that may occur due to nonsensitivity of corrective SCOPF.

Objective of the work. It can be seen that the existing control scheme does not allow power systems with high penetration of renewable and distributed generation to release their full potential. The scheme does not use possibility to utilize load-side control. Finally, slow congestion management leads to the need of (N-x) security criteria for the lines, which increases generation cost and requires new lines installation. Thus, we define the following set of objectives:

1. Choose power system model that would provide realistic dynamics of frequency and power flows and define set of system parameters that can be realistically measured and used for control.

2. For the chosen power system model derive control that would have following capabilities:

   (a) Improved frequency control. Maximal frequency deviation (nadir) as well as frequency restoration time must be reduced in comparison to the traditional control;

(b) Real-time congestion management. Control must respond to line flow to contingencies within the timeframe of secondary frequency control;

(c) Inter-area flows control. This control must be implemented as it is a part of the currently used AGC;

(d) Minimization of control cost function;

(e) Distributed implementation;

(f) Load-side control;

(g) Operation in feedback and feedforward modes, depending either on the available information about system state or on the disturbance measurements.

3. Prove global asymptotic stability of the control.

4. Provide numerical test that would support the theoretical results. Power system models used for the numerical experiments must include more complicated ones in comparison to the one used for theoretical results in order to ensure control robustness.

Research methodology. Despite the power balance oscillations being constantly present in the system, it is at most important to analyse systems behavior in the emergency case caused by power outage or line trip. Such situations are modeled by a step change in power generation, or consumption, or change in the system's topology, or combination of them. All these parameters are considered to be constant after this step change. Everywhere further systems dynamics are analysed after such type of step change disturbances.

While it is possible to formulate optimal control problem, communication limitations and lack of information about the system as well as constraints on the phase variables (system state) make it impossible to derive a general form optimal control solution. Thus, we firstly analyze after transient steady-state. Our goal is to minimize control cost function subject to frequency deviations being equal to zero and all line constraints. Solution for this optimization problem will theoretically give the steady-state control values. We show that frequency and power flows are defined uniquely by the control values, thus solution of the optimization problem is sufficient to deliver physical system into a state, where all the control requirements are fulfilled. However, due to the lack of information and communication limitations it is impossible to solve the optimization problem directly.

Therefore corresponding Karush-Kuhn-Tucker condition (KKT) [14] is analyzed. The complementary slackness conditions are replaced with piece-wise linear equations of special form. After that transition from algebraic equations of modified KKT condition to first order piecewise linear integral algebraic equations is done. This approach allows us to limit the amount of required information and communications to the acceptable margins.

The available information is used in the following way. It is known, that power balance is restored if and only if sum of control signals equals to the minus sum of the disturbances (change in power generation is equal to the change in power consumption). Therefore, any frequency control approximates size of the disturbance. We separate our control into two stages in order to utilize this property. First stage approximates the disturbance using the available information about the system. The second stage uses disturbance approximation as an input in order to calculate control values.

The describe method allows us to derive globally asymptotically stable control that delivers power system to the desired state at minimal control cost. However, we do not provide any analysis of the transient performance of the control. Therefore, numerical experiments are provided in order to ensure acceptable system dynamics. Power system model for the experiments is more detailed than the one used for the theoretical results. Disturbance is considered to be nonconstant. Some of the controllable buses control limits change over time. Control on some of the buses turns on several minutes after the disturbance appearance.

Scientific novelty. There exists a large number of works dedicated to the frequency control and congestion management. The novelty of the presented work in comparison to others can be summarized in the two items:

1. Frequency control and congestion management algorithm is developed for the power system model with second order turbine governor dynamics.

2. Global asymptotic stability is proved for this power system model.

To the authors knowledge stability of such control is proved either for lower order model, is local or both.

While usage of the detailed power system model grants realistic representation of the system dynamics, overcomplication unusually makes it impossible to provide any proof of control stability, while too simple model does not accurately represent system behavior and may be stable, while the actual system is not.

We use the simplest model that provides realistic dynamics of frequency under controls of proportional integral type in order to prove global asymptotic stability. Then we test the obtained control on the more detailed model in order to ensue correctness of the analytical results. Equations corresponding to the second order turbine governor dynamics are the key to realistic representation of the system response to fast changes of the control signal. It will be shown later that simpler model can provide unrealistically optimistic results, such as stability with any gain of proportional controller. The second order model represents an analytical basis for derivation of the control that as the numerical experiments will show remains stable even for more detailed models of power system.

Second order turbine governor dynamics introduce cascade (triangular) type block to the power system model. Thus direct stability analysis of overall system (power model and control) becomes difficult, as to the knowledge of the author it is not possible to derive general form of Lyapunov function for the system that consists of two blocks (physical system and control system) connected by the cascade block. Therefore stability is analysed in parts. Firstly, we derive properties of the control sufficient for the physical system stability. Then we derive control system that satisfies these properties. Such solution becomes possible due to the two stage control structure. Explicit disturbance approximation makes control dependant on a parameter (approximation) that is very close to the one independent of the system state (disturbance). As a result, control, stability to a large extent can be analysed as a stability of a feedforward control, despite the latter being feedback if necessary.

2 Overview of the existing results

In this section we provide an overview of the works dedicated to frequency control and congestion management. The detailed overviews of the problems in power systems can be found in surveys [15], [16], and [17]. Here we provide description of the works that are closely related to this thesis. Section has the following structure. Firstly we provide overview of frequency control works and general classification of the most used approaches within this topic. Then, we provide similar description of the works, dedicated to the congestion management. After that we highlight the main features of all considered works. Finally, we provide a comparison of the presented work with three theses on the same topic followed up by a general comparison with all the considered results. Works, dedicated to the frequency control problems:

- Paper [18] is dedicated to modification of the existing frequency control for the low-inertia systems. The authors provide modification of the AGC control called Enhanced-AGC. While AGC minimizes quadratic function in stationary point, Enhanced-AGC minimizes integral quadratic function on the observation period $[t_0, \infty)$ subject to the physical system linear dynamics equations. Such approach is one of the few that explicitly optimizes transient performance.

- Paper [19] is dedicated to enhance the existing frequency control via introduction of adaptive control gains. The authors use reduced turbine governor model, but they keep the nonlinear generator dynamics. The developed algorithm allows to reduce cost associated with the control actions due to the adaptive control gains.

- Paper [20] is dedicated to the demand response. The aim is to introduce load-side controller that would turn on and off the appliance to achieve balance between needs of the consumers and need of the grid. The authors consider aggregated model of the system dynamics.

- Paper [21] is dedicated to the demand response. The control is applied to transmission level star topology networks. The control is distributed, allowing to reduce communication between controllable loads.

- Paper [22] is dedicated to the combination of frequency control, congestion management. This paper has the most similarities with this work. It solves the same control problem for both generators and loads. It is based on the primal-dual approach for the first order turbine governor model. However, as it was shown in [23], it is not possible to expand this approach to the higher order model.

- Paper [24] is dedicated to usage of a fuzzy neural network to substitute traditional generators frequency control with an algorithm for the distributed energy resources.

- Paper [5] is dedicated to control of distributed energy resources and energy storage. The distributed gradient descend method is used for the control values to converge to the solution of optimization problem formulated for the stationary point.

- Paper [25] is dedicated to the distributed demand response algorithm. Here algorithm is based on the Markov decision approach, therefore optimization problem for the stationary point is formulated. Such approach allows the authors to derive algorithm capable of scheduling many small loads to contribute to the frequency reserve for a case of frequency drop.

- Paper [26] is dedicated to the derivation of distributed frequency control. The approach is similar to the standard AGC from the point of view that control in [26] integrates the frequency deviation. However, this integral is substituted with the frequency deviations from the adjacent buses.

- Paper [27] is dedicated to the load side primary frequency control. In this case proportional controller is substituted with bounded cost function inverse.

- Paper [28] is the extension of the previous work [27]. Here congestion management is implemented in addition to the frequency control. Here linear system of differential algebraic equations without governor turbine model is used in order to describe power system dynamics.

- Paper [29] similarly to the previous two works is based on the primal-dual approach without congestion management, but with the first order turbine governor dynamics.

- Papers [30] and [31] are two parts of the primal-dual frequency and congestion management control for generators and loads. It is a continuation of the works [28], [29], and [22]. Here, similarly to the previous works of these authors, linear system with first order turbine governor dynamics is considered.

- Paper [32] is dedicated to the load-side control based on a primal-dual approach. This algorithm allows to do frequency control and congestion management for linear physical system with no turbine governor dynamics.

- In [33] frequency control is derived for a star topology grids. The control is once again based on the primal dual algorithm. However, here the algorithm is based on the interior point method and not on gradient method, used in the majority of the papers.

- In [34] frequency control is derived for a tree topology grids. Distributed control is derived for a grid, described by a system of linear differential equations with first order turbine governor dynamics. Additionally, line limits are introduced; thus, the algorithm also performs congestion management.

- In [35] hierarchical approach is used. Here, similarly to [18], optimal control approach is used to minimize quadratic integral cost function.

- In [36] frequency control and congestion management are performed based on the primal-dual approach. Congestion management is introduced via addition of the penalty component to the cost function. Power system model includes non-constant voltages but omits governor turbine equations.

- The work [37] is an expansion of the previous work [34] on the average topology with an addition of congestion management.

- In [38] frequency control is derived based on the primal-dual approach with different cost function for the frequency sensitive loads, traditional generation and renewable generation.

- In [39] passivity based approach is used to derive frequency control for nonlinear system dynamics with time-varying voltages.

- In [40] distributed PI controller is derived. Stability is proven by integral Lyapunov functions for a linear system without turbine-governor dynamics.

- In [41] similarly to the previous work, PI controller is derived for a linear system. However, here physical system is described by a general system of liner differential equations.

In general, approaches in the majority of the papers above can be separated into three categories:

1. Primal-dual type approach firstly developed in [42–44]. This approach is used in works [22, 27–34, 36–38]. Primal-dual approach is based on optimization over the set of stationary points. The Karush-Kuhn-Tucker conditions [14] are formulated for this problem. Then, after some modifications, continuous version of gradient method (in [22,27–32,34,36–38]) or interior point method (in [33]) is applied. As a result, some of the optimization method equations coincide with the equations of the system dynamics (primal part) is provided by the physical systems. The other differential equations of the optimization algorithm (dual part) is provided by the controller dynamics.

2. Averaging type methods are presented in [26, 40, 41]. Here PI controllers (either modifications of the traditional control or a new approach) are used to provide frequency restoration.

3. Optimal control approach is considered in the papers [18, 35]. Here explicit analysis of the transient dynamics is considered. The authors introduce integral quadratic objective functions in order to minimize frequency deviations not only in the stationary point, but during the entire observation period.

It is necessary to point out, that several works above provide solution for the congestion management as an addition to the frequency control. In general, there exist very few works dedicated to the congestion management only. As can be seen from the survey [17] in majority of the cases congestion management is a part of more general problem. Exception of this rule can be found in the work [45], where differential evolution algorithm is used to ensure correct power flows in the AC model. In the list above frequency control is the main goal of all works. Thus, the control is derived as a continuous function in order to ensure mid-term stability. Power flows oscillations are significantly less dangerous to the system stability; thus, application of congestion management as a part of real time OPF is also of interest, since it is based on the construction of discrete control. Below are the works, dedicated to the real time OPF problem. There exists a wide range of works dedicated to this problem that can be found in [16]. However, here we consider algorithms that allow distributed implementation.

1. The paper [46] is dedicated to solution of non-convex OPF problem for radial networks via gradient projection algorithm. The intermediate iterations of the derived algorithm always satisfy operational constraints.

2. In [47] a model free extremum seeking algorithm is used to solve AC OPF problem for a radial network.

3. In [48] alternating direction multiplier method for an arbitrary topology network.

4. In [49] distributed feedback controller is developed. Primal-dual gradient method is used to provide fast (unlike in the previous work) control of the system in order to bypass standard hierarchical structure.

The approaches above ignore turbine dynamics. The trade-off here is control of not only active but also reactive power flows.

The control in this work will be derived in the piece-wise differential form, it is necessary to note some general results on such control types and corresponding stability estimation approaches [50–55]. However, decentralization requirement cannot be easily represented in the form of typical control constraints, since a set of admissible control types remains unchanged, but limitations are implied on the control inputs. The results specialized for the distributed control development are presented in [56–62]. Control decentralization usually rises questions of communication limitations and delays. Information about such properties with regards to the power systems can be found in [63–65]. Within this work firstly optimization problem that defines optimal state of the power system is derived. Then, control is obtained with the only requirement to deliver the system to the optimal state. Such approach does not provide analytical analysis of the transient behavior; however, this problem is substituted by numerical experiments. Similar approach is used in [22] and some other works devoted to the distributed control [27–32]. More results on the frequency control problem are given in [5, 24–39]. This results include centralized control schemes [38, 39] that considers non-constant voltage magnitudes, methods that allow us to control frequency without control of power flows (congestion management) or inter-area flows [5, 24–26] and [36, 37]. Some works use simpler first order dynamics of turbine governor equations or ignore the dynamics [26–32, 36, 37] compared to the model considered in this work. One of the reasons for the development of a new control is reduction of the system inertia due to the introduction of renewable generation. Analysis of the inertia reduction impact on the power system's dynamics are presented in [66]. Works, aimed to modify the existing control in order to account for the increasing amount of wind turbines are [67–72]. Additionally, some works are dedicated to the general low-inertia systems: [15, 18, 19]. One of the possible ways to increase controllability is usage of the controllable loads, works [22, 27–32] combines generator and load side controls, while other works [20, 21] are dedicated to the controllable loads only. As this work considers linear model of the system dynamics, we will mostly consider global asymptotic stability even for the cases when the developed control is nonlinear. However, results for standard control on more detailed models can be found in [73–79], in particular numerical stability analysis in [74–76] and analytical approaches in [73, 77–79]. This results correlate with the transmission planning works [80, 81] as the latter must take into account the stability constraints.

3 Novelty and Contribution to Knowledge

3.1 Comparison with Literature

Before we compare the approaches above with the approach in this work, let us consider 3 theses related to the same topic [1–3]. Main difference between the first two works is presence of congestion management and inter-area flows regulation. Without them problem becomes simpler, because in case of only frequency control we need to equate sum of control signals to the sum of the disturbances.

Let us firstly compare the presented work within the scope of only frequency control. Let us consider two theses [1, 2] dedicated to this problem. In the presented work the developed control algorithm requires less information about the system than the algorithms presented in these theses. Usually, it is difficult to accurately approximate time constants of turbine and governor. Algorithm in [1] requires knowledge of their ration (Assumption 5.5.4) to ensure algorithm stability. However, ratio of two inaccurately approximated values may differ significantly from the correct one. In the presented thesis knowledge of these parameters is required for the first three problems. However, in the presented work we only need to give an upper approximation of their minimum to ensure controller stability. For the rest of the problems the knowledge of these constants are not needed at all due to the approach to the disturbance approximation (section 9.1). If we consider thesis [2], the algorithms require knowledge of line parameters (control equations 3.52), which are excluded in the presented work in the problems that consider frequency control only because the latter requires only power balance restoration and does not work with power flows. Finally, they prove local asymptotic stability only without determining convergence radius. The authors consider nonlinear dynamics which results in the presence of sin functions in physical system differential equations. However, corresponding Lyapunov functions (e.g. (5.17) in [1] thesis and (3.37) in [2] thesis) limit arguments of sin function to be within its monotonous region near origin: $[-\pi/2, \pi/2]$. Thus, locality is either caused by cascade structure of turbine governor dynamics or controller dynamics. Both latter issues are considered in the presented thesis and global asymptotic stability is proven.

Finally, let us consider existing works dedicated to the problem, analysed in the presented work, namely frequency control together with congestion management. The thesis [3] considers only first order turbine-governor dynamics. The detailed description of this approach will be presented below, after additional discussion about the existing literature.

	Control in [1]	**The presented control**
Congestion management	Not present	Present (Problem 6, Section 13.3)
Inter-area flows regulation	Not present	Present (Problem 7, Section 13.4)
Measurement of turbine and governor constants	Needed	Not needed for Problems 2-7
Asymptotic stability	Local with no estimation of the convergence radius	Global

Table 3.1: Comparison with [1].

	Control in [2]	**The presented control**
Congestion management	Not present	Present (Problem 6, Section 13.3)
Inter-area flows regulation	Not present	Present (Problem 7, Section 13.4)
Measurement of line parameters, turbine and governor constants	Needed	Not needed (for frequency control)
Asymptotic stability	Local with no estimation of the convergence radius	Global

Table 3.2: Comparison with [2].

Similarly to the first two theses [1], [2], the works considered above are mainly concentrated on frequency control only and omit congestion management or inter-area flows regulation. The scope of works that consider all aspects of the control is reduced to the works [37], [82], [22]. However, works [37] and [82] do not consider load-side control; thus,

	Control in [3]	**The presented control**
Turbine-governor dynamics	First order	Second order

Table 3.3: Comparison with [3].

the problem considered in the presented thesis is analysed only in the work [22]. While derivation of the load-side control may be easier from the implementation perspective, however have low or zero inertia corresponding to load buses usually results in significant oscillations in transient. This work (as well as [82]) does not consider second order turbine governor dynamics. Such approach removes delay in the dynamics, thus relaxing some constraints on the control. For example, let $-K^I\omega$ be droop control. Then, the system remains stable for any $K^I > 0$. Moreover, taking K very close to $+\infty$ might demonstrate the best possible results (Section 5, Figure 5.2 in the presented thesis). Thus, it is not possible to predict how controller, derived for such system, would behave on more realistic one. In particular we showed in [23] that Unified Control [22] becomes unstable, if applied for a system with second-order turbine governor dynamics. We analysed this issue and modified it in [23]; however, only local stability was shown.

3.2 Novelty of the approach

In the previous section we made the general overview of the results in control theory that are close or correlate with our research. Let us now discuss the novelty of the proposed approach. The existing approaches to the frequency control can be separated into two main groups: controls based on the averaging approach and control based on the primal-dual algorithm. Within this work we propose a new approach based on the idea of separation of control and physical system dynamics as much as possible. Frequency control is aimed to restore power balance in the system. Therefore, control actions are complete if and only if sum of control signals is equal to the sum of the disturbances. Thus, every frequency control estimates size of the disturbance. Within this work we expand this idea. We derive our control as a feedback control consisting of two parts. First part uses system state, namely measurements of frequencies and electrical powers on every bus in order to obtain some approximation of the disturbance. Further we show that this approximation can differ from the actual disturbance, but it provides approximation accurate enough for the next part. The second part uses the calculated approximation in order to calculate control values in a distributed way. It can accept both disturbance approximation, obtained in the first part and disturbance measurement. This way the control acts as a feedback control. If for some reason the disturbance is known (e.g. system loses a bus with known consumption or generation), then the second part of the controller can act as a feedforward controller using disturbance vector as an input. Moreover, controller can operate in a mixed regime, when some components of the disturbance are approximated via the feedback part and some of the components are an input of the second part as a feedforward action. As a result, we utilize the fact that every disturbance is measured or approximated within every frequency control. However, we separate the disturbance approximation into separate decentralized block. Thus, distributed control block not only can act separately as a feedforward controller, if necessary. Moreover, the developed controller can combine this approaches. General control block-diagram is presented on the Figure 3.1. Here r is the vector of bus disturbances, $\overline{r}$ is vector of known disturbance measurements r^I is a vector of indicators that show if the measurement is available. Vector u is a vector of bus control signals sent to the turbines regulating valves, ω and p^e are vectors of bus frequency deviations and electrical powers respectively. The internal structure of the controller is presented on the Figure 3.2. Here $\tilde{r}$ is vector of bus disturbances approximations.

The algorithm of control derivation technique is given in the Figure 3.3. It is not clear how to explicitly analyse dynamics of the controller that includes frequency control, congestion management, and inter-area flows regulation during transient if we include communication limitations. Thus, we start analysis by formulation optimization problem for the stationary point (here our approach coincides with the primal-dual approach). Knowledge of the disturbance vector is sufficient for the control derivation. However, this information is not available; therefore, we approximate it using the system state. Next step is reduction of Karush-Kuhn-Tucker conditions. Our goal is to exclude or replace all physical variables with the exception of those used for the disturbance approximation. This allows us to decouple dynamics of the physical system from dynamics of the controller in the following scene: dynamics of the controller depends only on disturbance approximation based on the system

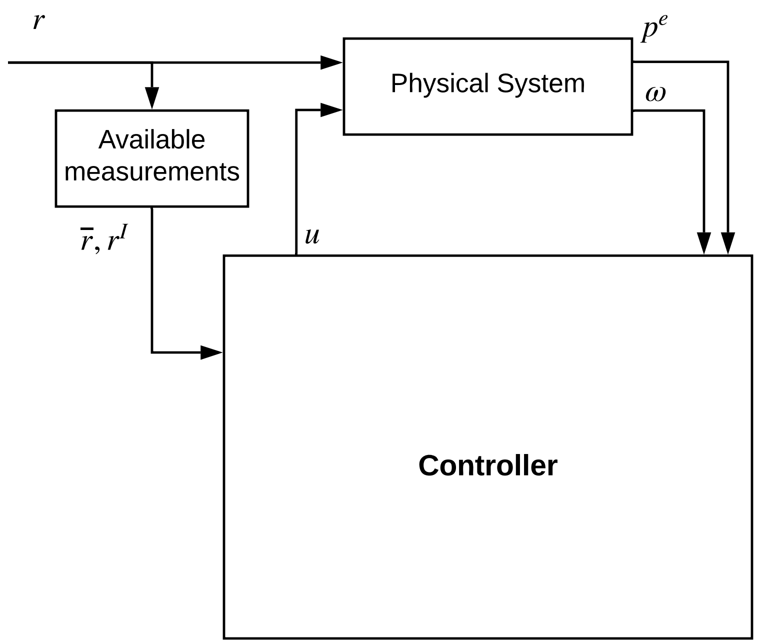

Figure 3.1: General Controller block-diagram.

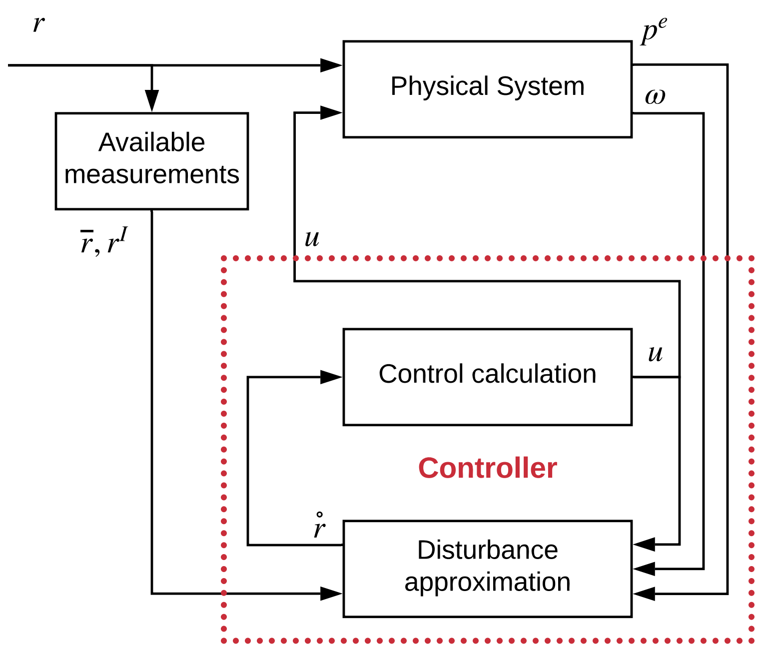

Figure 3.2: Controller block-diagram.

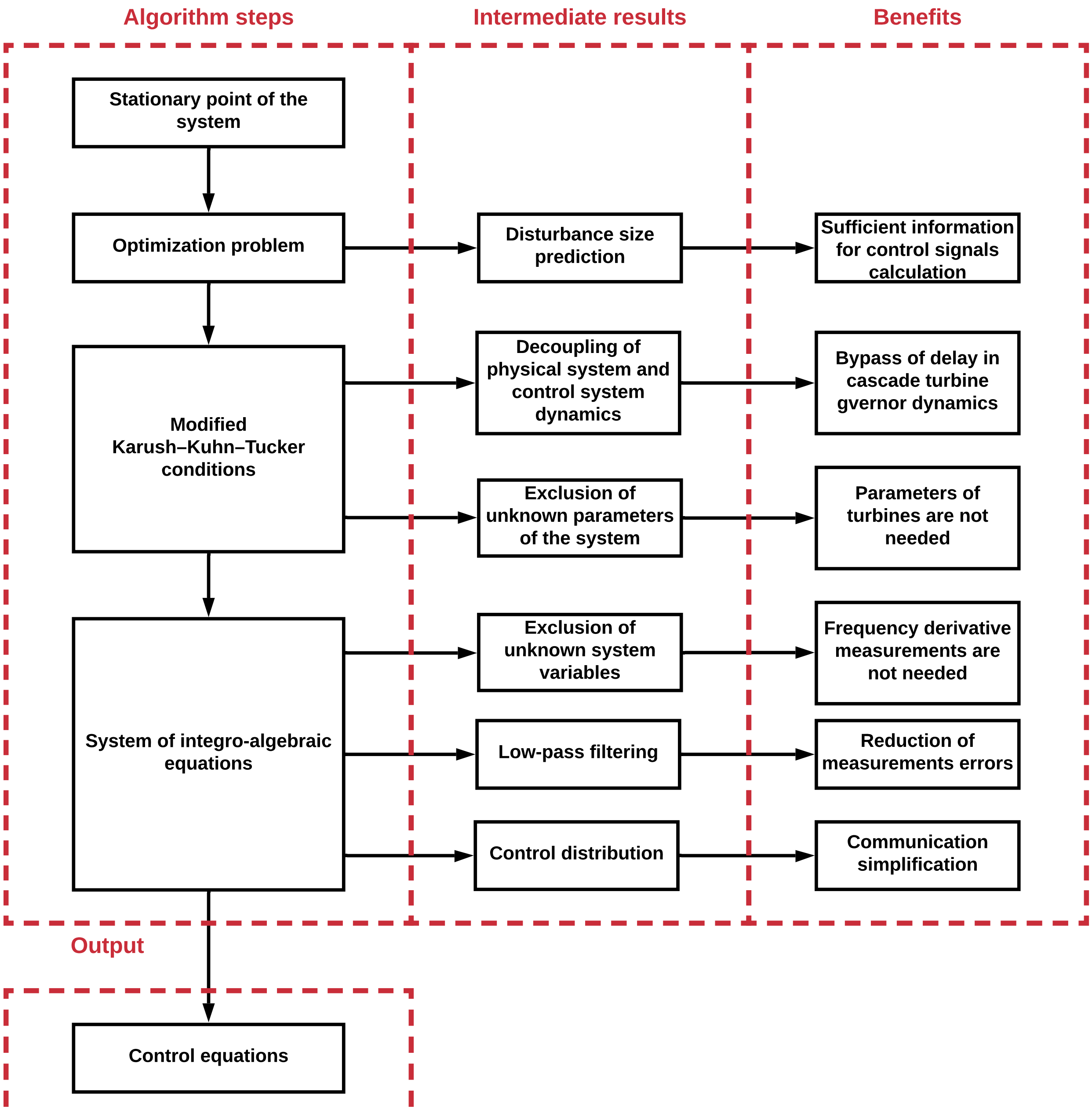

Figure 3.3: Algorithm of the control derivation.

state. All physical dynamics are suppressed in the disturbance approximation state, because disturbance is an external parameter with respect to the system dynamics.

Such approach allows us to do both: bypass the issues with cascade dynamics and exclude physical variables that we cannot measure (e.g. mechanical power injections). The bypass of the control dynamics provides the main novel contribution of this work. Namely, it allows to keep control response globally asymptotically stable even when the other types of control (as is shown in [83]) lose stability.

In addition during this stage we modify complimentary slackness conditions and replace them with piece-wise linear continuous equality constraints (constraints that are defined by piece-wise linear continuous functions). Finally, we transition from a system of algebraic equations to a system of integral algebraic equations in order to

1. Exclude frequency derivative from a set of required information. Although, it is possible to measure frequency derivative, its measurement is noisy and can be used only after some averaging. However, the latter requires observation window of ~ 5 seconds, which is too big since frequency control must respond immediately after the frequency change.

2. Low-pass filtering. All measurements as well as information obtained from the neighbouring buses goes through low-pass filter; thus, robustness of the algorithm increases.

3. Control distribution. The controller allows us to do distributed implementation.

The list above states goals that in other works were only fulfilled for a simpler turbine governor dynamics.

4 Thesis structure

Section 5 consists of all the notations used further in the thesis and contains list of the most used variables. In section 6 we provide general overview of the problems in power systems. Then in the section 7 we discuss in details issues related to frequency control and congestion management. Further sections of this work are organized in the following way. We start with the description of the known results in stability theory that are used within this work (section 8). In section 9 we discuss power system model used for the further research and justify our choice. The control derivation is separated in 7 problems described in sections 12.1 — 13.4. First 3 problems are dedicated to the centralized control and are focused on the derivation of the general control idea. The last 4 problems are more focused on the control properties, namely distributed communication, congestion management and inter-area flows control. This approach is used in order to consequently increase complexity of the control problems. For each problem separate control is derived. All controls perform frequency control and utilize load-side control. The details of each problem are shown in the table 4.1. Here "+" sign is used if the control aspect is present and "−" otherwise. Control in problem 2 does not have control limits, but can limit the number of controllable buses, therefore "±" sign is used.

Communication type	Problem number	Section	Control limits	Distributed communication	Congestion management	Inter-area flows regulation
Centralized	1	12.1	−	−	−	−
	2	12.2	±	−	−	−
	3	12.3	+	−	−	−
Decentralized	4	13.1	−	+	−	−
	5	13.2	+	+	−	−
	6	13.3	+	+	+	−
	7	13.4	+	+	+	+

Table 4.1: Problems structure

5 Notations

Set of real numbers is denoted by $\mathbb{R}$. Set of natural numbers is denoted by $\mathbb{N}$. For an arbitrary matrix X its transpose is denoted by X^T. Identity matrix of the size $n \times n$ is denoted by I^n. Vector of ones of size n is denoted by $\mathbf{1}^n = (1, \ldots, 1)^\top$. Matrix $\operatorname{diag}(x_1, \ldots, x_n) \in \mathbb{R}^{n \times n}$, $x_i \in \mathbb{R}$ — diagonal matrix with numbers x_i on the diagonal. Matrix $\operatorname{diag}(X_1, \ldots, X_n) \in \mathbb{R}^{m \times m}$, $X_i \in \mathbb{R}^{n_i \times n_i}$, $m = \sum_{i=1}^{n} n_i$ — block-diagonal matrix with matrices X_i on the diagonal. For any vector $x \in \mathbb{R}^n$ and set $K \subseteq \{1, \ldots, n\}$ vector x_K is subvector of x that consists of elements x_i, $i \in K$. For any matrix $X \in \mathbb{R}^{n \times m}$ and sets K_1, K_2 matrix X_{K_1} is row submatrix that consists of elements x_{ij}, $i \in K_1$, $j \in \{1, \ldots, m\}$, matrix X_{K_1,K_2} is submatrix that consists of elements x_{ij}, $i \in K_1$, $j \in K_2$. Comparison operators ($<$, $>$, $\leq$, $\geq$) applied to vectors are considered to be element wise. For a power network graph set of buses adjacent to bus i is denoted by $\operatorname{Adj}(i)$, set of lines adjacent to bus i is denoted by $\overline{\operatorname{Adj}}(i)$. Further the following piece-wise linear functions will be used:

- Function $\nu^n : \mathbb{R}^n \times \mathbb{R}^n \times \mathbb{R}^n \to \mathbb{R}^n$,

$$\nu_i^n(x, y, z) = \max\{\min\{x_i, y_i\}, z_i\},\ i \in \{1, \ldots, n\}. \tag{5.1}$$

- Function $\phi^n : \mathbb{R}^n \times \mathbb{R}^n \to \mathbb{R}^n$,

$$\phi_i^n(x, y) = \begin{cases} x_i, & \text{if } x_i \geq 0 \text{ or } y_i \geq 0, \\ 0 & \text{otherwise.} \end{cases},\ i \in \{1, \ldots, n\}. \tag{5.2}$$

It is necessary to mention that $(\nu^n(x, y, z))_i = \nu^1(x_i, y_i, z_i)$, $(\phi^n(x, y))_i = \phi^1(x_i, y_i)$.

Γ	power system graph;	C	incidence matrix of the graph Γ;
E	set of edges (lines);	S	incidence matrix of inter-area flows;
N	set of vertexes (buses);	w_i	participation factors of the controlled buses;
G	set of generator buses;		
L_1	set of load buses with inertia;	W	diagonal matrix of w_i;
L_0	set of load buses without inertia;	r_i	bus power disturbance ;
q	number of lines;	ω_i	bus frequency deviations;
n	number of buses;	θ_i	bus phase angles deviations;
g	number of generator buses;	p_j	power flows deviations;
l_1	number of load buses with inertia;	p_i^e	bus electrical powers;
l_0	number of load buses without inertia;	p_i^m	generators mechanical power injections;
n^{area}	number of areas;	v_i	regulating valves positions;
$\alpha(k)$	set of border buses of the area k;	u_i	control signals;
$\beta(k)$	set of buses from areas $\hat{k} \neq k$ adjacent to buses from $\alpha(k)$;	$\overline{u}_i$	upper control limits;
		$\underline{u}_i$	lower control limits;
$\gamma(k)$	set of lines connecting border buses with other areas;	$\overline{p}_j$	upper line flow limits;
		$\underline{p}_j$	lower line flow limits;
m_i	synchronous machines inertia;	ζ_k	inter-area flows reference values;
d_i	sum of synchronous machines damping and response of frequency dependant loads;	$\overline{r}_I$	measurements of bus disturbances;
		r_i^I	indicators of bus disturbances measurements availability;
t_i^m	generator time constants;	$\mathring{r}_i$	output of the disturbance approximation control block (either available measurement $\overline{r}_i$ or approximation $\tilde{r}_i$);
t_i^v	regulating valves time constants;		
b_j	line parameters in inverse ratio to the line suseptances;		
M	diagonal matrix of m_i;	$\tilde{p}_i^m$	mechanical power injections approximations;
D	diagonal matrix of d_i;		
B	diagonal matrix of b_i;	y^i	auxiliary variables.

6 Power System's Structure

The first electrical lightning system was a network of Yablochkov candles. It was launched on May 30, 1878 in Paris on Avenue de l'Opera. The first power system was created by Edison in 1882 and consisted of generator and distribution network, which delivered power to the customers on Pearl Street in Manhattan. Nowadays power systems vary in size, power, and components. Nevertheless, it is possible to point out a number of their basic characteristics.

1. Power systems are three phase systems with almost constant voltages.

2. Mainly synchronous machines are used to generate electrical power. Energy of primal source (e.g. chemical energy of fuel or potential energy of water) is converted to mechanical in turbine, and then converted to electrical by synchronous generator.

3. Electrical energy can be transmitted through long distances and to a large number of consumers.

Deliverance of electrical power to the consumer is a transportation problem that has two features:

1. Generated and consumed powers must always be equal in the power system. Despite existence of storage possibility in the form of energy storage, it is not possible to store significant amounts of power due to the high energy storage installation and maintenance cost.

2. Unlike in majority of transportation networks (e.g. pipelines networks), generally in power systems it is not possible to directly control power flow on every line. Line power flows are defined by the second Kirchhoff's law and can be changed only via adjusting generation or demand of the controllable buses.

It is possible to identify basic power system components shown in the Figure 6.1 [84]. Historically power system is divided into physical and electrical components. At the first stage fuel energy is converted into heat in the boiler. Then, produced steam sets in motion turbine, which produces mechanical power. Mechanical power is injected into synchronous

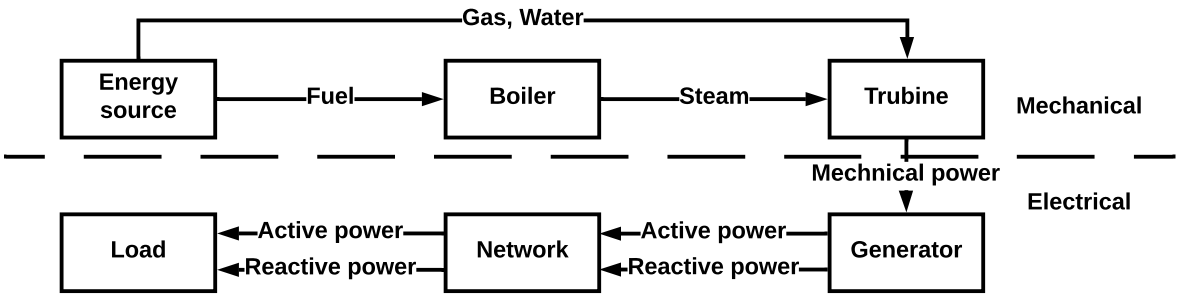

Figure 6.1: Power system structure

generator, which produces electrical power. The latter is transmited to the consumer through the network.

6.1 Synchronous machines

Generators in power networks are synchronous machines [10]. They are divided into high-speed (3000-1500 rpm) driven by steam or gas turbines and low-speed (1000-50 rpm) driven by hydro turbines.

All synchronous machines consist of two parts made of magnetic steel: stator which has armature windings and rotor. Armature winding consists of three identical equidistant windings. Rotor is a set of electromagnets supplied by DC current from the excitation system. The current produces magnetic flux with the strength proportional to the current. This magnetic flux rotates with respect to the armature windings. Thus, sinusoidal electromotive force is induced on each of three windings, which produces AC current. Electrical frequency of a generator can be calculated according to the following formula:

$$f = \frac{pn}{120}, \tag{6.1}$$

where p is the number of rotor poles, n is rotor rotational speed (rpm) and f is electrical frequency (Hz). For example, in order to produce 50 Hz electricity 2-pole rotor should rotate at 3000 rpm.

By design type, rotors are divided into two categories: with salient and non-salient magnetic poles. In salient poles rotors excitation windings are placed on explicitly projected t-shaped poles. Such rotors are used in low-speed generators used on hydro power plants. Due to their low speed centrifugal force as well as windage losses are low. Such rotor construction allows us placement of multiple poles, thus providing possibility to operate at different speed depending on the number of excited poles.

Non-salient poles rotors are used in high-speed generators. They have cylindrical form and excitation windings are placed in parallel slots on the surface of the rotor as it is technologically impossible to create salient pole rotors for such generators due to high centrifugal force. Such generators have 2 or 4 poles which corresponds to rotational speed of 3000 rpm or 1500 rpm respectively.

Frequency of the induced electromotive force is proportional to the rotation speed of the rotor. Multiple synchronous generators must operate at the same electrical frequency; thus, their rotational speeds must be proportional to each other. Additionally, frequency must be kept within close neighborhood of the nominal value. This requirement is enforced by significant drop of turbines' efficiency in case of non optimal speed operation. Moreover, high frequency oscillations (over 2 Hz) may result in turbine damage. Therefore, in case of high frequency oscillations generation unit will automatically disconnect from the system.

6.2 Generating unit structure

Structure of a generating unit is presented in the Figure 6.2 [85]. Here p^{ref} is nominal value of electrical power, p^e is value of electrical power, f is frequency, ω is rotor's rotation speed, V^{ref} is nominal voltage magnitude value, V_g is voltage magnitude value, I_g is current value.

Energy carrier (steam in this case) is delivered to the turbines through governor valves and sets turbine's rotor in motion. Turbine and generator rotors are located on one shaft that has shaft counter. DC current is provided to the generator rotor by the exciter.

Generator outputs power through a three-phase line connected to a step-up transformer needed to reduce losses as they are proportional to current squared. Finally, the transformer is connected to power network through circuit-breaker, which disconnects generating unit from the network in case of emergency.

Two main control systems are presented on a generator unit. Frequency regulator adjusts position of governor valves; thus, changes power output in order to perform frequency control.

Voltage regulator changes current of the exciter, thus changing generator output voltage.

6.3 Wind generators

In case of wind generators, mechanical energy injected to the generator is provided by wind tribune. Its rotational speed varies in between 15-20 spins per minute. Wind turbine is connected to the generator by a gearbox. The major difference of conventional generating units compared to the wind ones from the perspective of frequency control is low inertia of the latter [10]. As a result, volume of kinetic energy available for arresting frequency oscillation is reduced. Effect of inertia in frequency control is discussed in more details in section 7.4.

6.4 Active and reactive power

Let us consider a synchronous machine connected to an infinite bus. Under the assumption that generator rotor is ideally cylindrical and air resistance is equal to zero generator active and reactive power outputs are defined by the following formulas:

$$P_G = \frac{|\mathcal{E}||V|}{X} \sin\theta, \tag{6.2a}$$

$$Q_G = \frac{|\mathcal{E}||V|}{X} \cos\theta - \frac{|V|^2}{X}, \tag{6.2b}$$

where P_G is active power, Q_G is reactive power, $|\mathcal{E}|$ is EMF magnitude, $|V|$ is voltage magnitude of an infinite bus, X is its reactance, θ is rotor angle with respect to an infinite bus.

In power systems voltages can deviate from the nominal values only by several percent. Thus, fraction in equation (6.2a) is close to constant and active power is defined by rotor angle θ. In equation (6.2b) voltage of an infinite bus is the only quadratic term; thus, it has the major impact on reactive power value. Variables P_G, θ and Q_G, V are strongly coupled, while dependencies out of this couples are almost non existent in transmission networks.

6.5 Types of power systems dynamics

Power systems function is generation of electrical energy and its transportation to consumers. This operations requires usage of large variety of different components that perform different

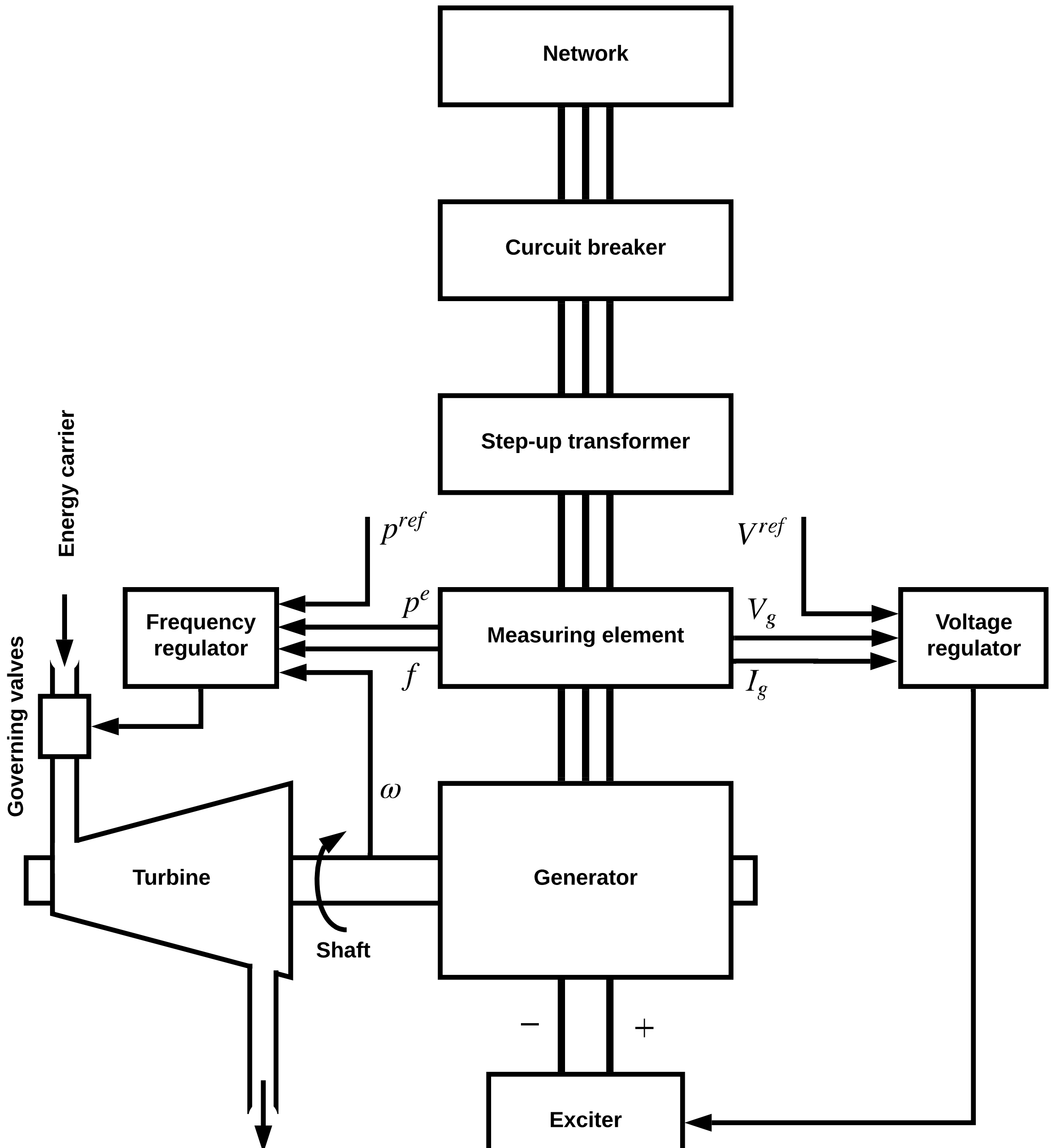

Figure 6.2: Generating unit structure

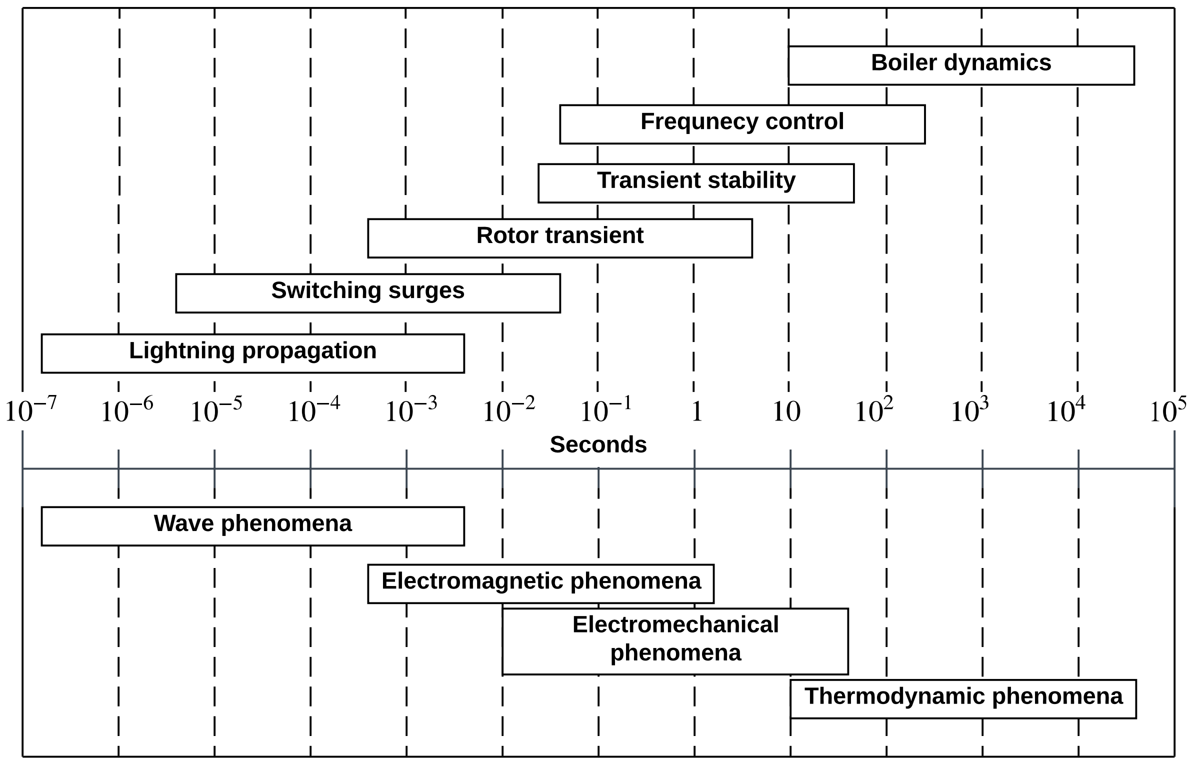

Figure 6.3: Power system dynamics classification.

functions at different timescales. Nevertheless, it is possible to divide all dynamical processes into categories based on timescales, causes and types of effect (Figure. 6.3 [85], [84]). One of the primary points of interest is system's reaction to change of consumption or appearance of disturbance caused by a loss of the power system element (e.g. loss of generator or line). Nevertheless, it is necessary to note that some processes (for example, frequency control) can cover several time intervals.

6.6 Power system stability

System stability is ability of power system to remain in the neighbourhood of predefined stationary point even if some disturbances appear. Disturbance types were briefly discussed in the previous section. Based on these types power system stability is divided into several categories (Figure 6.4 [86], [87]). This division is based on usage of different mathematical models required for accurate representation of system's behavior.

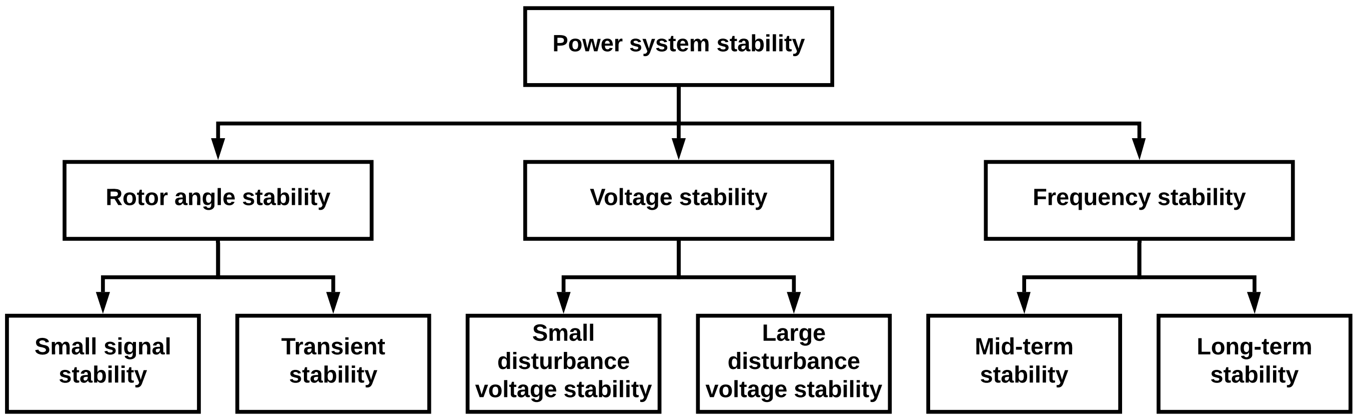

Figure 6.4: Power system stability types classification.

6.7 Rotor angle stability

Rotor angle stability is capability of synchronous machines of the system to keep syncronism. During normal operation magnetic field in synchronous machine rotates at the speed of rotor.

If due to some disturbance rotor speed deviates from the synchronous speed of magnetic field, the latter ceases to be stationary with respect to the rotor. As a result, current is induced on damper windings. This current, according to the Lenz's law produce torque opposite to the direction of magnetic field rotation, thus restoring synchronism.

If disturbance is large, deviation of rotor speed may lead to a loss of sychnronism. In this case generating unit is either disconnected from the network or is returned to synchronous regime by out-of-step conditions liquidation system.

Rotor angle stability is traditionally divided into two categories:

1. Small signal stability is an ability of power system to remain sycnhronism after small disturbances. In this case disturbances size allows us to analyse system using linearized model.

2. Transient stability is an ability of power system to remain sycnhronism after large disturbances. Linearization is not applicable due to loss of model accuracy. Usually, post-disturbance state of the power system differes from the one before the disturbance.

6.8 Voltage stability

Voltage stability is the capability of power system to keep acceptable voltage values on all system's buses not only during normal operating conditions but also after appearance of disturbances. Let us consider equation (6.2a).Maximal active power that can be transported to an infinite bus is equal to

$$P_{\max} = \frac{|\mathcal{E}|^2}{X}. \tag{6.3}$$

It is achieved when $|\mathcal{E}| = |V|$. Further increase of power consumption on the infinite bus will lead to reduction of active power flow and consequently stability loss. Additionally, voltage converges to zero, which results in voltage collapse.

Voltage stability is divided into two categories:

1. Small disturbance voltage stability. Disturbance is caused by for example, daily change in power consumption. System's steady-state is used to analysed voltage stability.

2. Large disturbance voltage stability. Disturbance is caused by a failure (e.g. loss of a generator or a line). Dynamical model of the system is considered for a time interval varying from couple of seconds to several minutes.

6.9 Frequency stability

Frequency stability is capability of power system to keep frequency at nominal value as during the normal system operation as well as during disturbances. Main difference here from the previous types of stability is slow dynamical processes. Reason for that is dependence of frequency on rotational speed of synchronous machines of the system.

Frequency stability is divided into the following types:

1. Mid-term stability. Here system's dynamical response to a disturbance caused by any possible reason (including daily consumption changes and system's components failures).

2. Long-term stability. Steady-state of the system is analysed, after attenuation of all dynamical effects.

6.10 Power system control types

The following criteria are used to identify reliability of power systems:

1. Power system must quickly adapt to changes of loads since no means to store electrical energy of significant sizes exist.

2. Voltage changes must be strictly limited.

3. Frequency oscillations must be strictly limited.

4. Power system must withstand loss of system's element.

In order to satisfy these criteria a set of various controls is applied to the system depending on the state of the latter (Figure 6.5, [85], [88]):

1. At normal state power balance is held, frequency is at nominal value, all system parameters such as voltages and power flows are within acceptable limits. Disturbances that may appear in the system are caused by daily load changes.

2. At alert state values of power system parameters such as voltages may be close to the acceptable limits. Moreover, system does not satisfy safety criteria (e.g. inter-area flows are different from the nominal). Otherwise all system's components operate normally; however, disturbance that would otherwise be considered safe may lead to system components failure.

3. At emergency state power is supplied to the majority of the consumers; however, power system suffers from significant frequency and voltages deviations from nominal values. Some elements of the system such as lines or generating units may not work. If failures happen on multiple elements, system may go into in extremis state.

4. In extremis state is defined as a power system state when control over the system is lost. As a result, system may separate into multiple synchronous islands and shut down fully or partially.

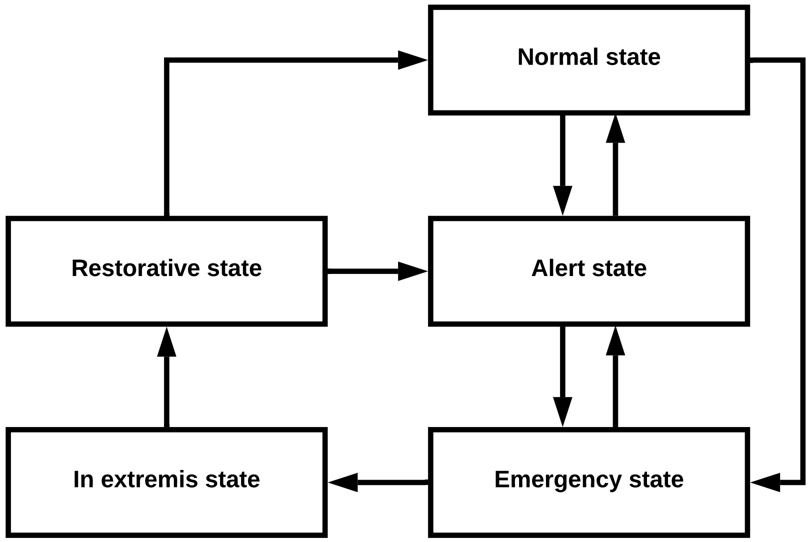

Figure 6.5: Power system states classification.

5. At restorative state automatic and manual actions (such as generating units and loads reconnection, synchronization of islands) are taken to return power system to normal state.

Figure 6.6 [89] represents statistics based information about types of failures developments. Each arrow represents type of failure or control action, percentages are counted from total amount of failures. In some cases multiple events may develop simultaneously; thus, for example, after stage 6 some of percentages of following events is bigger than 100%.

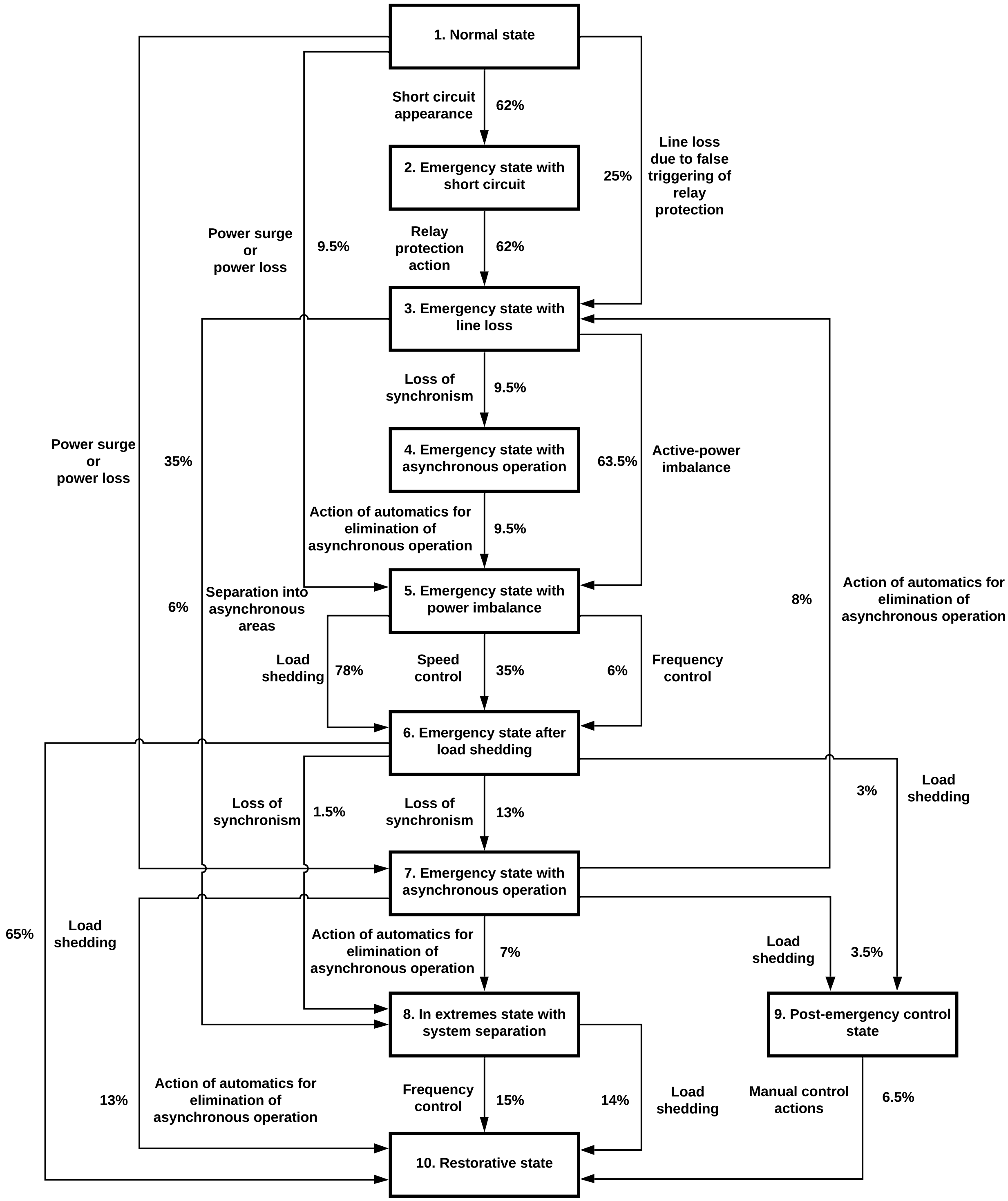

Figure 6.6: Power system cascade failures development types.

7 Frequency control

This section is dedicated to the problem of keeping frequency at the nominal value. Since connection between reactive power and frequency is weak in transmission networks [90], everywhere further only active power is considered.

In power systems frequency is an indicator of the power balance. If power consumption is higher than generation, synchronous generators start to slow down; thus, frequency drops. The opposite situation happens, when there is surplus of power in the system.

There exists multiple techniques aimed two keep power balance [10]. The large slow (from several hours to several days) changes in power consumption are addressed via unit commitment procedure that defines which generators must be turned on or off or ramped up or down. In the case of large unexpected power loss, if the system is in an emergency state, load shedding is carried out (Figure 6.6). The remaining niche includes system operation at timescale below the timescale of unit commitment with the state being in normal or alert state. Further, we will analyse the existing control and derive the new control scheme for this type of system operation.

Frequency oscillations are countered by frequency control. Frequency control (shown in the Figure 6.2) opens or closes governor valves changing input of energy carrier into turbines. As a result, it drives mechanical power output of the turbine to the desired value.

In addition to keeping frequency at the nominal value control solves two additional problems. Regulation of inter-area flows and congestion management (control of line power flows). Some of the power systems are divided into several areas. Reasons for such division might be different: system's size, loads distribution, regional or country borders. Inter-area flow of an area is a sum of flows through lines that connect area to the rest of the system. Control of inter-area flows is required due to the number of reasons: (a) it allows us to limit power flows through long distances, thus reducing power losses, (b) after power imbalance being compensated by generators of the same area; operation of the other areas remains unchanged. Deviations of inter-area flows do not lead to equipment damage; nevertheless, control of inter-area flows is important for the system's robustness.

Congestion management is needed due to the following reasons: (a) amount of power that can be transmitted through a line is limited by formula (6.3), violation of this limit leads to the voltage collapse, (b) lines have thermal limits, their violation leads to line overheat and trip. In case of transmission lines thermal limits are the restricting ones. Despite the possibility of line trip, short-term violation of thermal limits does not lead to negative consequences.

7.1 Traditional control scheme

Control scheme, used today in power systems, consists of three parts: primary, secondary and tertiary controls

- Primary control is dynamic control aimed to suppress frequency oscillations.
- Secondary frequency control is dynamic control, which purpose is frequency restoration as well as inter-area flows control. It works in a centralized way in every area. If spinning reserves are insufficient to restore frequency additional generation units are put into operation.
- Tertiary frequency control solves secure constraints optimal power flow problem, which includes congestion management. Tertiary control is the only static control presented here: it ignores networks dynamics and is performed at regular time intervals.

In the following paragraphs controls will be described in more details.

7.2 Primary frequency control

Historically centrifugal governor was used for primary frequency control, which is also called droop control. Nowadays control is implemented via electronics. Primary frequency control is the fastest among all three. It works in a distributed way using only local information during several tens of seconds after disturbance appearance. It uses spinning reserves in order to work. Primary frequency control cannot restore frequency to the nominal values and only limits frequency deviations. This control is a proportional controller with deadband:

$$u^I(t) = \begin{cases} 0, & \text{if } |\omega(t) - \Omega| \leq \Delta\omega, \\ -k^I P^n \Omega^{-1} \left((\omega(t) - \Omega) - \Delta\omega \,\mathrm{sign}(\omega(t) - \Omega) \right) & \text{in other cases.} \end{cases} \tag{7.1}$$

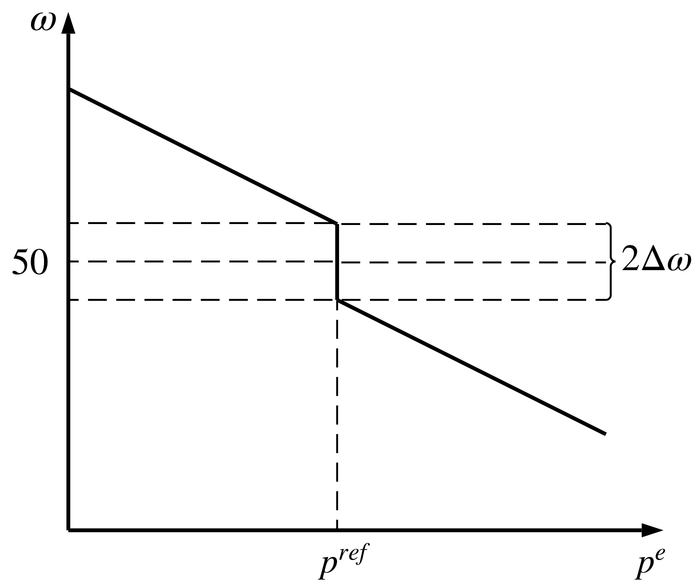

Figure 7.1: Primary frequency control graph.

Here Ω is nominal frequency (50 or 60 Hz), $\Delta\omega$ is a deadband size, P^n is installed generator power, u^I is control value, and $k^I > 0$ is a dimensionless control gain, which usually varies from 15 to 25 and is defined by the system operator so that the system is stable.Parameter $\Delta\omega$ is called deadband. Control signal for $|\omega(t)| < \Delta\omega$ is equal 0. The deadband is used due to the following reasons:

1. If frequency is close to nominal, control signal of different generators can have opposite signs due to measurements errors. As a result, generators will "fight" each other.

2. Deadbands of different sizes allow some generators (e.g. hydro generators) to respond to a disturbance quicker than the other.

Figure 7.1 represents dependence of generator electrical power output on the frequency value. As can be seen, frequency drop leads to increase of power output. The opposite happens in case of frequency increase. Primary frequency control operates at all system's states presented in section 6.10. Nevertheless, in some power systems in case of high frequency oscillations (when the system is in critical state) primary frequency control switches from frequency control to speed control. The latter is represented by proportional controller with higher control gain k^I [10].

7.3 Secondary frequency control

Secondary frequency control is responsible for delivering frequency to the nominal value. This control works in a centralized way: frequency measurements are taken from one or several reference generators, and then system operator calculates control values and sends them synchronously to every controllable bus. Secondary frequency control is represented by an integral controller. Frequency deviation measured at reference buses are integrated in order to obtain control signals u^{II}. Let G be set of system's generators, ω_{ref} be frequency on the reference generator that sends frequency measurements to the system operator. Then, secondary frequency control is represented by the following formulas:

$$y(t) = -k^{II} \int_0^t (\omega_{ref}(\tau) - \Omega) d\tau, \tag{7.2a}$$

$$u_i^{II} = \frac{y}{w_i},\ i \in G. \tag{7.2b}$$

Here $w_i,\ i \in G$ are generators participation factors, $k^{II} > 0$ (MW/Hz) is an integration coefficient. Its choice is discussed in section 7.4.

Participation factors have the following interpretation. Let us consider the case, when system suffers from a step change disturbance, which is then compensated by frequency control action (7.2). Then, participation factors are equal to coefficients of quadratic function, which is being minimized during secondary frequency control operation:

$$\frac{1}{2} \sum_{i \in G} w_i (u_i^{II})^2. \tag{7.3}$$

Frequency control response is presented in the Figure 7.2. Change of electrical power nominal value moves droop characteristic along the p^e axis, thus allowing to return frequency to the nominal value.

Secondary frequency control in addition to frequency restoration is also responsible for control of inter-area flow. In order to do so, value of inter-area flow deviation is added to integrated of (7.2a). After such modification values of y function are not unique for the entire system, but are unique for each area of the system.

Let power system be divided into $k^{\max}$ areas, and ref_k is in index reference generator in

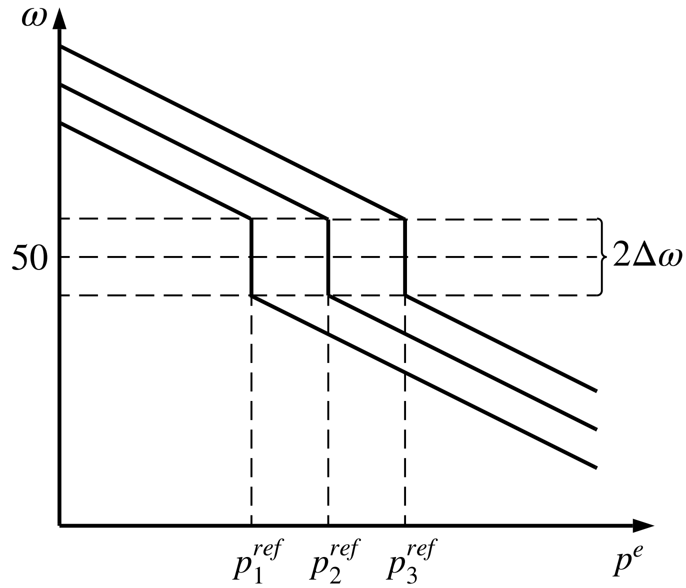

Figure 7.2: Droop characteristics for different reference values u^{II}

the area $k \in \{1, \dots, k^{\max}\}$. Then, equations (7.2) are updated to the following form:

$$y_k(t) = -k^{II} \int_0^t (\omega_{ref_k}(\tau) - 50) + K_k^{area}(\hat{P}_k(\tau) - \hat{P}_k^{ref}) d\tau,\ k \in \{1, \dots, k^{\max}\},\ l \in \{1, \dots, k^{\max}\}, \tag{7.4a}$$

$$u_i^{II} = \frac{y_k}{w_i},\ i \in G_k,\ k \in \{1, \dots, k^{\max}\}. \tag{7.4b}$$

Here $\hat{P}_k$ is inter-area flow, $\hat{P}_k^{ref}$ is nominal value of inter-area flow. Coefficient K_k^{area} is chosen so that value inter-area flow deviation would affect function y much less, than value of frequency deviation. Thus, in case of disturbance appearance, generators from all areas participate in frequency restoration, ensuring system's safety. Then, after frequency oscillations are suppressed, generation is adjusted subject to the inter-area flows nominal values. Hence, after the transient, disturbance is compensated only by the generators of the disturbance's area.

7.4 Frequency dynamics in power systems

Power system's reaction to a step change disturbance is represented in the Figure 7.3. Here r is total power consumption of the system, Δr is the step change disturbance. Upper plot represents frequency response to the disturbance, lower plot shows participation of kinetic energy, primary and secondary controls in mechanical power output.

During the first 5-10 seconds after the disturbance appearance draw of additional electrical energy is compensated only by the change of the generator's kinetic energy. Primary and secondary control respond to the frequency change; however, due to the delay in turbine governor dynamics, they do not change mechanical power output during this period. As a result, generator continues to supply power system with energy; however, generator's speed as well as system's frequency drop. If system does not have any control, then frequency will continue to drop (graph $f_{kinetic}$ on the upper plot).

Primary frequency control reacts to the frequency drop by opening governor valves hence, increasing input of energy carrier to the turbine (green area, u^I). Then, mechanical power delivered by the energy carrier becomes bigger than the disturbance size Δr, hence, kinetic energy loss is compensated. Primary frequency control is represented by proportional controller; thus, it cannot fully compensate the disturbance, and should the system have no secondary frequency control, the system frequency will stabilize at some suboptimal value (graph f_{PFC} on the upper plot).

Finally, secondary frequency control (blue area, u^{II}) changes mechanical power output by Δr, thus restoring frequency. Oscillations of the mechanical power output can be observed. They appear due to the control lag caused by the delay of governor and turbine dynamics as well as difference between responses of the system's generators.

Example 7.1 (Primary and secondary control coefficients)**.** Let us consider New England IEEE 39 bus system [8], shown in the Figure 7.4. It consists of 39 buses including 10 generators marked G1,...,G10. Per unit system is used: all parameters are scaled with respect to the base power value of 100 MVA. Parameters of the system are given in the tables 7.1 and 7.2 here $k^I = 20$. In the table we present values $P_i^n k^I$ in the column droop response (where P_i^n is a reference power of the generator Gi.Turbine and governor constants are taken from [90].

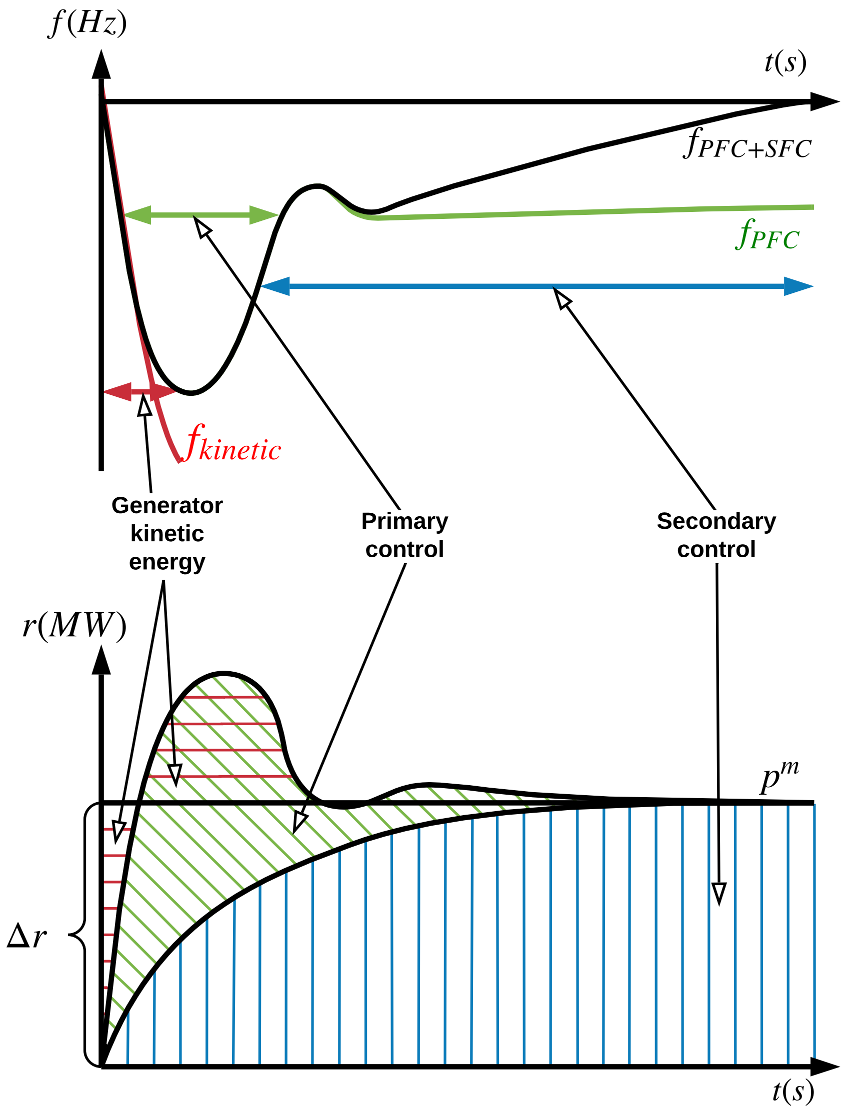

Figure 7.3: Power imbalance compensation.

Generator number	Bus number	Inertia (s)	Damping (p.u.)	Droop response (p.u.)
1	39	50.0000	12.5000	0.1326
2	31	4.2000	28.6465	0.3039
3	32	3.0300	32.5000	0.3448
4	33	3.5800	31.6000	0.3353
5	34	2.8900	25.4000	0.2695
6	35	2.6000	32.5000	0.3448
7	36	3.4800	28.0000	0.2971
8	37	2.6400	27.0000	0.2865
9	38	2.4300	41.5000	0.4403
10	30	3.4500	50.2646	0.5333

Table 7.1: IEEE New England 39 bus system generators' parameters.

Line number	Output bus	Input bus	Line reactance (p.u.)
1	1	2	0.0374
2	1	39	0.0232
3	2	3	0.0139
4	2	25	0.0077
5	2	30	0.0165
6	3	4	0.0204
7	3	18	0.0124
8	4	5	0.0125
9	4	14	0.0125
10	5	8	0.0110
11	5	6	0.0025
12	6	7	0.0090
13	6	11	0.0079
14	7	8	0.0045
15	8	9	0.0350

16	9	39	0.0235
17	10	11	0.0041
18	10	13	0.0041
19	10	32	0.0201
20	11	12	0.0423
21	12	13	0.0423
22	13	14	0.0097
23	14	15	0.0209
24	15	16	0.0089
25	16	17	0.0083
26	16	19	0.0180
27	16	21	0.0126
28	16	24	0.0055
29	17	18	0.0076
30	17	27	0.0161
31	19	33	0.0136
32	19	20	0.0132
33	20	34	0.0180
34	21	22	0.0129
35	22	23	0.0087
36	22	35	0.0130
37	23	24	0.0324
38	23	36	0.0247
39	25	26	0.0290
40	25	37	0.0215
41	26	27	0.0134
42	26	28	0.0429
43	26	29	0.0568

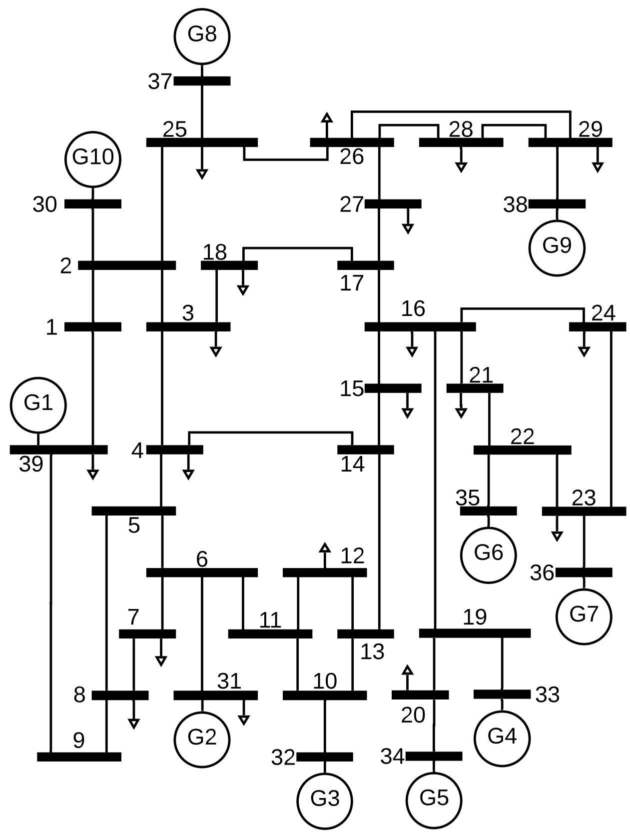

Figure 7.4: New England IEEE 39 bus system.

44	28	29	0.0137
45	29	38	0.0146
46	6	31	0.0238

Table 7.2: IEEE New England 39 bu system line parameters

It is assumed that partial outage happens resulting in step change disturbance of 100 MW on the generator 10 (Figure 7.5). In the Figure 7.6 initial frequency drop corresponds to the loss of kinetic energy. Then, primary frequency control operates during 5-40 seconds after the disturbance. Finally, secondary frequency control restores frequency 6 minutes after the disturbance. Primary and secondary frequency control responses are shown in the Figure 7.7. Even though controls change positions of the governor valves it is convenient to measure

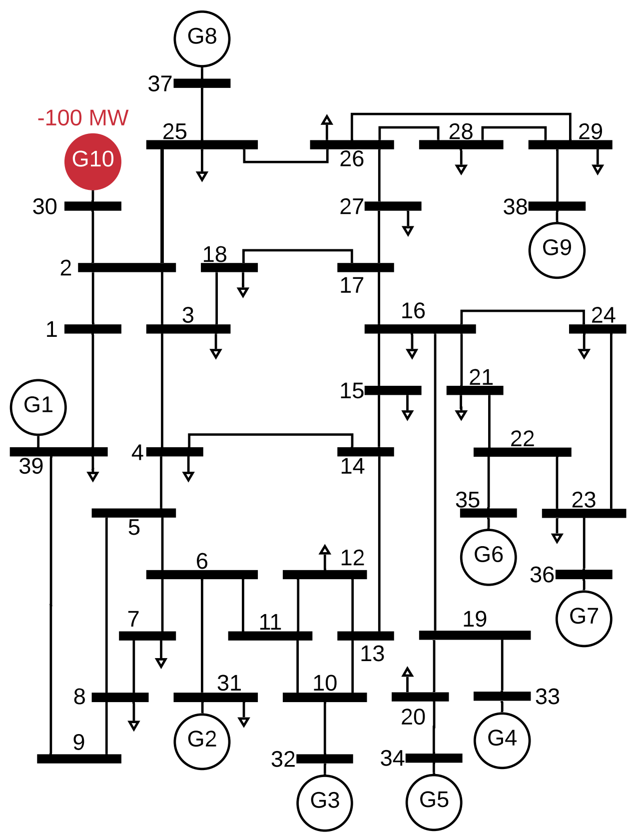

Figure 7.5: New England IEEE 39 bus system. Partial outage.

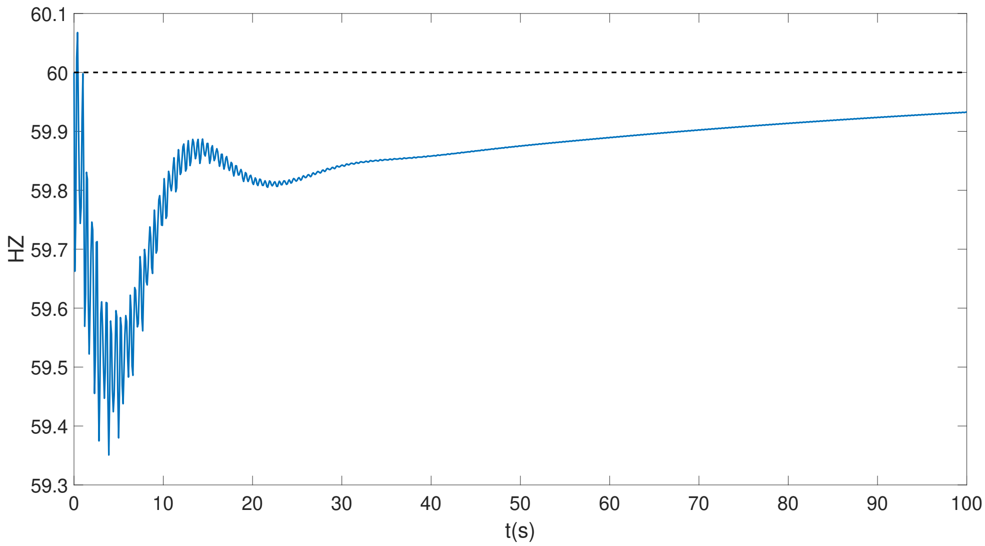

Figure 7.6: Frequency, normal droop constants

it in MW similar to the generator output. If, for example, control signal is changed by 1 MW, generator output will also be changed by 1 MW after attenuation of all transient processes. Since primary frequency control is represented by proportional controller (7.1) its signal graph (blue line) is very close to mirrored graph of frequency in the Figure 7.6. Signal of secondary frequency control (orange line) converges to the 100 MW disturbance value, thus restoring frequency. As a consequence value of primary frequency control converges to 0.

After control signal is sent it takes some time for the mechanical power output to adjust. Turbogenerators act as low pass filters that have control signal as input and mechanical power as output. This dynamics is shown in the Figure 7.8. Such behavior of turbines introduces control, thus imposing limits on the control gains K^I and k^{II}. It can be seen, that approximately at 10 seconds mechanical power output reaches its local maximum. At the same time frequency in the Figure 7.6 reaches its local minimum, which results in rapid growth of control signal and consequently frequency at 20 seconds. If control gains will be increased such effect will lead to increase of frequency oscillations (Figures 7.9 — 7.11) and loss of stability (Figures 7.12 — 7.14). As a result, droop coefficients K^I are taken to be $0.03 - 0.07$ and gain of the secondary frequency control $k^{II} \approx 0.002$ [10].

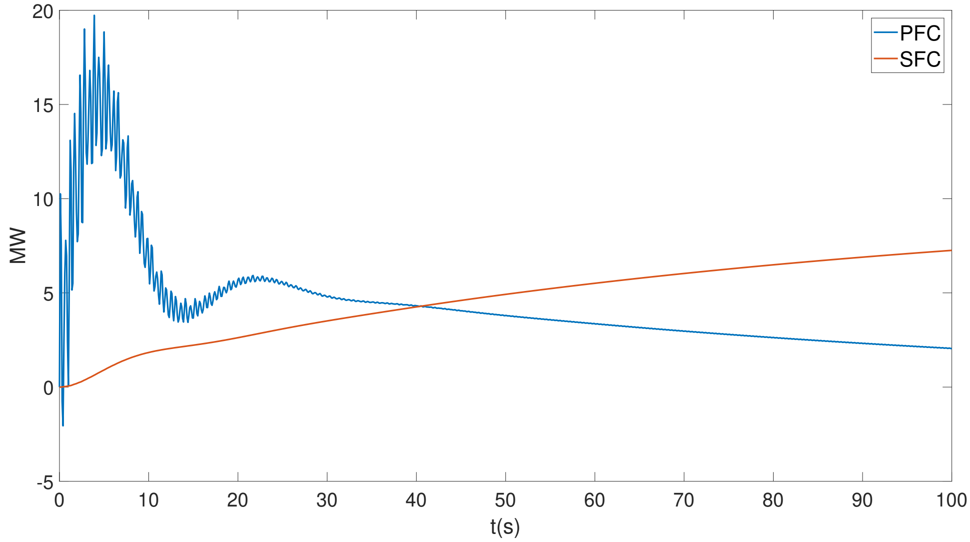

Figure 7.7: Control signals, normal droop constants

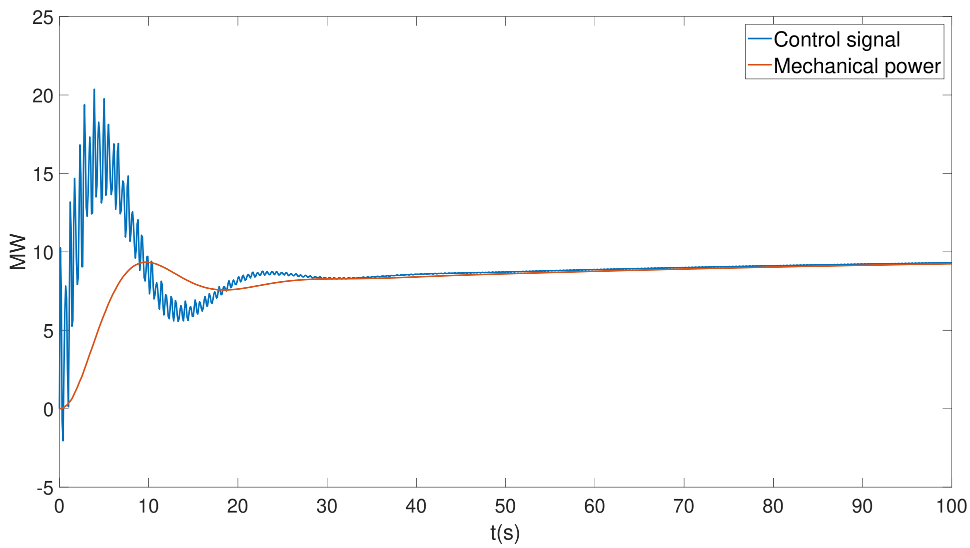

Figure 7.8: Control signal and mechanical power output, normal droop constants

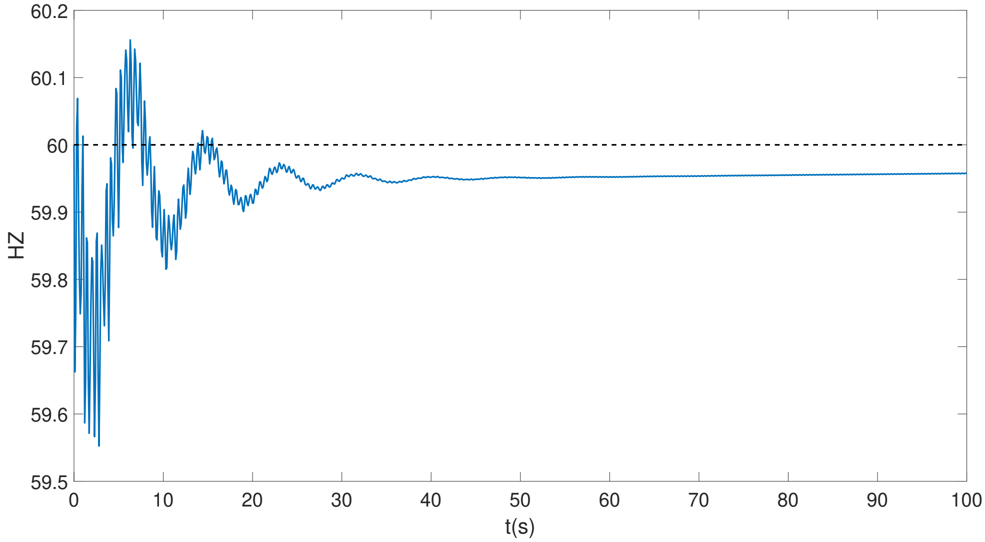

Figure 7.9: Frequency, droop constants x5

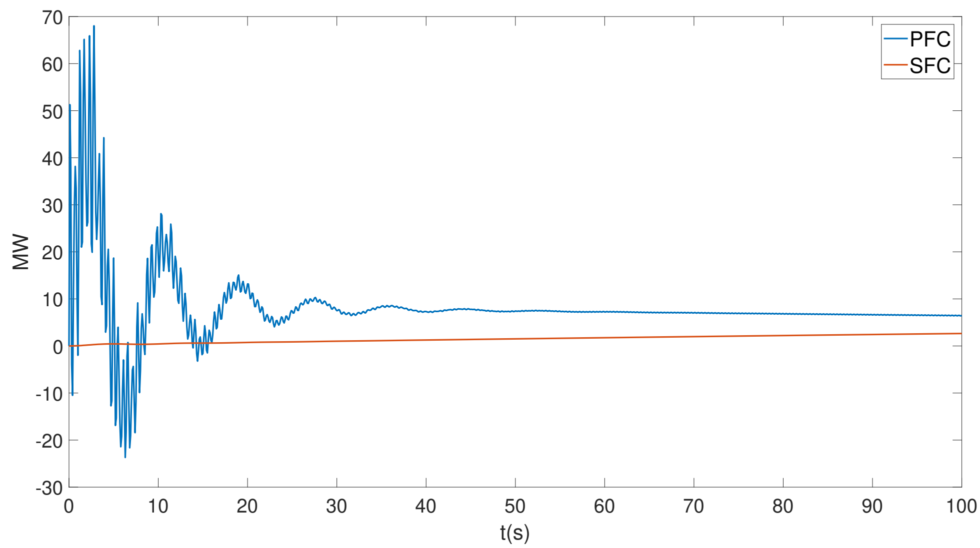

Figure 7.10: Control signals, normal droop x5

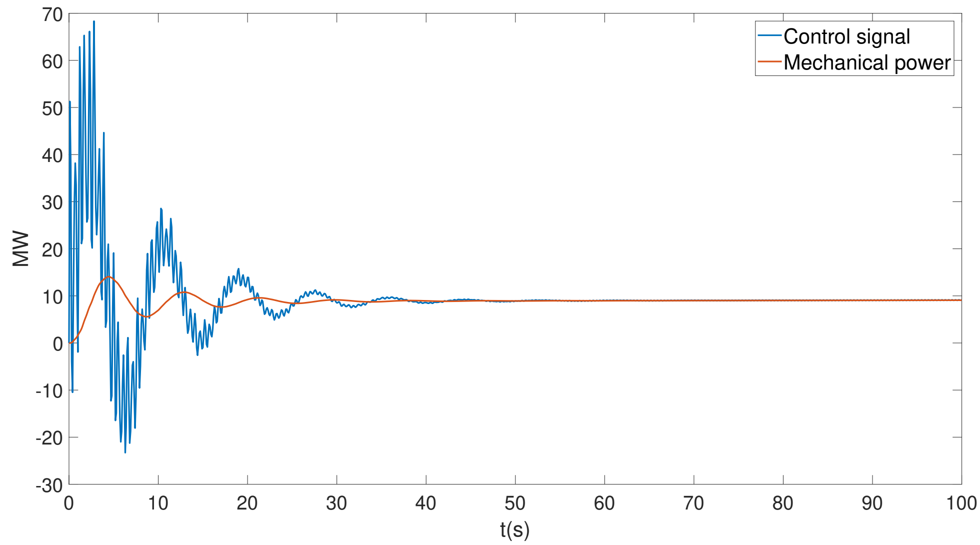

Figure 7.11: Control signal and mechanical power output, droop constants x5

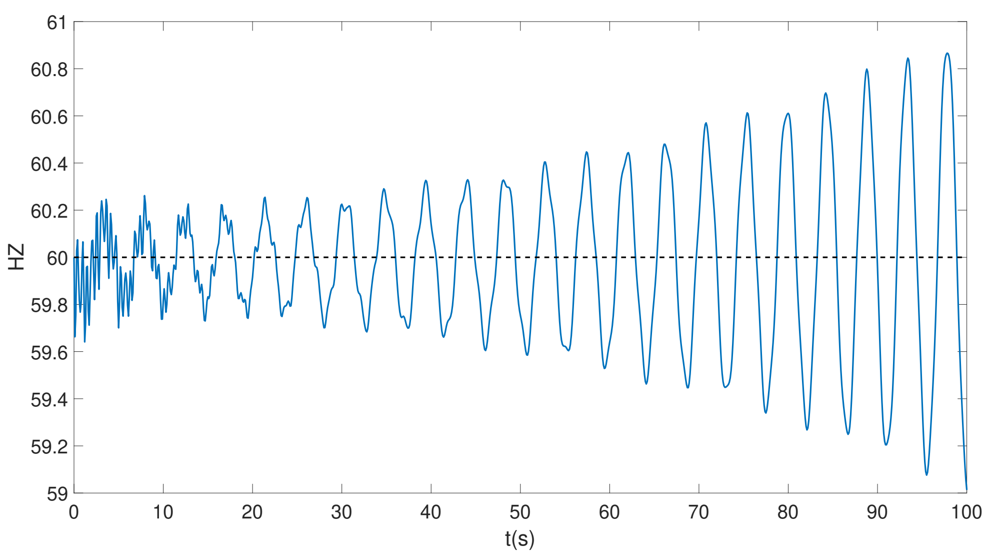

Figure 7.12: Frequency, droop constants x20

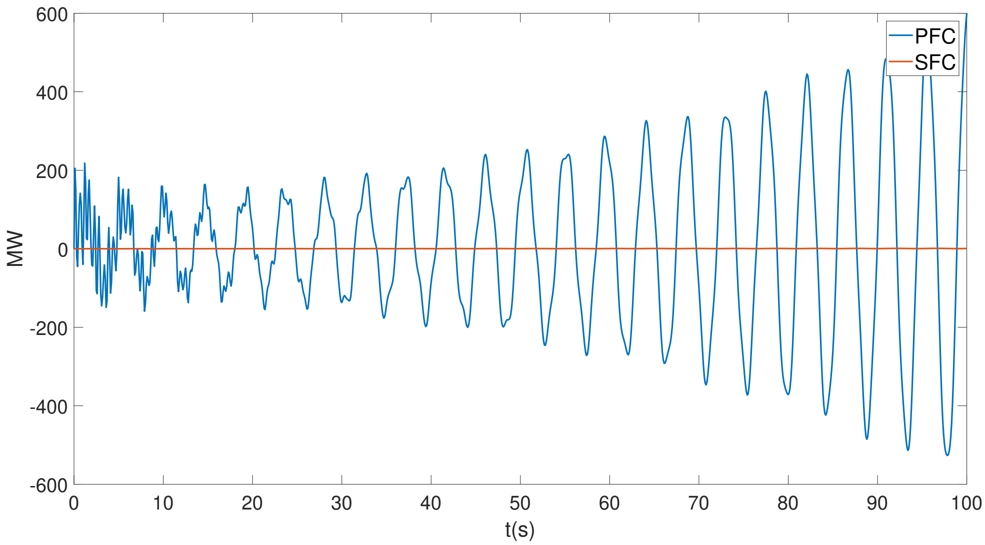

Figure 7.13: Control signals, normal droop x20

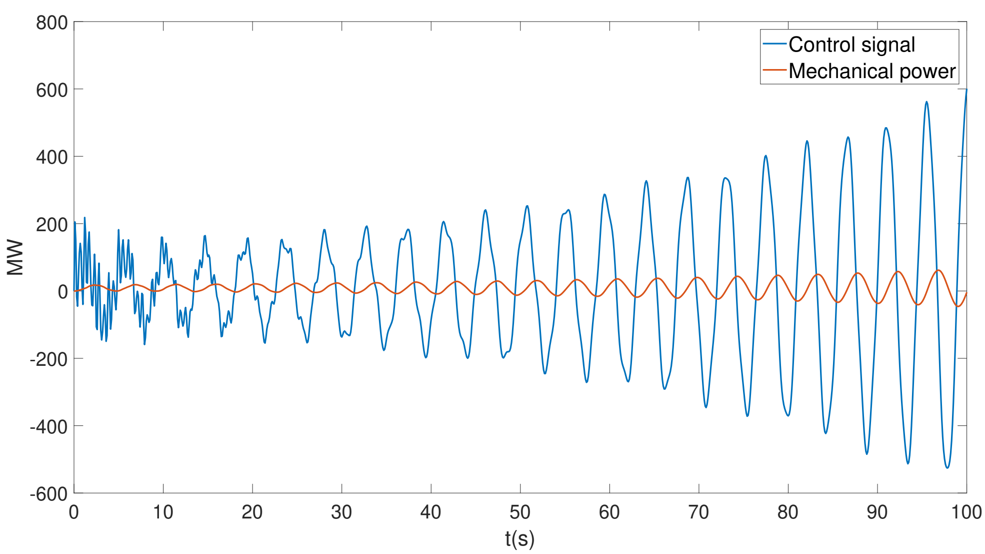

Figure 7.14: Control signal and mechanical power, normal droop x20

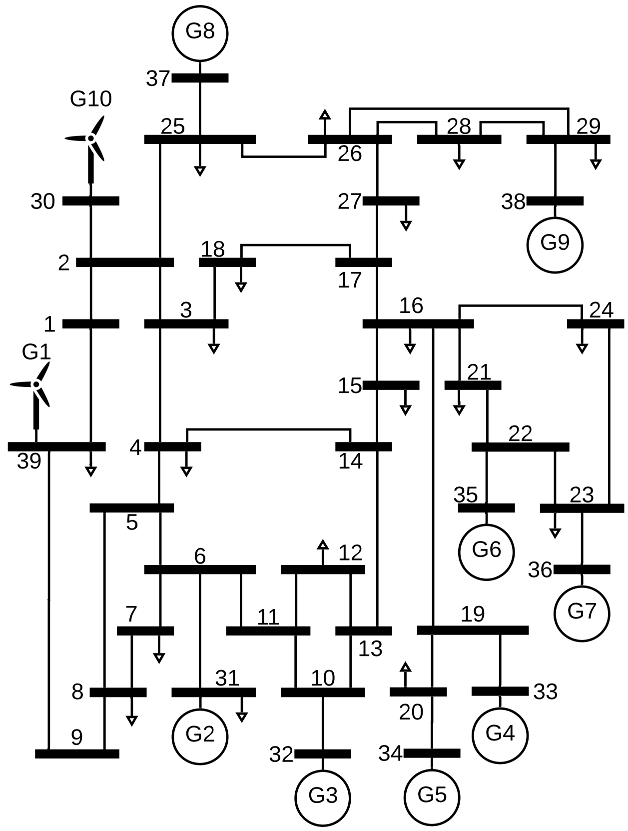

Figure 7.15: New England system with two wind farms.

Example 7.2 (Low-inertia system)**.** In section 6.3 it was mentioned that one of the issues of renewable generation is low inertia. Let us consider New England network from the example 7.1. However, now two generators G1 and G10 are replaced with wind farms of the same capacity. Inertia of both generators is reduced 10 times to represent dynamics of the wind generators. Thus, after the same loss of 100 MW on G10 frequency oscillates at greater rate as it is shown in the Figure 7.16.

7.5 Tertiary control. Optimal power flow and security constrained optimal power flow.

While primary and secondary frequency controls are used to regulate dynamic processes in power systems, tertiary frequency control is used periodically to adjust generation according to the prices given by the power market, and performs congestion management. In order

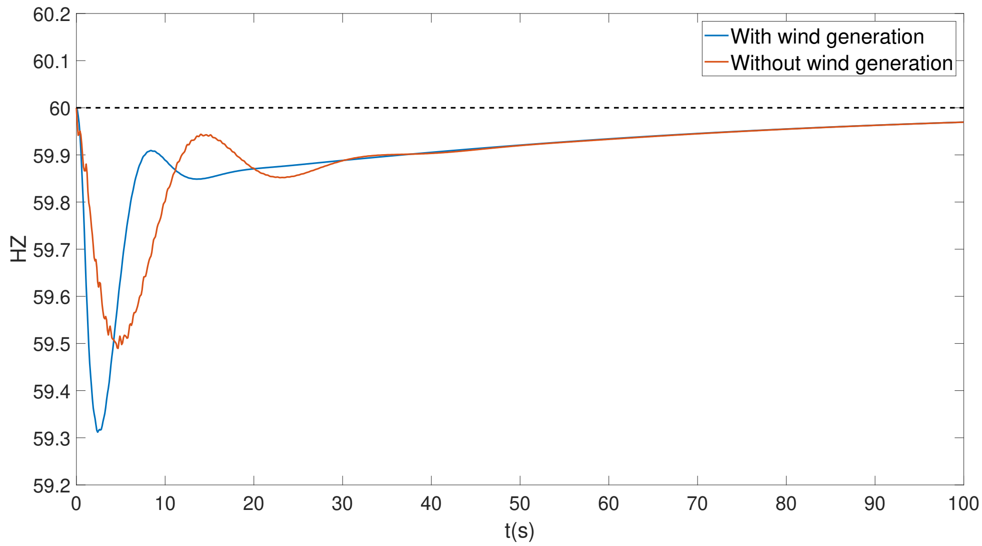

Figure 7.16: Frequency for systems with and without renewable generation.

to do so optimal power flow problem (OPF) is solved for the desired time interval (15-120 minutes). Additionally, it is run again after any failure in order to readjust power generation.

Optimal power flow problem is an optimization, usually non-convex problem. Non-convexity appears due to the formulas that define active and reactive power flows as well as due to the cost function in some cases. Nevertheless, for some systems direct current OPF (DC OPF) is solved. In this case reactive power flows are ignored and voltage magnitudes $|V|$ and electromagnetic force $|\mathcal{E}|$ are considered to be constant. Let the power system be defined by the oriented graph (N, E), where N is the set of buses, $|N| = n$, E is the set of lines, $|E| = q$. Formulation of DC OPF is a simplified version of the formulation in [91]:

$$\min_{\substack{(u_i,\theta_i,p_{ij}:\\ i\in N, ij\in E)}} \quad c(u_1, \ldots, u_n), \tag{7.5a}$$

$$0 = \sum_{j:ji\in E} p_{ji} - \sum_{j:ij\in E} p_{ij} + u_i + z_i, \; i \in N, \tag{7.5b}$$

$$p_{ij} = b_{ij} \sin(\theta_i - \theta_j), \; ij \in E, \tag{7.5c}$$

$$\underline{u}_i \leq u_i \leq \overline{u}_i, \; i \in N, \tag{7.5d}$$

$$\underline{p}_{ij} \leq p_{ij} \leq \overline{p}_{ij}, \; ij \in E. \tag{7.5e}$$

Here variables of the system are

- $u_i,\ i \in \{1, \ldots, n\}$ — active power, generated on the bus i;
- $p_{ij},\ ij \in E$ — power flow on the line ij.

System's parameters are:

- $z_i,\ i \in \{1, \ldots, n\}$ — consumption on the bus i;
- $b_{ij},\ ij \in E$ — line parameter calculated according to the formula $b_{ij} = \frac{|V_i||V_j|}{X_{ij}}$, where $|V_i|$ and $|V_j|$ are fixed voltage magnitudes of buses i and j respectively, X_{ij} — line reactance;
- $\overline{u}_i,\ \underline{u}_i,\ i \in \{1, \ldots, n\}$ — upper and lower generation limits on the bus i;
- $\overline{p}_{ij},\ \underline{p}_{ij},\ ij \in E$ — upper and lower power flow limits on the line ij.

Function $c(\cdot)$ is some generation cost function, defined by the rules of power market. Consumptions r_i are predicted based on the previously gathered statistics.

Solving (7.5) allows us to minimize generation and perform congestion management. However, in practice a modification of this problem, called security constrained optimal power flow (SCOPF) is solved. It is needed to ensure system's compliance with all line limits in case of a line or a bus failure, when statistics based prediction is incorrect. It is said that the system satisfies (N-x) criteria, if it can remain its efficiency after x of its elements (lines or buses) fail. The DC SCOPF solved during the tertiary control has the following form. Let $\alpha_i \in \{0, 1\},\ i \in \{1, \ldots, n\}$ and $\beta_{ij} \in \{0, 1\},\ ij \in E$ be indicators of working capacity of buses and lines respectively. If $\alpha_i = 1$ then bus i works, if $\alpha_i = 0$ then bus i does not work, and the same notations applied to lines' indicators. Then, for (N-x) criteria the following inequality holds:

$$1 \leq \sum_{i=1}^{n} \alpha_i + \sum_{ij \in E} \beta_{ij} \leq N - x. \tag{7.6}$$

Let X^α be combinations of all possible combinations of α_i (for each α_i there exists set of β_{ij} such that inequality (7.6) holds). Then, its cardinality is equal to

$$|X^\alpha| = \sum_{j=0}^{x} \frac{n!}{(n-j)!j!}. \tag{7.7}$$

Let all sets from X^α be enumerated: $(\alpha_1^k, \ldots, \alpha_n^k),\ k \in \{1, \ldots, |X^\alpha|\}$. Then, for each number k it is possible to introduce set $X^\beta(k)$ that consists of all possible combinations of β_{ij} such that inequality (7.6) holds. Here

$$|X^\beta(k)| = \sum_{j=0}^{x-\alpha_0^k} \frac{q!}{(q-j)!j!}, \tag{7.8}$$

where $\alpha_0^k = \sum_{i=1}^n \alpha_i^k$. As before it is possible to enumerate all elements of $X^\beta(k)$: $(\beta_{ij}^l, ij \in E)$, $l \in \{1, \ldots, |X^\beta(k)|\}$. Then, one formulation of the SCOPF with (N-x) criteria is a simplified version of the formulation in [91]:

$$\min_{\substack{(u_i,\theta_i,\Delta p_i^k,\theta_i^{kl},p_{ij},p_{ij}^{kl}:\\ i\in N, ij\in E,\\ k\in\{1,\ldots,|X^\alpha|\}, l\in\{1,\ldots,|X^\beta(k)|\})}} \quad c(u_1, \ldots, u_n), \tag{7.9a}$$

$$0 = \sum_{j:ji\in E} p_{ji} - \sum_{j:ij\in E} p_{ij} + u_i + z_i,\ i \in N, \tag{7.9b}$$

$$p_{ij} = b_{ij}\sin(\theta_i - \theta_j),\ ij \in E, \tag{7.9c}$$

$$\underline{u}_i \le u_i \le \overline{u}_i,\ i \in N, \tag{7.9d}$$

$$\underline{p}_{ij} \le p_{ij} \le \overline{p}_{ij},\ ij \in E, \tag{7.9e}$$

$$0 = \sum_{j:ji\in E} p_{ji}^{kl} - \sum_{j:ij\in E} p_{ij}^{kl} + \alpha_i^k(u_i + z_i + \Delta p_i^k),\ i \in N,\ k \in \{1, \ldots, |X^\alpha|\},\ l \in \{1, \ldots, |X^\beta(k)|\}, \tag{7.9f}$$

$$p_{ij}^{kl} = \beta_{ij}^{kl} b_{ij}\sin(\theta_i^{kl} - \theta_j^{kl}),\ ij \in E,\ k \in \{1, \ldots, |X^\alpha|\},\ l \in \{1, \ldots, |X^\beta(k)|\}, \tag{7.9g}$$

$$\underline{u}_i \le u_i + \Delta p_i^k \le \overline{u}_i,\ i \in N,\ k \in \{1, \ldots, |X^\alpha|\},\ l \in \{1, \ldots, |X^\beta(k)|\}, \tag{7.9h}$$

$$\underline{p}_{ij} \le p_{ij}^{kl} \le \overline{p}_{ij},\ ij \in E,\ k \in \{1, \ldots, |X^\alpha|\},\ l \in \{1, \ldots, |X^\beta(k)|\}. \tag{7.9i}$$

Here similarly to (7.5) generation cost function is minimized for power system with all its elements working. However, additional constraints are introduced that correspond to failure of 1 to x elements of the system. The system responds according to the rules of primary and secondary frequency controls; therefore, generation in (7.9f) is adjusted by Δp^k for each type of bus failure. It can be seen, that this adjustments do not depend on the type of line failure $l(k)$. It is done due to the fact, that primary and secondary frequency controls do not take into consideration line limits. Let us consider the case, when for some k all $\alpha_i^k = 1$ and some $\beta_i^k = 0$. For such type of failure control action $y^k = 0$, since frequency control takes into consideration only disturbances in power balance. Moreover, since frequency control is blind to line constraints it can increase power flow on the congested lines. Therefore, tertiary control has to preventivelly adjust generation so neither any failure or control action would not violate line limits. Hence SCOPF (7.9) is called SCOPF with preventive (N-x) criteria. Such preventive approach results in the underloading of the majority of lines as well as cheap generators consequently in increase of generation cost.

If primary and secondary controls would have more complicated structure that would recognize and correct line flows violations than optimization problem (7.9) can be relaxed into the following problem, called SCOPF with corrective (N-x) criteria:

$$\min_{\substack{(u_i,\theta_i,\Delta p_i^{kl},\theta_i^{kl},p_{ij},p_{ij}^{kl}:\\ i\in N, ij\in E,\\ k\in\{1,\ldots,|X^\alpha|\}, l\in\{1,\ldots,|X^\beta(k)|\})}} \quad c(u_1,\ldots,u_n), \tag{7.10a}$$

$$0 = \sum_{j:ji\in E} p_{ji} - \sum_{j:ij\in E} p_{ij} + u_i + z_i,\ i\in\{1,\ldots,n\}, \tag{7.10b}$$

$$p_{ij} = b_{ij}\sin(\theta_i - \theta_j),\ ij\in E, \tag{7.10c}$$

$$\underline{u}_i \le u_i \le \overline{u}_i,\ i\in\{1,\ldots,n\}, \tag{7.10d}$$

$$\underline{p}_{ij} \le p_{ij} \le \overline{p}_{ij},\ ij\in E, \tag{7.10e}$$

$$0 = \sum_{j:ji\in E} p_{ji}^{kl} - \sum_{j:ij\in E} p_{ij}^{kl} + \alpha_i^k(u_i + z_i + \Delta p_i^{kl}),\ i\in N,\ k\in\{1,\ldots,|X^\alpha|\},\ l\in\{1,\ldots,|X^\beta(k)|\}, \tag{7.10f}$$

$$p_{ij}^{kl} = \beta_{ij}^{kl} b_{ij}\sin(\theta_i^{kl} - \theta_j^{kl}),\ ij\in E,\ k\in\{1,\ldots,|X^\alpha|\},\ l\in\{1,\ldots,|X^\beta(k)|\}, \tag{7.10g}$$

$$\underline{u}_i \le u_i + \Delta p_i^{kl} \le \overline{u}_i,\ i\in N,\ k\in\{1,\ldots,|X^\alpha|\},\ l\in\{1,\ldots,|X^\beta(k)|\}, \tag{7.10h}$$

$$\underline{p}_{ij} \le p_{ij}^{kl} \le \overline{p}_{ij},\ ij\in E,\ k\in\{1,\ldots,|X^\alpha|\},\ l\in\{1,\ldots,|X^\beta(k)|\}. \tag{7.10i}$$

Here control adjustments Δp^{kl} depend on both type of bus failure and type of line failure. It is possible to switch from corrective constraints in (7.10) to preventive by adding additional constraint $p^{k,l_1} = p^{k,l_2}$ for all $k\in\{1,\ldots,|X^\alpha|\}$, $l_1,l_2\in\{1,\ldots,|X|^\beta(k)\}$. Therefore, SCOPF with corrective constraints always has value of objective function better or equal to the one of SCOPF with preventive constraints. in majority of the systems x is set to 1, since is highly unlikely that more than one failure would happened in between to tertiary control operation.

7.6 Reasoning behind new control scheme

The frequency control scheme described above is used in every power systems possibly with some modifications. Nevertheless, there exists a number of reasons for developing a new one. The following issues compose a basis for update and modification of the used control algorithms.

1. Usage of renewable energy sources. As it was shown in section 6.1, generator units that work from the renewable sources have low inertia. In traditional power systems rapid frequency drop as a consequence of a disturbance is not possible. Traditional generators have high inertia; thus, loss of kinetic energy does not change their speed rapidly. Usage of renewable sources reduces overall inertia of the system. As a result, frequency responds abruptly even to small disturbances. The existing control scheme cannot respond to such quick changes in frequency and consequently cannot provide sufficient reliability level for the systems with high penetration of renewables.

2. Usage of controllable loads can improve frequency dynamics. Short-term shut down (or reduction of power consumption) of some loads can provide necessary balancing action after a disturbance of significant size. Generator-side control is implemented via position changes of governing valves of turbines. However, valves are set in motion by hydraulics or servomotors, which requires some time. Moreover, after governor valves change their position, change of the turbines' mechanical power output takes some time (usually 5-20 seconds) due to dynamics of energy carrier. As a result, during first seconds after disturbance generators do not change their output and frequency dynamics depends only on the change of kinetic energy of the systems' synchronous machines. Thus, load-side control can help rebuffing frequency drop at the very beginning. Additionally, short-term shut down of some loads such as air conditioning units causes little or no complications on the consumer side.

3. AGC requires centralized operation within each area or entire system. Synchronized information collection followed by control signal broadcast imposes limit on the control signals update frequency. In practice equations (7.4) are discretized with discretization

time. If control will be performed in the distributed way, so only neighbours can communicate trough point to point connections, the discretization can be reduced to tens of milliseconds, which may improve control performance. Additionally, even after aggregation, number of load buses is several times bigger, than number of generator buses. Load-side control organized in the centralized way would require complicated communication system that would support control with synchronized communication, which makes centralized generator and load control difficult to implement.

4. Congestion management is performed as a part of tertiary control, which is done once per 15-120 minutes. Corrective control is used only after a failure occurs. As a result, (N-x) criteria is implemented to ensure system's stability. It is necessary, since real-time congestion management is not a part of traditional control scheme. If $x+1$ of the system will fail, line limits violations, caused by this failure will not be cleared until the next tertiary control. Real-time congestion management would allow to switch from preventive (N-x) criteria to corrective one reducing generation cost.

The issues above are considered in a large variety of works considered in section 2. The novelty of the presented work is in the usage of high order turbine governor model that ensures realistic modeling of the power system dynamics, hence provides possibility of control implementation.

8 Preliminaries of stability theory

Here the known results from stability theory, needed further in the work, are presented. Let us introduce the autonomous system of differential equations

$$\dot{x} = f(x),\ x(0) = x^0, \tag{8.1}$$

where $f : \mathbb{R}^n \to \mathbb{R}^n$, f is continuous and Lipschitz on R^n. Its solution is denoted by $x(t, x^0) = x(t)$.

Definition 8.1. Solution $x(t, 0) \equiv 0$ of the system (8.1) is called globally asymptotically stable if for any $x^0 \in \mathbb{R}^n$ $\lim_{t\to\infty} x(t, x^0) = 0$.

Definition 8.2. Function $W : \mathbb{R}^n \to \mathbb{R}$ is called positive (negative) definite if $W(x) > 0$ ($W(x) < 0$) for all $x \in \mathbb{R}^n \setminus \{0\}$ and $W(0) = 0$.

Theorem 8.1 (Lyapunov asymptotic stability theorem [92]). *Assume there exists a continuously differentiable function $V : \mathbb{R}^n \to \mathbb{R}$ such that $V(x) = V(x(t))$ has the following properties: $V(x)$ is positive definite and $\dot{V}(x) = V'(x(t))f(x(t))$ is negative definite. Then, solution $x(t, 0) \equiv 0$ is globally asymptotically stable.*

Function V in the theorem 8.1 is called Lyapunov function.

Definition 8.3. A set $\mathcal{M} \subseteq \mathbb{R}^n$ is an invariant set with respect to the system (8.1) if

$$\mathcal{M} = \{x(t, x^0) \mid t \geq 0, x^0 \in \mathcal{M}\}. \tag{8.2}$$

Theorem 8.2 (Barbashin-Krasovskii-LaSalle theorem [93], [94]). *Assume there exists a continuously differentiable Lyapunov function $V : \mathbb{R}^n \to \mathbb{R}$ such that $V(x) = V(x(t))$ has the following properties: $V(x)$ is positive definite and $\dot{V}(x) = V'(x(t))f(x(t)) \leq 0$ for any $x(t) \in \mathbb{R}^n$. Let $\ker \dot{V}(x) = \{x(t) \in \mathbb{R}^n : \dot{V}(x(t)) = 0\}$ and let $\mathcal{M}$ be the largest invariant set contained in $\ker \dot{V}(x)$. Then, any solution $x(t, x^0)$ converges to a trajectory from $\mathcal{M}$.*

Definition 8.4. Function $V : \mathbb{R}^n \to \mathbb{R}$ with argument x is called positive (negative) definite over subvector x_I, $I \subseteq \{1, \ldots, n\}$ if there exists such positive (negative) definite function $W : \mathbb{R}^{|I|} \to \mathbb{R}$ that $V(x) \geq W(x_I)$.

Definition 8.5. Solution $x(t, 0) \equiv 0$ of the system (8.1) is called globally asymptotically over subvector x_I, $I \subseteq \{1, \ldots, n\}$ if for any x^0 $\lim_{t\to\infty} x_i(t, x^0) = 0$, $i \in I$.

Theorem 8.3 (Rumyantsev partial stability theorem [95])**.** *Assume there exists a continuously differentiable Lyapunov function $V : \mathbb{R}^n \to \mathbb{R}$ such that $V(x) = V(x(t))$ has the following properties: $V(x)$ is positive definite and $\dot{V}(x) = V'(x(t))f(x(t))$ is negative definite over subvector x_I, $I \subseteq \{1, \ldots, n\}$. Then, solution $x(t, 0) \equiv 0$ is asymptotically stable over subvector x_I.*

9 Power system model

Here we model power system network. If we choose model to be too detailed it might be not possible to derive any analytical results. If the chosen model is overly simplified, it might not correctly describe the dynamics of the network. Therefore, for the analytical results we use simpliest model that provides accurate simulation of the system dynamics with primary frequency control (proportional controller).

Per unit system is used. This allows us to exclude transformers from the model and also assume that network electrical frequency is equal to the rotational speed of the generators. Additional assumptions are taken in accordance with [85] and [90]. Namely, as it was shown in section 6.4, reactive powers and voltages have little effect on frequency. Therefore, voltage magnitudes are assumed to be constant and equal 1 p.u. and reactive power is not considered. Second order generator model is used as sufficient for the analysis of frequency, which dynamics is within a timeframe of seconds.

We use different system models for the theoretical results and numerical simulations in section 14 in order to ensure applicability of the derived control in practice. Namely, model used for theoretical results has linear DC linear power flows and second order turbine and governor dynamics, while model used in numerical experiments has nonlinear DC power flows and more realistic turbine and governor model for steam and hydro turbines.

Control is denoted by a continuous vector function $u \in C(\mathbb{R}^n)$. In generator units (section 6.2) control signals are sent to the regulation valves servomotors, which act as low pass filters. Therefore, in practice control can be discontinuous. Such property must be utilized if optimal control approach is utilized to find control functions. However, we will derive control by a transition from the optimization problem on the set of the stationary points to integral algebraic system of equations. Therefore, we do not use discontinuities and, consequently, assume the control to be continuous in order to analyse system stability.

In further section we will explicitly define control inputs and information availability. We do not consider issues of the communication delays and discretization.

9.1 Model for derivation of theoretical results

General form of the model for theoretical results is given in the Figure 9.1. Classical generator model is used [85]:

$$m\dot{\omega} = -d\omega - p^e + p^m + r, \tag{9.1}$$

$$\dot{\theta} = \omega. \tag{9.2}$$

Here variables have the following meanings:

- θ is phase angle;
- ω is deviation of frequency from the nominal angle;
- p^e is electrical power;
- p^m is mechanical power, injected by the turbine.

Here and further only deviations of frequency will be used. Frequency value itself will not be present. Therefore, frequency deviations are denoted by ω instead of $\Delta\omega$. As a part of the assumption, reactive power does not affect the considered problem; therefore, everywhere further electrical power p^e corresponds to active power.

Generator's parameters have the following values:

- m is generator and turbine inertia;
- d is generator damping;
- r is unknown sum of load and change in generation due to failure. This parameter is further referred as disturbance.

Here inertia constants of turbine and generator are summed into one, product $-d\omega$ approximates combination of fast electromagnetic processes.

$$t^m\dot{p}^m = -p^m + v, \tag{9.3}$$

$$t^v\dot{v} = -v + u. \tag{9.4}$$

Here variables have the following meanings:

- u is control signal,

$$u \in [\underline{u}, \overline{u}]; \tag{9.5}$$

- v is governor valve position.

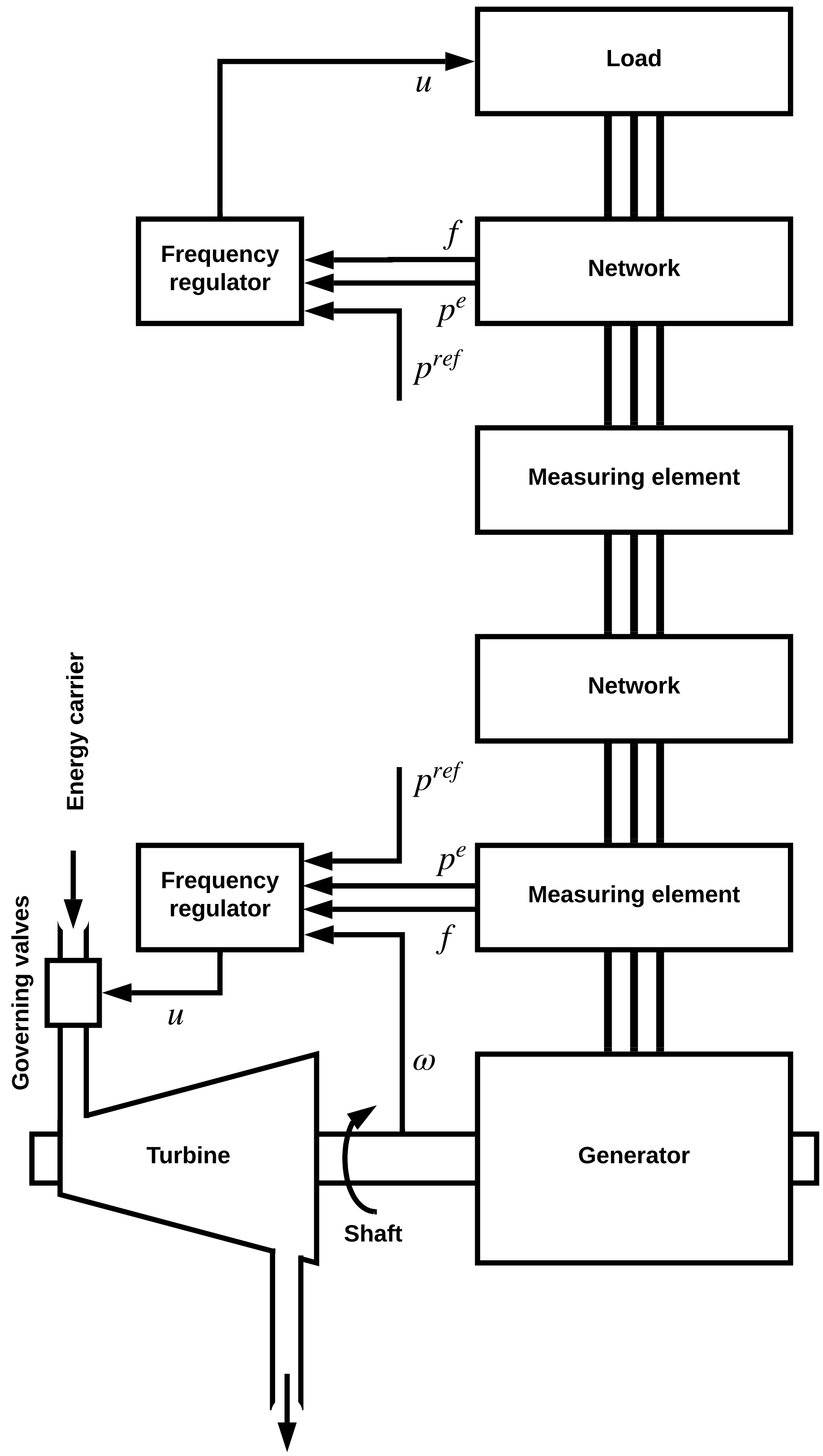

Figure 9.1: Power network structure.

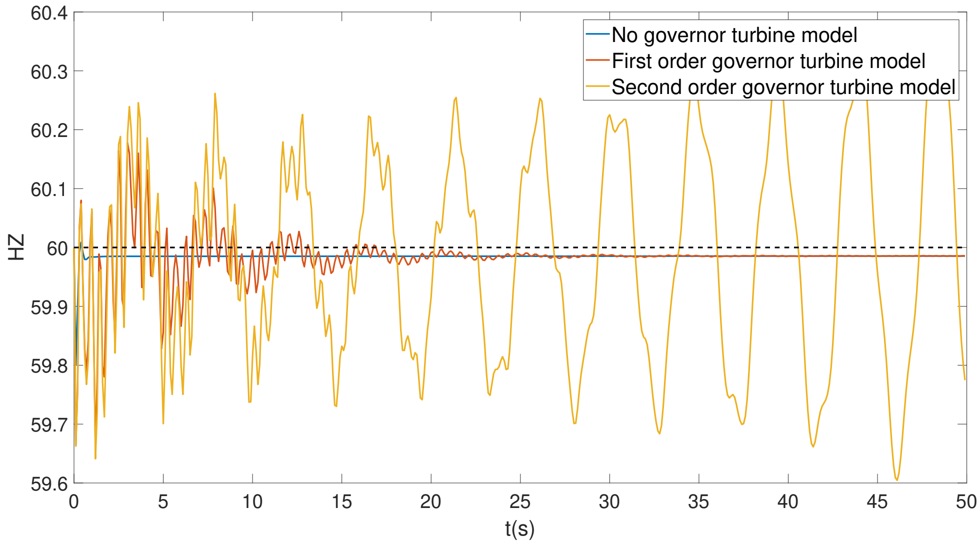

Figure 9.2: Governor turbine model.

Equation (9.3) describes lag of governor valves. Equation (9.4) describes turbine dynamics. Parameters have the following meanings [90], [96]:

- t^v is time constant characterizing response of governor valve to the control signal;
- t^m is time constant characterizing energy carrier dynamics in turbine.

Choice of the second order turbine governor model is necessary for accurate representation of system's response to control signals. Let us consider case, when droop control constants K^I are increased 30 times above standard values. For simplicity, it is assumed, that the system has no secondary frequency control. As it was shown in section 7.4 system should become unstable. Then, results of numerical experiments for the models with no turbine governor dynamics model ($p^m \equiv u$) and with turbine governor model of the first ($v \equiv u$) and second order are considered Figure 9.2. It can be seen, that in the first case system remains stable, and thus, such model is insufficient for accurate representation of frequency dynamics. In the second case the system suffers from significant frequency oscillation; however, is still stable. On the contrary second order governor turbine model is sufficient to represent correct behavior of the system.

Balance equations for load buses with synchronous machines are similar to the equations of the classical generator model [90]:

$$m\dot{\omega} = -d\omega - p^e + u + r, \tag{9.6}$$

$$\dot{\theta} = \omega. \tag{9.7}$$

As presence of synchronous machines is not guaranteed on every bus, balance equations for load buses without synchronous machines are also introduced [90]:

$$0 = -d\omega - p^e + u + r, \tag{9.8}$$

$$\dot{\theta} = \omega. \tag{9.9}$$

Difference between 9.8 and 9.6 appears due to the lack of synchronous machines' inertia in the latter case. Parameter d in equations for load buses is a sum of two components: damping of synchronous machines (if present) and response of frequency dependent loads.

Load side control can be implemented via switching on and off electrical appliances. Such process has discrete structure. For simplicity, it is assumed that due to aggregation of the loads in each bus discretization step is small, so load side control can be considered continuous. Since switching on and off is almost instant process, control u is added directly to the power balance equations 9.8 and 9.6.

It is assumed that some loads may be located on the same bus as generator. Then, bus is still considered a generator bus and equations (9.1), (9.2), (9.3), (9.4) remain unchanged. However, in this case m is a sum of inertia's of all synchronous machines, and d is a sum of damping of synchronous machines (if present) and response of frequency dependent loads.

Lines power flows are modeled by DC flows. All voltage magnitudes in per unit system are considered to be equal 1. As a result, power flow equation for a line connecting to buses with phase angles θ_1 and θ_2 is a simplification of equation (6.2a):

$$p = b\sin(\theta_1 - \theta_2), \tag{9.10}$$

where $b = \frac{|V_1||V_2|}{X} = \frac{1}{X}$. Then, sin function is linearized in the origin:

$$p = b(\theta_1 - \theta_2). \tag{9.11}$$

Power system is defined by an oriented connected graph $\Gamma = (N, E)$, where N is set of buses, $|N| = n$. It is assumed that a bus is defined by its index. Set of generator buses is denoted by G, $|G| = g$. Without loss of generality it is assumed, that generator buses are the first g buses of the system: $G = \{1, \dots, g\} \neq \emptyset$. The other buses are load buses. Their set is denoted by $L = \{g+1, \dots g+l\}$. Load buses are divided into buses with non-zero and zero inertia: $L = L_1 \cup L_0$, $L_1 = \{g+1, \ \dots, g+l_1\}$, $L_0 = \{g+l_1+1, \dots, g+l_1+l_0\}$.

Set E is set of lines ($|E| = q$). It is assumed that lines in E are sorted in lexicographic order, thus, each line ij is indexed by unique $k \in \{1, \dots, q\}$. Further, variables and parameters associated with lines will be used with both types of indices ij and k (for example, line flow can be denoted by p_{ij} and p_k).

System's dynamics is described by the following system of differential algebraic equations:

$$\dot{\theta}_i = \omega_i, \ i \in N, \tag{9.12a}$$

$$m_i \dot{\omega}_i = -d_i \omega_i - p_i^e + p_i^m + r_i, \ i \in G, \tag{9.12b}$$

$$t^m \dot{p}_i^m = -p_i^m + v_i, \ i \in G, \tag{9.12c}$$

$$t^v \dot{v}_i = -v_i + u_i, \ i \in G, \tag{9.12d}$$

$$m_i \dot{\omega}_i = -d_i \omega_i - p_i^e + u_i + r_i, \ i \in L_1, \tag{9.12e}$$

$$0 = -d_i \omega_i - p_i^e + u_i + r_i, \ i \in L_0, \tag{9.12f}$$

$$p_{ij} = b_{ij}(\theta_i - \theta_j), \ ij \in E, \tag{9.12g}$$

$$p_i^e = \sum_{j:(i,j) \in E} p_{ij} - \sum_{j:(j,i) \in E} p_{ji}. \ i \in N. \tag{9.12h}$$

This system is derived from the equations (9.1)-(9.11). Here

- θ_i, $i \in N$ is phase angle on the bus i;
- ω_i, $i \in N$ is frequency deviation from the nominal value on the bus i;
- p_i^e, $i \in N$ is electrical power generated on the bus i;
- p_{ij}, $ij \in E$ is power flow on the line connecting buses i and j. If $p_{ij} > 0$, than power flow is directed from bus i to j, if $p_{ij} < 0$, then it is direct from j to i. This variables can be used with a single index corresponding to the line ij: p_k;
- p_i^m, $i \in G$ is mechanical power, injected by the turbine on the bus i;
- v_i, $i \in G$ is governor valve position on the bus i.

System's parameters

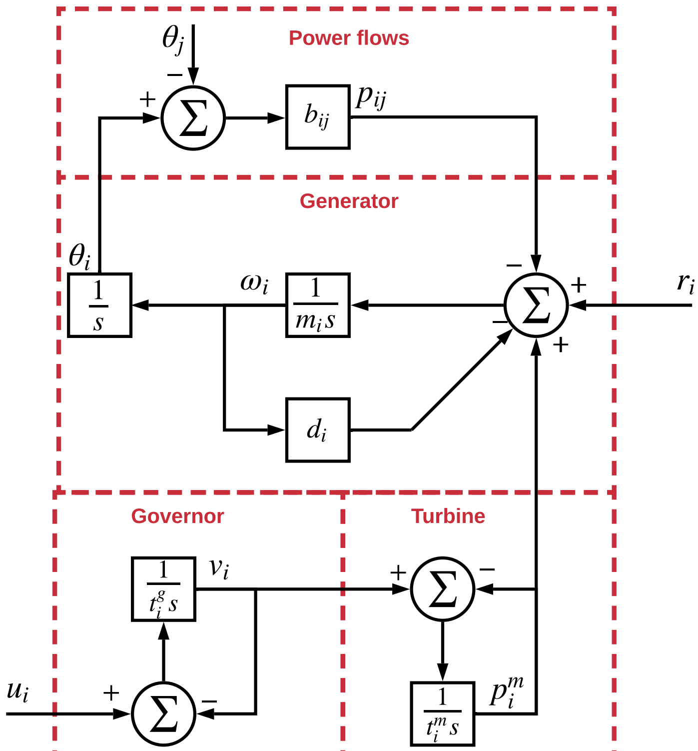

Figure 9.3: Generating unit block-diagram

- $m_i,\ i \in G \cup L_1$ is inertia of synchronous machines on the bus i;
- $d_i,\ i \in N$ is sum of damping of synchronous machines (if present) and response of frequency dependent loads on the bus i;
- $r_i,\ i \in N$ is sum of load and unknown disturbance on the bus i;
- $b_{ij},\ ij \in E$ is line parameter reciprocal to reactance. This parameter can be used with a single index corresponding to line ij: b_k;
- $t_i^v,\ i \in G$ is time constants characterizing response of governor valve to the control signal on the bus i;
- $t_i^m,\ i \in G$ is time constants characterizing energy carrier dynamics in turbine on the bus i.

Control signals: $u_i,\ i \in N$.

Further, matrix representation of the system (9.12) will be used:

$$\dot{\theta} =\omega, \tag{9.13a}$$

$$M_{G,G}\dot{\omega}_G =- D_{G,G}\omega_G - p^e_G + p^m + r_G, \tag{9.13b}$$

$$T^m\dot{p}^m =- p^m + v, \tag{9.13c}$$

$$T^v\dot{v} =- v + u_G, \tag{9.13d}$$

$$M_{L_1,L_1}\dot{\omega}_{L_1} =- D_{L_1,L_1}\omega_{L_1} - p^e_{L_1} + u_{L_1} + r_{L_1}, \tag{9.13e}$$

$$0 =- D_{L_0,L_0}\omega_{L_0} - p^e_{L_0} + u_{L_0} + r_{L_0}, \tag{9.13f}$$

$$0 =BC^T\theta - p, \tag{9.13g}$$

$$0 =Cp - p^e. \tag{9.13h}$$

Here vector representation of the variables is used: $\theta = (\theta_1, \dots \theta_n)^T$, $\omega = (\omega_1, \dots, \omega_n)^T$, $p = (p_1, \dots, p_q)^T$, $p^m = (p^m_1, \dots, p^m_g)^T$, $v = (v_1, \dots, v_g)^T$, $u = (u_1, \dots, u_n)^T$ as well as matrix representation of parameters: $M = \operatorname{diag}(m_1, \dots, m_{g+l_1})$, $D = \operatorname{diag}(d_i, \dots, d_n)$, $r = (r_1, \dots, r_n)$, $B = \operatorname{diag}(b_1, \dots, b_q)$, $T^m = \operatorname{diag}(t^m_1, \dots, t^m_g)$, $T^v = \operatorname{diag}(t^v_1, \dots, t^v_g)$. Matrix C is incidence matrix of Γ.

In matrix form we can separate differential and algebraic equations as follows:

$$\dot{x}^1 =A^{11}x^1 + A^{12}x^2 + Z^1u + r^1, \tag{9.14a}$$

$$0 =A^{21}x^1 + A^{22}x^2 + Z^2u + r^2, \tag{9.14b}$$

where

$$A^{11} = \begin{pmatrix} 0 & (I^n_G)^\top & 0 & 0 & (I^n_{L_1})^\top \\ 0 & -M^{-1}_{G,G}D_{G,G} & M^{-1}_{G,G} & 0 & 0 \\ 0 & 0 & -(T^m)^{-1} & (T^m)^{-1} & 0 \\ 0 & 0 & 0 & -(T^v)^{-1} & 0 \\ 0 & 0 & 0 & 0 & -M^{-1}_{L_1,L_1}D_{L_1,L_1} \end{pmatrix}, \; A^{12} = \begin{pmatrix} (I^n_{L_0})^\top & 0 & 0 \\ 0 & -M^{-1}_{G,G}I^n_G & 0 \\ 0 & 0 & 0 \\ 0 & 0 & 0 \\ 0 & -M^{-1}_{L_1,L_1}I^n_{L_1} & 0 \end{pmatrix},$$

$$Z^1 = \begin{pmatrix} 0 \\ 0 \\ 0 \\ (T^v)^{-1}I^n_G \\ M^{-1}_{L_1,L_1}I^n_{L_1} \end{pmatrix}, \; x^1 = \begin{pmatrix} \theta \\ \omega_G \\ p^m \\ v \\ \omega_{L_1} \end{pmatrix}, \; r^1 = \begin{pmatrix} 0 \\ M^{-1}_{G,G}r_G \\ 0 \\ 0 \\ M^{-1}_{L_1,L_1}r_{L_1} \end{pmatrix},$$

$$A^{21} = \begin{pmatrix} 0 & 0 & 0 & 0 & 0 \\ 0 & 0 & 0 & 0 & 0 \\ -BC^\top & 0 & 0 & 0 & 0 \end{pmatrix}, \; A^{22} = \begin{pmatrix} -D_{L_0,L_0} & -I^n_{L_0} & 0 \\ 0 & I^n & -C \\ 0 & 0 & I^q \end{pmatrix},$$

$$Z^2 = \begin{pmatrix} I^n_{L_0} \\ 0 \\ 0 \end{pmatrix}, \; x^2 = \begin{pmatrix} \omega_{L_0} \\ p^e \\ p \end{pmatrix}, \; r^2 = \begin{pmatrix} r_{L_0} \\ 0 \\ 0 \end{pmatrix}.$$

It can be seen that A^{22} is triangular matrix and $\det A^{22} \neq 0$. Thus, the system has a unique solution for any continuous vector-function u and the system (9.13) can be reduced to a system of differential equations [97]. Hence, everywhere below functions $\theta, \omega,\ p^m,\ v, p, p^e$ are understood as a unique solution of the system (9.13).

Equations (9.13c) and (9.13d) do not depend on other system's equations. Therefore, equations (9.13c), (9.13d) can be analysed separately from the rest of the system. Hence the following lemma is correct.

Lemma 9.1. *System (9.13c), (9.13d) is asymptotically stable.*

Proof. Let us consider homogeneous system corresponding to (9.13c), (9.13d):

$$\dot{p}^m = (T^m)^{-1}(-p^m + v), \tag{9.15a}$$

$$\dot{v} = (T^v)^{-1}(-v). \tag{9.15b}$$

Its matrix has form:

$$\begin{pmatrix} -(T^m)^{-1} & (T^m)^{-1} \\ \mathbf{0} & -(T^v)^{-1} \end{pmatrix}. \tag{9.16}$$

This matrix is triangular with negative diagonal elements. Hence it is negative-definite and system (9.13c), (9.13d) is asymptotically stable. $\square$

Corollary 9.2. *Let $u(t) \to u_G^*$. Then, $p^m(t) \to u_G^*$ and $v(t) \to u_G^*$.*

This result is a consequence of the system (9.13c), (9.13d) asymptotic stability. It shows that mechanical power of the turbine converges to the control value at exponential rate.

The other equations of the system (9.13), namely (9.13a), (9.13b), (9.13e), (9.13f), (9.13g), (9.13h) can be reduced to a system of differential equations by expressing variables ω_{L_0}, p and p^e from equations (9.13f), (9.13g), (9.13h) and excluding this variables from the system. The obtained system is given by the following equations:

$$M\dot{\omega}_G = - D_{G,G}\omega_G - C_G BC^T\theta + p^m + r_G, \tag{9.17a}$$

$$M\dot{\omega}_{L_1} = - D_{L_1,L_1}\omega_{L_1} - C_{L_1} BC^T\theta + u_{L_1} + r_{L_1}, \tag{9.17b}$$

$$\dot{\theta}_{G\cup L_1} = \omega_{G\cup L_1}, \tag{9.17c}$$

$$D_{L_0,L_0}\dot{\theta}_{L_0} = - C_{L_0} BC^T\theta + u_{L_0} + r_{L_0}. \tag{9.17d}$$

Equations for variables p^m are not a part of this system; therefore, corresponding homogeneous system has the following form:

$$M\dot{\omega}_{G\cup L_1} = - D_{G\cup L_1,G\cup L_1}\omega_{G\cup L_1} - C_{G\cup L_1} BC^T\theta, \tag{9.18a}$$

$$\dot{\theta}_{G\cup L_1} = \omega_{G\cup L_1},\ \theta_{G\cup L_1}(0) = \theta^0_{G\cup L_1}, \tag{9.18b}$$

$$\dot{\theta}_{L_0} = - D^{-1}_{L_0,L_0} C_{L_0} BC^T\theta,\ \theta_{L_0}(0) = \theta^0_{L_0}. \tag{9.18c}$$

Lemma 9.3. *System (9.17) is asymptotically stable over $\omega_{G\cup L_1}$.*

Proof. Lyapunov function

$$\mathcal{L}_0(\omega_{G\cup L_1}, \theta) = \frac{1}{2}\left(\omega^T_{G\cup L_1} M\omega_{G\cup L_1} + \theta^T CBC^T\theta\right) \tag{9.19}$$

is positive definite $\omega_{G\cup L_1}$. Its time derivative with respect to homogeneous system (9.18):

$$\begin{aligned}\dot{\mathcal{L}}(\omega_{G\cup L_1},\theta) &= \omega_{G\cup L_1}^T(-D_{G\cup L_1,G\cup L_1}\omega_{G\cup L_1} - C_{G\cup L_1}BC^T\theta)+\\ &+\theta^T CB(C_{G\cup L_1})^T\omega_{G\cup L_1} - \theta^T CB(C_{L_0})^T D_{L_0}^{-1}C_{L_0}BC^T\theta =\\ &= -\omega_{G\cup L_1}^T D_{G\cup L_1,G\cup L_1}\omega_{G\cup L_1} - \theta^T CB(C_{L_0})^T D_{L_0}^{-1}C_{L_0}BC^T\theta.\end{aligned} \tag{9.20}$$

Derivative $\dot{\mathcal{L}}(\omega_{G\cup L_1},\theta)$ is negative definite over $\omega_{G\cup L_1}$. Therefore, system (9.17) is asymptotically stable over $\omega_{G\cup L_1}$. □

Theorem 9.4. *Let $u(t)\to u^*$. System (9.13) is asymptotically stable over ω, p^m, v, p, p^e. Variables ω, p^m, v, p, p^e converge to vectors ω^*, $(p^m)^*$, v^*, p^*, $(p^e)^*$ respectively. Additionally,*

$$\omega_i^* = \omega_j^* = \frac{\sum_{i\in N} u_i^* + r_i}{\sum_{i\in N} d_i},\ i,j\in N. \tag{9.21}$$

Proof. Asymptotic stability of p^m and v was shown in lemma 9.1, asymptotic stability of $\omega_{G\cup L_1}$ is a result of lemma 9.3 due to the fact that p^m and v do not depend on the rest of the system's variables. Vector p^m can be considered as converging inhomogeneity in equation (9.13b). Hence p^m does not depend on the convergence of (9.12a), (9.12b), (9.12e), (9.12f), (9.12g), (9.12h).

Let us now prove asymptotic stability over ω_{L_0} and their convergence to ω^*. Let us assume that the system does not have any synchronous machines: $G\cup L_1=\emptyset$. Then, $L_0=N$, and equation (9.17d) has form:

$$-CBC^T\theta + u + r = D\dot{\theta} = D\omega. \tag{9.22}$$

Sum of the equation's rows gives:

$$\sum_{i\in N} d_i\omega_i(t) = \sum_{i\in N} u_i(t) + r_i \to \sum_{i\in N} u_i^* + r_i. \tag{9.23}$$

Differentiation of both sides of the equation (9.22) gives

$$D\dot{\omega} = -CBC^T\omega. \tag{9.24}$$

Matrix $-CBC^T$ is symmetric negative semi-definite; therefore, $\omega(t)$ converges to some ω^*. Vector ω^* is a solution of the system

$$CBC^T\omega^* = 0, \tag{9.25a}$$

$$\sum_{i\in N} d_i\omega_i^* = \sum_{i\in N} u_i^* + r_i. \tag{9.25b}$$

First equation of this system gives $\omega_i^* = \omega_j^*\ \forall i,j \in N$. Therefore, the second equation is equivalent to

$$\omega_1^* = \frac{\sum_{i\in N} u_i^* + r_i}{\sum_{i\in N} d_i}, \tag{9.26}$$

which proves convergence of $\omega(t)$ to $\frac{\sum_{i\in N} u_i^*+r_i}{\sum_{i\in N} d_i}$.

Let us now consider the case, when system has at least one synchronous machine: $G\cup L_1 \neq \emptyset$. Then, differentiation of (9.17d) gives

$$D_{L_0,L_0}\dot{\omega}_{L_0} = -C_{L_0}BC^T\omega = -C_{L_0}B'C_{L_0}^T\omega_{L_0} - C_{L_0}BC^T \begin{pmatrix} \omega_{G\cup L_1} \\ 0 \end{pmatrix}. \tag{9.27}$$

Here matrix B' is a submatrix of B obtained by exclusion of all rows and columns corresponding to lines ij such that $i \notin L_0$ and $j \notin L_0$. Matrix $C_{L_0}B'C_{L_0}^T$ is obtained by exclusion corresponding rows and columns from weighted Laplacian matrix CBC^T. Thus, $C_{L_0}B'C_{L_0}^T$ can be represented as $C'B'(C')^T + H$, where C' is incidence matrix of subgraph that consists of buses L_0, H is diagonal positive semi-definite matrix, which diagonal elements are sums of parameters of lines that connect the subgraph to the rest of the system. Therefore, matrix $C_{L_0}B'C_{L_0}^T = C'B'(C')^T + H$ is positive semi-definite as a sum of two symmetric positive semi-definite matrices. This matrix can have zero eigenvalues if and only if $\ker(C'B'(C')^T) \cap \ker(H) \neq \emptyset$. But $\ker(C'B'(C')^T) = \{\mathbf{1}_{l_0}\}$, and $H\mathbf{1}_{l_0} \neq 0$, as graph Γ is connected and H has at least one nonzero entry. Thus, $\ker(C'B'(C')^T) \cap \ker(H) = \emptyset$ and $C_{L_0}B'C_{L_0}^T = C'B'(C')^T + H \succ 0$. System (9.27) is a system with negative definite matrix; therefore,

$$-C_{L_0}BC^T \begin{pmatrix} \omega_{G\cup L_1} \\ 0 \end{pmatrix} \to -C_{L_0}BC^T \begin{pmatrix} \omega^*_{G\cup L_1} \\ 0 \end{pmatrix} = \text{const}\,. \tag{9.28}$$

As a result, variables $\omega_{L_0}(t)$ are asymptotically stable and converge to some ω^*. Similar to the previous case ω^* satisfies (9.25); therefore, $\omega_i = \omega_j = \frac{\sum_{i\in N} u_i^*+r_i}{\sum_{i\in N} d_i}$, $i,j \in N$.

Asymptotic stability p^e can be obtained from the equations (9.13a), (9.13e) and (9.13f):

$$\begin{gathered} p_G^e = -M_{G,G}\dot{\omega}_G - D_{G,G}\omega_G + p^m + r_G \to \\ \to -D_{G,G}\omega_G^* + u_G^* + r_g = (p^e)_G^*, \end{gathered} \tag{9.29a}$$

$$
\begin{aligned}
p^e_{L_1} &= -M_{L_1,L_1}\dot{\omega}_{L_1} - D_{L_1,L_1}\omega_{L_1} + u_{L_1} + r_{L_1} \to \\
&\to -D_{L_1,L_1}\omega^*_{L_1} + u^*_{L_1} + r_g = (p^e)^*_{L_1},
\end{aligned} \tag{9.29b}
$$

$$
\begin{aligned}
p^e_{L_0} &= -D_{L_0,L_0}\omega_{L_0} + u_{L_0} + r_{L_0} \to \\
&\to -D_{L_0,L_0}\omega^*_{L_0} + u^*_{L_0} + r_g = (p^e)^*_{L_0}.
\end{aligned} \tag{9.29c}
$$

□

Let us now show asymptotic stability of p. From (9.13g) and (9.13h)

$$p^e = CBC^T\theta. \tag{9.30}$$

Since vector p^e is asymptotically stable we have $CBC^T\theta(t) \to (p^e)^*$. Let θ^* be some solution of the equation $CBC^T\theta^* = (p^e)^*$. Then, $CBC^T\theta(t) \to CBC^T\theta^*$. Since $\ker(CBC^T) = \ker(C^T)$ we have $p(t) = C^T\theta(t) \to C^T\theta^* = p^*$.

9.2 Model for a numerical experiment

For this case we use more complicated system model in comparison to the one, used for the analytical results. Firstly, we use nonlinear model of the power flows instead of the equations (9.13g):

$$p_{ij} = b_{ij}\sin(\theta_i - \theta_j),\ ij \in E, \tag{9.31}$$

or in vector form

$$p = B\sin(C^\top\theta). \tag{9.32}$$

Secondly, generators are divided into 3 categories: G^s — set of generators with tandem compound single-reheat turbines [85], [90]; G^h — set generators with hydro turbines, [85], [90]; G^g — set of other generators with generic second-order turbine model, $G = G^s \cup G^h \cup G^g$, $|G^s| = g^s,\ |G^h| = g^h,\ |G^g| = g^g$. Dynamics of steam turbine and governor is given by the following equations:

$$
\begin{aligned}
p^m_{G^s} =& \alpha x^{1s} + \beta x^{2s} + \gamma x^{3s}, && (9.33a)\\
T^{1s}\dot{x}^{1s} =& -x^{1s} + v_{G^s}, && (9.33b)\\
T^{2s}\dot{x}^{2s} =& -x^{2s} + x^{1s}, && (9.33c)\\
T^{3s}\dot{x}^{3s} =& -x^{3s} + x^{2s}, && (9.33d)\\
T^{4s}\dot{v}_{G^s} =& -v_{G^s} + x^{4s}, && (9.33e)\\
T^{5s}\dot{x}^{4s} =& -x^{4s} + R^s\omega_{G^s} + u_{G^s}. && (9.33f)
\end{aligned}
$$

Here vectors $x^{is}(t) \in \mathbb{R}^{g^s}$, $i \in \{1, \dots, 4\}$ are auxiliary variables, used to describe dynamics. Parameters T^{ih} $i \in \{1, \dots, 5\}$ are diagonal positive definite matrices of size $g^s \times g^s$. $R^s \in \mathbb{R}^{g^s \times g^s}$ is a diagonal positive definite matrix of droop coefficients. Coefficients α, β and γ are positive and $\alpha + \beta + \gamma = 1$.

Dynamics of hydro turbines are given below:

$$
\begin{aligned}
p^m_{G^h} =& x^{1h} - 2v_{G^h}, && (9.34a)\\
T^{1h}\dot{x}^{1h} =& -x^{1h} + 3v_{G^h}, && (9.34b)\\
T^{2h}\dot{v}_{G^h} =& x^{2h}, && (9.34c)\\
T^{3h}\dot{x}^{2h} =& -x^{2h} - (R^{th} + R^h)v_{G^h} - R^{th}x^{3h} - \omega_{G^h} + (R^h)^{-1}u_{G^h}, && (9.34d)\\
T^{4h}\dot{x}^{3h} =& -x^{3h} - v_{G^h}. && (9.34e)
\end{aligned}
$$

Similarly to the previous case $x^{is}(t) \in \mathbb{R}^{n^s}$ $i \in \{1, \dots, 3\}$ are auxiliary variables. Parameters T^{ih} $i \in \{1, \dots, 4\}$ are diagonal positive definite matrices of size $g^h \times g^h$. Matrices $R^h, R^{th} \in \mathbb{R}^{g^h \times g^h}$ are diagonal positive definite matrices of static droop and transient droop coefficients respectively.

Finally, turbine governor dynamics of the rest of the buses is described by a second order model:

$$
\begin{aligned}
T^{1g}\dot{p}^m_{G^g} =& -p^m_{G^g} + v_{G^g}, && (9.35a)\\
T^{2g}\dot{v}_{G^g} =& -v_{G^g} + R^g\omega_{G^g} + u_{G^g}. && (9.35b)
\end{aligned}
$$

Here T^{1g} and T^{2g} are diagonal positive matrices of size $g^g \times g^g$. Matrix $R^g \in \mathbb{R}^{g^g \times g^g}$ is diagonal positive definite matrix of droop coefficients. As a result full model for the numerical experiment is given by the following system:

$$\dot{\theta} =\omega, \tag{9.36a}$$

$$M_{G,G}\dot{\omega}_G =- D_{G,G}\omega_G - p^e_G + p^m + r_G, \tag{9.36b}$$

$$p^m_{G^s} =\alpha x^{1s} + \beta x^{2s} + \gamma x^{3s}, \tag{9.36c}$$

$$T^{1s}\dot{x}^{1s} =- x^{1s} + v_{G^s}, \tag{9.36d}$$

$$T^{2s}\dot{x}^{2s} =- x^{2s} + x^{1s}, \tag{9.36e}$$

$$T^{3s}\dot{x}^{3s} =- x^{3s} + x^{2s}, \tag{9.36f}$$

$$T^{4s}\dot{v}_{G^s} =- v_{G^s} + x^{4s}, \tag{9.36g}$$

$$T^{5s}\dot{x}^{4s} =- x^{4s} + R^s\omega_{G^s} + u_{G^s}, \tag{9.36h}$$

$$p^m_{G^h} =x^{1h} - 2v_{G^h}, \tag{9.36i}$$

$$T^{1h}\dot{x}^{1h} =- x^{1h} + 3v_{G^h}, \tag{9.36j}$$

$$T^{2h}\dot{v}_{G^h} =x^{2h}, \tag{9.36k}$$

$$T^{3h}\dot{x}^{2h} =- x^{2h} - (R^{th} + R^h)v_{G^h} - R^{th}x^{3h} - \omega_{G^h} + (R^h)^{-1}u_{G^h}, \tag{9.36l}$$

$$T^{4h}\dot{x}^{3h} =- x^{3h} - v_{G^h}, \tag{9.36m}$$

$$T^{1g}\dot{p}^m_{G^g} =- p^m_{G^g} + v_{G^g}, \tag{9.36n}$$

$$T^{2g}\dot{v}_{G^g} =- v_{G^g} + R^g\omega_{G^g} + u_{G^g}, \tag{9.36o}$$

$$M_{L_1,L_1}\dot{\omega}_{L_1} =- D_{L_1,L_1}\omega_{L_1} - p^e_{L_1} + u_{L_1} + r_{L_1}, \tag{9.36p}$$

$$0 =- D_{L_0,L_0}\omega_{L_0} - p^e_{L_0} + u_{L_0} + r_{L_0}, \tag{9.36q}$$

$$0 =B\sin(C^T\theta) - p, \tag{9.36r}$$

$$0 =Cp - p^e. \tag{9.36s}$$

This model provides one of the best possible DC approximations of the network dynamics. Thus, it is chosen to provide numerical experiment of the control dynamics in section 14.

10 Control derivation algorithm

In the previous section we formalized description of the power system. That allows us to formalize control derivation idea, which idea was presented in section 3.2. We start with the optimization problem defined for the set of stationary points of the physical system (9.13). Firstly we introduce the participation factors function similarly to (7.3).

Definition 10.1. The participation factors function:

$$f(\hat{u}) = \frac{1}{2}\sum_{i \in N} w_i(\hat{u}_i)^2 = \frac{1}{2}\hat{u}^T W \hat{u}, \tag{10.1}$$

where $W = \mathrm{diag}(w_1, \ldots, w_n) \succ 0$.

In addition we introduce three sets of linear inequality and equality constraints: control limits, line limits and inter-area limits. For simplicity, within this section we define a convex set determined by this constraints by X. The optimization problems considered in the further sections are modifications of the following:

$$\min_{u, x^1, x^2} f(u), \tag{10.2a}$$

$$0 = A^{11}x^1 + A^{12}x^2 + Z^1 u + r^1, \tag{10.2b}$$

$$0 = A^{21}x^1 + A^{22}x^2 + Z^2 u + r^2, \tag{10.2c}$$

$$(x^1, x^2) \in X. \tag{10.2d}$$

This is a quadratic problem with linear constraints, thus, if all parameters of the equations are known, it can be easily solved. However there are three difficulties that render such approach impossible:

1. The problem must be solved in a distributed way. There exists a wide range of distributed solvers for OPF problem. They are analysed in section 2. The main issue of these distributed solvers is insufficient control response speed to the system dynamics.

2. Some parameters of the system, i.e. turbine and governor time constants are unknown.

3. Disturbance vector is unknown.

In order to address first two items control calculation block in the Figure (3.2) is written in the form of integral algebraic equations that converge to solution of the optimization problem (10.2). In order to address the third issue disturbance approximation block is introduced. Similarly to the control calculation block it also consists of integral algebraic equations.

Further sections describe in details disturbance approximation and control calculation. However they all have the same general structure. Firstly the general form of integral algebraic equations is presented. This is done in order to explicitly limit the available information obtained via system measurements and communications. In case of disturbance approximation we then provide explicit form of the equations. In case of control calculation we update optimization problem, then provide KKT condition based on which control equations satisfying control form are derived.

Systems of equations for both disturbance approximation and control calculation are derived in the form of first order integral algebraic equations. In case of disturbance approximation equations are divided into two blocks with different roles: 1) calculation of auxiliary variables vector $\tilde{p}^m$ (approximation of mechanical power injections); 2) calculation of disturbance approximation. Same approach is used for the control calculation block: 1) calculation of auxiliary variables vector y; 2) calculation of the control variables. Such approach allows us to keep all calculations in the easy for numerical implementation first-order form and exclude requirement for any derivatives that may introduce noise to the system.

Example 10.1. Consider both Primary and Secondary frequency control described in section 7.1. For simplicity, we omit control deadbands. Corresponding block-diagram is given in Figure 10.1. In the form of first order integral algebraic equations the control has the following form:

$$u(t) = y(t), \tag{10.3a}$$

$$y_i(t) = \begin{cases} -k_i^I \omega(t) - \frac{1}{w_i} k^{II} \int_0^t \omega_{ref}(\tau) d\tau, & \text{if } i \in G, \\ 0, & \text{otherwise,} \end{cases} \quad i \in N. \tag{10.3b}$$

Here y is a scalar of auxiliary variables. As it was show in the example 7.2 system stability depends on the coefficients k^I and k^{II}. If the system is stable, than due to the integral part of

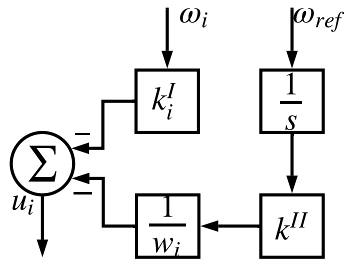

Figure 10.1: Block diagram of primary and secondary frequency control.

the controller frequency deviations $\omega = 0$ in stationary point. As a result, proportional part of the controller also equals zero and control values u_i in inverse ratio to the coefficients w_i. Thus control delivers minimum of the participation function in the set of stationary points with frequency deviations equal 0.

11 Disturbance vector approximation

In this section we consider the disturbance approximation block of the control scheme (Figure 3.2). Normally, in frequency control approaches goal of disturbance approximation is not stated explicitly. However, frequency in power system can be restored if and only if power balance is restored. Thus, sum of frequency control signals must be equal to the minus sum of the disturbances. This is necessary and sufficient condition of the frequency restoration. Therefore, any frequency control approximates disturbance size near the stationary point at latest. Disturbance approximation will be done in any case if the frequency is to be restored. Therefore, we separate this approximation into an explicit control block.

In the previous section we gave general form of the optimization problem on the set of stationary points (10.2). It is a strictly convex problem, thus it has a unique solution. For a system with a fixed set of parameters A^{11}, A^{12}, A^{22}, A^{22}, and feasible set X the solution is uniquely defined by the disturbance vector r. Therefore knowledge of this vector (or its approximation) is not only necessary and sufficient information needed for frequency control, but also a sufficient information for congestion management and inter-area flows control.

In the case, when disturbance is approximated with sufficient accuracy, the control calculation block (Figure 3.1) can do all necessary actions for frequency control, congestion management and inter-area flows control with minimal cost relying only on the disturbance approximation. As a result we separate control inputs (both feedback system state and feedforward disturbance measurements) from the calculation of the control values. All information input goes into the disturbance approximation block. Firstly, this provides control flexibility, as it can work in feedback and feedforward modes or in any combination of them. Most importantly system state is used only to approximate disturbance which does not depend on system state or control systems, thus oscillation of either does not lead to positive feedback, which appearance was shown in the Figure (9.2). As a result in the further sections we will prove global asymptotic stability of the control for the second order turbine-governor dynamics.

11.1 Information availability

The developed control must work in both feedback and feedforward modes. If disturbance measurements are known, then there is no need to approximate the disturbance. However these measurements usually are not known for all or any buses. Moreover, we consider case, when some of the bus disturbance measurements become available or unavailable during transient and control must switch between feedback and feedforward mode.

Let us consider the case, when disturbance measurements are not available. It must be approximated using the available information about the system state and bus parameters. It is not possible to calculate mechanical power injections p^m and valve positions v. Moreover, time constants T^m and T^v are also unknown [85]. Therefore, it is not possible to restore dynamics of the physical system (9.13). The only available information is presented below.

- current frequency deviations values $\omega(t)$;
- stored frequency deviations values in definite integral form: $\int_0^t \omega(\tau)d\tau$;
- stored values of electrical power in definite integral form: $\int_0^t p^e(\tau)d\tau$;
- synchronous machines inertia M;
- synchronous machines damping and coefficients of frequency dependent loads D;
- indicators of buses types $\kappa = (\kappa_1, \dots, \kappa_n)^\top$,

$$\kappa_i = \begin{cases} 0, & \text{if } i \in L_0, \\ 1, & \text{if } i \in L_1, \quad i \in N; \\ 2, & \text{if } i \in G, \end{cases} \tag{11.1}$$

- identifications of available disturbance measurements $r^I = (r_1^I, \dots, r_n^I)^\top$,

$$r_i^I = \begin{cases} 1, & \text{if measurement is available on the bus } i, \\ 0, & \text{if measurement is not available on the bus } i, \end{cases} \quad i \in N; \tag{11.2}$$

- values of available disturbance measurements $\int_0^t \overline{r} d\tau$, where $\overline{r} = (\overline{r}_1, \dots, \overline{r}_n)^\top$,

$$\overline{r}_i = \begin{cases} r_i, & \text{if } r_i^I = 1, \\ 0, & \text{otherwise}, \end{cases} \quad i \in N; \tag{11.3}$$

.

In addition to the limitations above we will allow to use only local information to approximate bus disturbance: bus i can only use $\omega_i(t)$, $\int_0^t \omega_i(\tau)d\tau$, $\int_0^t p_i^e(\tau)d\tau, m_i.d_i$, and κ_i. While control calculations can be done almost instantly, given low computational complexity, measurements of the system state require some time [63–65] and may cause delay. While we do not consider this issue explicitly we enforce this locality condition in order to provide more realistic system behavior.

11.2 Approximation equations

We will approximate the disturbance using generator swing equations (9.13b) and balance equations (9.13e) and (9.13f). Let us firstly move disturbance to the left side of this equations and everything else to the right side:

$$r_G = M_{G,G}\dot{\omega}_G + D_{G,G}\omega_G + p_G^e - p_G^m, \tag{11.4a}$$

$$r_{L_1} = M_{L_1,L_1}\dot{\omega}_{L_1} + D_{L_1,L_1}\omega + p^e - u_{L_1}, \tag{11.4b}$$

$$r_{L_0} = D_{L_0,L_0}\omega_{L_0} + p_{L_0}^e - u_{L_0}. \tag{11.4c}$$

Within this equations measurements of $\dot{\omega}$, p^e and p^m are unknown. In order to exclude the first two we integrate right and left hand sides of the equations:

$$\int_0^t r_G d\tau = M_{G,G}(\omega_G(t) - \omega_G(0)) + \int_0^t D_{G,G}\omega_G(\tau) + p_G^e(\tau) - p_G^m(\tau)d\tau, \tag{11.5a}$$

$$\int_0^t r_{L_1} d\tau = M_{L_1,L_1}(\omega(t)_{L_1} - \omega(0)_{L_1}) + \int_0^t D_{L_1,L_1}\omega_{L_1}(\tau) + p_{L_1}^e(\tau) - u_{L_1}(\tau)d\tau, \tag{11.5b}$$

$$\int_0^t r_{L_0} d\tau = \int_0^t D_{L_0,L_0}\omega_{L_0}(\tau) + p_{L_0}^e(\tau) - u_{L_0}(\tau)d\tau. \tag{11.5c}$$

Vector of mechanical powers p^m together with constants T^m and T^v is unknown; therefore, an auxiliary variable $\tilde{p}^m$ is used. It plays role of mechanical power injections approximation and is defined by

$$\tilde{T}\tilde{p}^m(t) = \int_0^t \left(-\tilde{p}^m(\tau) + u_G(\tau)\right) d\tau,\ \tilde{T} = \mathrm{diag}(\tilde{t}_1, \ldots, \tilde{t}_n) \succ 0. \tag{11.6}$$

Here choice of $\tilde{T}$ is based on the stability requirement and is discussed in the theorem 12.3. From the equations (9.13c) and (9.13d) mechanical power p^m converges to the control u.

Thus, equation (11.6) is chosen to define $\tilde{p}^m$ as the simplest approximation of mechanical power dynamic. Thus, we approximate the disturbance using the following formula:

$$\int_0^t \tilde{r}_i d\tau = \begin{cases} m_i(\omega_i(t) - \omega_i(0)) + \int_0^t d_i\omega_i(\tau) + p_i^e(\tau) - \tilde{p}_i^m(\tau)d\tau, & i \in G, \\ m_i(\omega(t)_i - \omega(0)_i) + \int_0^t d_i\omega_i(\tau) + p_i^e(\tau) - u_i(\tau)d\tau, & i \in L_1, \\ \int_0^t d_i\omega_i(\tau) + p_i^e(\tau) - u_i(\tau)d\tau, & i \in L_0, \end{cases} \quad i \in N. \tag{11.7}$$

Finally, we use the calculated disturbance only if disturbance measurements are unavailable. Therefore, output of the disturbance approximation control block has the following output:

$$\int_0^t \mathring{r}_i d\tau = \begin{cases} \tilde{r}_i, & r_i^I = 0, \\ \overline{r}_i, & r_i^I, \end{cases} \quad i \in N. \tag{11.8}$$

In general $\int_0^t \tilde{r}(\tau)d\tau$ is calculated according to the following formulas (block diagram in Figure 11.1):

$$\begin{aligned} \int_0^t \mathring{r}_i(\tau)d\tau = \tilde{F}\Bigg(\omega_i(t), \int_0^t \omega_i(\tau)d\tau, \int_0^t p_i^e(\tau)d\tau, \int_0^t u_i(\tau)d\tau, \int_0^t \tilde{p}^m(\tau)d\tau, \\ m_i, d_i, \int_0^t \overline{r}_i(\tau)d\tau, r_i^I, \kappa_i\Bigg) + \mathring{r}_i^0, \end{aligned} \tag{11.9a}$$

$$\tilde{p}_i^m(t) = \tilde{G}\left(\int_0^t \tilde{p}^m(\tau)d\tau, \int_0^t u_i(\tau)d\tau\right) + \tilde{p}^{m0}, \tag{11.9b}$$

for $i \in N$. Here $\tilde{F} : \mathbb{R}^8 \times \{0,1\} \times \{0,1,2\} \to \mathbb{R}$ and $\tilde{G} : \mathbb{R}^2 \to \mathbb{R}$ are functions of the following form. For $z \in \mathbb{R}^8,\ z_9 \in \{0,1\}, z_{10} \in \{0,1,2\}$.

$$\tilde{F}(z) = \begin{cases} z_8, & \text{if } z_9 = 1, \\ z_7z_2 + z_3 - z_4, & \text{if } z_9 = 0 \text{ and } z_{10} = 0, \\ z_7z_2 + z_3 - z_4 + z_6z_1, & \text{if } z_9 = 0 \text{ and } z_{10} = 1, \\ z_7z_2 + z_3 - z_5 + z_6z_1, & \text{if } z_9 = 0 \text{ and } z_{10} = 2. \end{cases} \tag{11.10}$$

Function $\tilde{F}$ is continuous over z. Note that r_i^I and κ_i are constant, thus this function is continuous within the disturbance approximation block. For $z \in \mathbb{R}^2$

$$\tilde{G}(z) = \frac{1}{\tilde{t}}(z_2 - z_1). \tag{11.11}$$

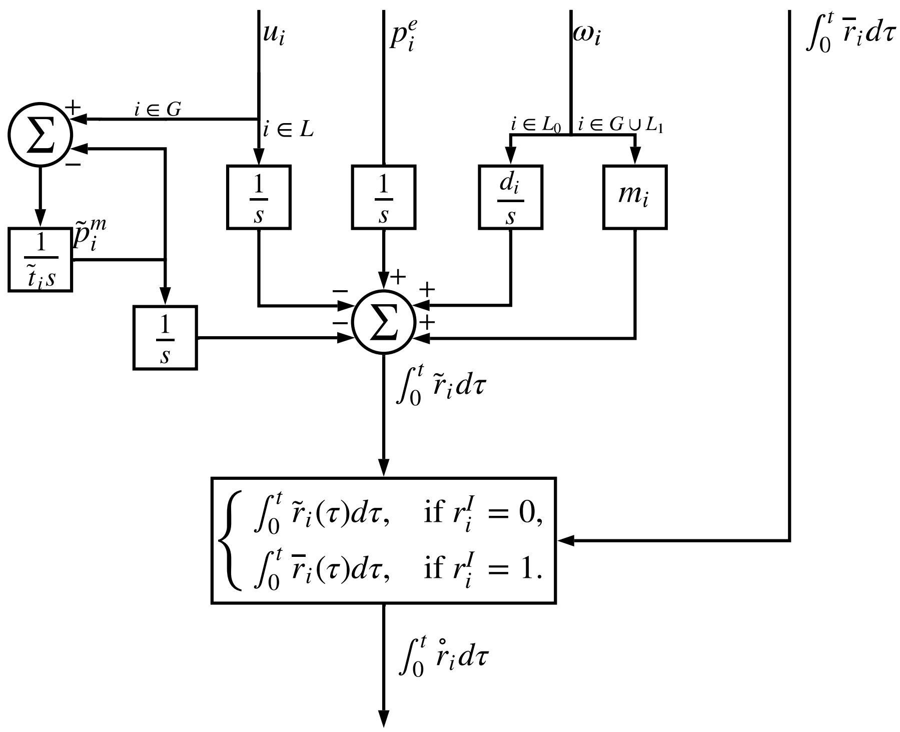

Figure 11.1: Disturbance approximation block diagram.

11.3 Conclusion

Disturbance is approximated directly or indirectly by every frequency control (i.e. traditional frequency control does it via integration of frequency deviation). Control restores power balance if and only if sum of control signals is equal to the minus sum of the disturbances. We utilize this idea and separate disturbance approximation into a separate control block (3.1). This control block either uses bus disturbances measurements or estimates disturbances using system state if measurements are unavailable. The disturbance is approximated either from the balance equations for the load buses or generator swing equations for the generator buses with approximation for mechanical power injections. Thus, turbine dynamics, which are unknown, are excluded from the estimation. The control uses system state as an input, but uses it only to estimate disturbance, which is an external force independent from the system dynamics. As a result, unknown transient processes in turbine and governor do not effect disturbance approximation control block output. Such approach allows to solve issues with the cascade structure of the turbine and governor equations, which introduce instabilities that cannot be observed in simpler models, as it was shown in [98]. In the further sections we will prove global asymptotic stability of the control for the system with the cascade structure of turbine and governor, which is one of the key points of the presented work.

Disturbance approximation approach is utilized in frequency control as a part of mandatory actions but also in the congestion management and inter-area flows control problems. In order to deliver system (9.13) to the desired state we formulate optimization problem on the set of stationary points (10.2). This problem is strictly convex, thus it has always a unique solution. Therefore, for any set of fixed system parameters A^{11}, A^{12}, A^{21}, A^{22}, and feasible set X its solution is uniquely defined by the disturbance vector r. Therefore, information, given by the disturbance approximation control block, is sufficient to not only do frequency control, but also to perform congestion management and inter-area flows control.

Due to the lack of information about the system state it is not possible to recover bus disturbances, therefore we recover its integral instead. Further we will show sufficiency of this information. In this work we provide analytical results for the case, when $r = \text{const}$. Therefore, for the load buses theoretically it is possible to estimate integral of the disturbance for some $t > 0$ using formulas (11.5b) and (11.5c) and then use it in all further calculations. However, this statement is only true if all parameters and system state are measured ideally without any errors. Moreover, such approach is not applicable for non-constant r for which we provide numerical experiments in section 14.

It can be seen from the general form of the disturbance approximation (11.9) that the same approach is used on every bus and only local information is required. Therefore, this approximation method supports decentralized implementation. Additionally, lack of any need for communication ensures that communication delays cannot affect this estimation.

12 Centralized control

12.1 Problem 1. Frequency control with no control limits.

The simplest frequency control problem is considered within this section. It is assumed that communications is done in a centralized way. In this problem it is assumed that all generators have sufficient spinning reserves so control limits are never reached, line limits are never reached and control is present on all buses.

12.1.1 Problem statement

It is needed to keep power balance in the system at minimal cost of the participation function (10.1). Let us define corresponding stationary point of the system:

Definition 12.1. Optimal type 1 steady-state (OS1) is a point $(\hat{u}^*, \hat{\theta}^*, \hat{\omega}^*, \hat{p}^{m*}, \hat{v}^*, \hat{p}^*, \hat{p}^{e*})$ that delivers a solution of the following optimization problem:

$$\min_{\hat{u},\hat{\theta},\hat{\omega},\hat{p}^m,\hat{v},\hat{p},\hat{p}^e} f(\hat{u}), \tag{12.1a}$$

$$(\hat{\theta}, \hat{\omega}, \hat{p}^m, \hat{v}, \hat{p}, \hat{p}^e) \in \Psi, \tag{12.1b}$$

where $\Psi = \{(u^*, \theta^*, \omega^*, p^{m*}, v^*, p^*, p^{e*})\}$ is the set of stationary points of the system (9.13).

From (9.17d) it can be seen that in all stationary points $\omega^* = 0$, thus, power balance is restored in OS1. Let us now define control form.

Problem 1 (Frequency control without control limits)**.** *Let s be the size of auxiliary variables vector y. Then, it is required to find Lipschitz continuous controller functions*

$$F : \mathbb{R}^s \times \mathbb{R}^{n\times n} \to \mathbb{R}^n, \tag{12.2a}$$

$$G : \mathbb{R}^n \times \mathbb{R}^n \times \mathbb{R}^s \to \mathbb{R}^s, \tag{12.2b}$$

such that

1. *Control u is defined by a system of integral-algebraic equations*

$$u(t) = F(y(t), W), \tag{12.3a}$$

$$y(t) = \int_0^t G(\mathring{r}(\tau), u(\tau), y(\tau))d\tau + y^0,\ y^0 \in \mathbb{R}^s. \tag{12.3b}$$

2. *Control u must be globally asymptotically stable.*

3. *System (9.13) with control u must converge to OS1.*

It can be seen that if the solution of the system (12.3) exists, then vector functions u and y are continuous. Our goal is to prove global asymptotic stability of the control in order to ensure its reliable operations for any state of the system. In addition control must converge to a constant vector. This requirement is necessary from the practical point of view: we consider constant disturbance, thus, after some time, control must be constant too. Additionally, according to the Theorem 9.4 this requirement sufficient for the global asymptotic stability of the frequency deviations.

The solving process is divided into two stages:

1. Formulation of an optimization problem that defines stationary point to which the system (9.13) should converge under developed control. It is possible to derive equations for the stationary point of the corresponding Lagrange function. However, its solution requires knowledge of the vector r, which is unavailable.

2. Transition from algebraic equations of the stationary point to a system of integral equations. The solution of optimization problem from the first item gives a set of algebraic equations depending on r. Thus, the system of integral equations that depends on $\int_0^t r d\tau$ and converges to the solution of optimization problem is derived.

12.1.2 Optimal steady-state analysis

Let us explicitly write constraints of the optimization problem for the OS1:

$$\min_{\hat{\theta},\hat{\omega},\hat{p}^m,\hat{v},\hat{p},\hat{p}^e,\hat{u}} f(\hat{u}), \tag{12.4a}$$

$$0 = \hat{\omega}, \tag{12.4b}$$

$$0 = -D_{G,G}\hat{\omega}_G - \hat{p}^e_G + \hat{p}^m + r_G, \tag{12.4c}$$

$$0 = -\hat{p}^m + \hat{v}, \tag{12.4d}$$

$$0 = -\hat{v} + \hat{u}_G, \tag{12.4e}$$

$$0 = -D_{L_1,L_1}\hat{\omega}_{L_1} - \hat{p}^e_{L_1} + \hat{u}_{L_1} + r_{L_1}, \tag{12.4f}$$

$$0 = -D_{L_0,L_0}\hat{\omega}_{L_0} - \hat{p}^e_{L_0} + \hat{u}_{L_0} + r_{L_0}, \tag{12.4g}$$

$$\hat{p} = BC^T\hat{\theta}, \tag{12.4h}$$

$$\hat{p}^e = C\hat{p}. \tag{12.4i}$$

Constraints (12.4b)-(12.4i) guarantee any feasible point of the problem to be a stationary point of the system (9.13) with frequency deviations being equal 0. From (12.4b) $\hat{\omega}$ is equal 0 and can be excluded from the rest of the system. From (12.4d) and (12.4e) $\hat{p}^m = \hat{v} = \hat{u}$; thus, variables p^m and v can be replaced with u in the system. As a result, equations (12.4c), (12.4f) and (12.4g) are equivalent to

$$0 = -\hat{p}^e + \hat{u} + r. \tag{12.5}$$

Let us consider the sum of the right-hand sides:

$$0 = -\mathbf{1}_n^T\hat{p}^e + \mathbf{1}_n^T(\hat{u} + r). \tag{12.6}$$

However, $\mathbf{1}_n^T p^e = -\mathbf{1}_n^T Cp = 0$ as a sum all flows in the system. Thus, problem (12.4) can be simplified to the following:

$$\min_{\hat{u}} \frac{1}{2}\hat{u}^T W\hat{u}, \tag{12.7a}$$

$$\mathbf{1}_n^T(\hat{u} + r) = 0. \tag{12.7b}$$

Let $\hat{u}^*$ be solution of this problem. This problem is strictly convex, thus, $\hat{u}^*$ is the unique solution [14]. Corresponding Lagrange function:

$$L(\hat{u}, \hat{\lambda}) = \frac{1}{2}\hat{u}^T W\hat{u} - \hat{\lambda}\mathbf{1}_n^T(\hat{u} + r). \tag{12.8}$$

Corresponding stationary point is defined by the system of algebraic equations:

$$W\hat{u} - \mathbf{1}_n\hat{\lambda} = 0, \tag{12.9a}$$

$$\mathbf{1}_n^T(\hat{u} + r) = 0, \tag{12.9b}$$

which is equivalent to

$$\hat{u} = W^{-1}\mathbf{1}_n\hat{\lambda}, \tag{12.10a}$$

$$\mathbf{1}_n^T(W^{-1}\mathbf{1}_n\hat{\lambda} + r) = 0. \tag{12.10b}$$

Solving this system gives

$$\hat{u}^* = -W^{-1}\mathbf{1}_n\frac{\mathbf{1}_n^T r}{\mathbf{1}_n^T W^{-1}\mathbf{1}_n}. \tag{12.11}$$

Lemma 12.1. *Let $u(t) \to \hat{u}^*$, then system (9.13) converges to the optimal type 1 steady-state.*

Proof. From the Theorem 9.4 variables ω, p^m, v, p, p^e of the system (9.13) converge to constant vectors. Let us now show that θ also converges to a stationary point.

Vector $\hat{u}^*$ is a unique solution of the problem (12.10) and, consequently, a part of the solution of (12.4) and (12.1). Additionally, from the theorem (9.4) frequency in stationary point is uniquely defined by control values, thus, from (12.4b) frequency deviations are equal 0, thus $\dot{\theta} = 0$ and θ converges to some constant vector. □

If $u(t) \equiv \hat{u}^*$, then, according to the Theorem 9.4, system (9.13) converges to OS1. However, in order to calculate $\hat{u}^*$ it is necessary to use r, which is unknown. Thus transition to integral algebraic equations is done in the next section.

12.1.3 Transition to control equations

Transition to a system of algebraic integral system is done be replacement of the equation (12.10b) with an integral version of it. Idea behind this transition is the following: it is not possible to solve equation (12.10b) directly, thus, it makes sense to apply some iterative method. Newton method as a one with high convergence speed for the highly sparse systems [99] seems to be an appropriate candidate. Since equation (12.10b) does not depend on $\hat{u}$, corresponding Newton method iteration is given by

$$\hat{\lambda}^{k+1} = \hat{\lambda}^k + (\mathbf{1}_n^T W^{-1}\mathbf{1}_n)^{-1}\mathbf{1}_n^T(-W^{-1}\mathbf{1}_n\hat{\lambda}^k + r). \tag{12.12}$$

Equivalently

$$\mathbf{1}_n^T W^{-1}\mathbf{1}_n(\hat{\lambda}^{k+1} - \hat{\lambda}^k) = \mathbf{1}_n^T(-W^{-1}\mathbf{1}_n\hat{\lambda}^k + r). \tag{12.13}$$

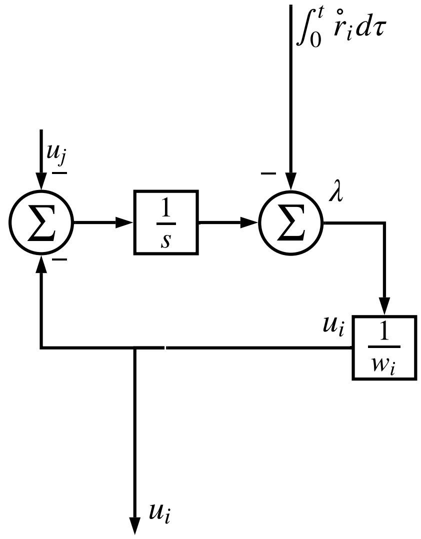

Figure 12.1: Control block diagram for the Problem 1.

Replacement of $\mathbf{1}_n^T W^{-1}\mathbf{1}_n(\hat{\lambda}^{k+1} - \hat{\lambda}^k)$ with $\dot{\lambda}$ and transition to the continuous algorithm gives

$$\dot{\lambda} = -\mathbf{1}_n^T(W^{-1}\mathbf{1}_n\lambda + r). \tag{12.14}$$

It can be seen that equation (12.14) can also be obtained from the (12.10b) by replacing right-hand side zero with the derivative of λ. Here $\hat{\lambda}$ is used instead of λ in order to separate vector λ in the optimization problem (12.7) and function λ in (12.14). The obtained differential equation is replaced with the equivalent integral in order to satisfy control form (12.3):

$$\lambda(t) = \int_0^t -\mathbf{1}_n^T(W^{-1}\mathbf{1}_n\lambda(\tau) + r)d\tau + \lambda_0. \tag{12.15}$$

Replacement of r with $\mathring{r}$ from the previous section gives overall control system

$$u(t) = W^{-1}\mathbf{1}_n\lambda(t), \tag{12.16a}$$

$$\lambda(t) = -\int_0^t \mathbf{1}_n^T(u(\tau) + \mathring{r}(\tau))d\tau + \lambda_0. \tag{12.16b}$$

Block-diagram corresponding to the control equations is shown in Figure 12.1.

12.1.4 Control stability and applicability

From (11.8)

$$\mathring{r}_G(t) = r_G + p^m(t) - \tilde{p}^m(t). \tag{12.17}$$

As a result, (9.13) values $r_G(t)$ depend only on p^m defined by equations (9.13c) and (9.13d). Thus, in order to prove asymptotic stability of $u(t)$ it is sufficient to prove asymptotic stability of the system (12.16), (9.13c) and (9.13d). This system contains both integral and differential equations. For simplicity they are all reduced to the differential ones:

$$\dot{\lambda} = -\mathbf{1}_n^T(W^{-1}\mathbf{1}_n\lambda + r) + \mathbf{1}_g^T \operatorname{diag}(r_G^I)(p^m - \tilde{p}^m), \tag{12.18a}$$

$$\dot{p}^m = -(T^m)^{-1}p^m + (T^m)^{-1}v, \tag{12.18b}$$

$$\dot{v} = -(T^v)^{-1}v + (T^v)^{-1}W_{G,G}^{-1}\mathbf{1}_g\lambda, \tag{12.18c}$$

$$\dot{\tilde{p}}^m = -\tilde{T}^{-1}\tilde{p}^m + \tilde{T}^{-1}W_{G,G}^{-1}\mathbf{1}_g\lambda. \tag{12.18d}$$

Or in matrix form

$$\dot{x} = Ax + R, \tag{12.19}$$

where

$$x = \begin{pmatrix} \lambda \\ p^m \\ v \\ \tilde{p}^m \end{pmatrix}, A = \begin{pmatrix} -\mathbf{1}_n^T W^{-1}\mathbf{1}_n & -\mathbf{1}_g^T & 0 & \mathbf{1}_g^T \operatorname{diag}(r_G^I) \\ 0 & -(T^m)^{-1} & (T^m)^{-1} & 0 \\ (T^v)^{-1}W_{G,G}^{-1}\mathbf{1}_g & 0 & -(T^v)^{-1} & 0 \\ \tilde{T}^{-1}W_{G,G}^{-1}\mathbf{1}_g & 0 & 0 & -\tilde{T}^{-1} \end{pmatrix}, R = \begin{pmatrix} -\mathbf{1}_n^T r \\ 0 \\ 0 \\ 0 \end{pmatrix}. \tag{12.20}$$

For this system the following result is obtained.

Lemma 12.2. *In stationary point $(\lambda^*, p^{m*}, v^*, \tilde{p}^{m*})$ of the system (12.18) λ^* coincides with $\hat{\lambda}^*$ in (12.10)*

Proof. It can be seen that in stationary point $(p^m)^* = (\tilde{p}^m)^*$. Thus, equation (12.18a) is equivalent to (12.10b) if $\dot{\lambda} = 0$. □

Theorem 12.3 (Control stability). *Let*

$$\tilde{t}_i \leq \max\{t_i^m, t_i^v\},\ i \in G. \tag{12.21}$$

Then system (12.19) is globally asymptotically stable.

Proof. Let us consider characteristic equation for the matrix A:

$$\det(A - I^{1+3g}\eta) = 0. \tag{12.22}$$

If we take determinant of the lower $3g \times 3g$ block we get

$$P_1(\eta) = \det \begin{pmatrix} -(T^m)^{-1} - I^g\eta & (T^m)^{-1} & 0 \\ 0 & -(T^v)^{-1} - I^g\eta & 0 \\ 0 & 0 & -\tilde{T}^{-1} - I^g\eta \end{pmatrix} = \tag{12.23}$$
$$= \prod_{i\in G}\left(-\frac{1}{t_i^m} - \eta\right)\left(-\frac{1}{t_i^v} - \eta\right)\left(-\frac{1}{\tilde{t}_i} - \eta\right).$$

Thus, for $P_1(\eta) = 0$ it is necessary $\eta = \Re\eta < 0$. If $P_1(\eta) \neq 0$, then according to the Schur complement formula

$$\det(A - I^{1+3g}\eta) = P_1(\eta)P_2(\eta), \tag{12.24}$$

where $P_2(\eta)$ is given by the formula

$$P_2(\eta) = \det\Bigg(-\mathbf{1}_n^T W^{-1}\mathbf{1}_n - \eta - \begin{pmatrix} -\mathbf{1}_g^T & 0 & \mathbf{1}_g^T \operatorname{diag}(r_G^I) \end{pmatrix} \cdot$$
$$\cdot \begin{pmatrix} -(T^m)^{-1} - I^g\eta & (T^m)^{-1} & 0 \\ 0 & -(T^v)^{-1} - I^g\eta & 0 \\ 0 & 0 & -\tilde{T}^{-1} - I^g\eta \end{pmatrix}^{-1} \begin{pmatrix} 0 \\ (T^v)^{-1}W_{G,G}^{-1}\mathbf{1}_g \\ \tilde{T}^{-1}W_{G,G}^{-1}\mathbf{1}_g \end{pmatrix}\Bigg) =$$
$$= \det\Bigg(-\mathbf{1}_n^T W^{-1}\mathbf{1}_n - \eta - \begin{pmatrix} -\mathbf{1}_g^T & 0 \end{pmatrix} \cdot \tag{12.25}$$
$$\cdot \begin{pmatrix} -((T^m)^{-1} - I^g\eta)^{-1} & -(T^m)^{-1}(-(T^m)^{-1} - I^g\eta)^{-1}(-(T^v)^{-1} - I^g\eta)^{-1} \\ 0 & -((T^v)^{-1} - I^g\eta)^{-1} \end{pmatrix} \cdot$$
$$\cdot \begin{pmatrix} 0 \\ (T^v)^{-1}W_{G,G}^{-1}\mathbf{1}_g \end{pmatrix} + \mathbf{1}_g \operatorname{diag}(r_G^I)(-\tilde{T}^{-1} - I^g\eta)\tilde{T}^{-1}W_{G,G}^{-1}\mathbf{1}_g\Bigg) =$$
$$= -\sum_{i\in N}\frac{1}{w_i} - \eta + \sum_{i\in G}\frac{r_i^I}{w_i}\left(\frac{1}{t_i^m t_i^v(\frac{1}{t_i^m} + \eta)(\frac{1}{t_i^v} - \eta)} - \frac{1}{\tilde{t}_i(\frac{1}{\tilde{t}_i} + \eta)}\right).$$

For simplicity let us denote $y_1^i = \frac{1}{t_i^m}$, $y_2^i = \frac{1}{t_i^v}$, $y_3^i = \frac{1}{\tilde{t}_i}$, $i \in G$. Then

$$P_2(\eta) = -\sum_{i=1}^{n}\frac{1}{w_i} - \eta + \sum_{i=1}^{g}\frac{r_i}{w_i}\left(\frac{y_1^i y_2^i}{(y_1^i + \eta)(y_2^i + \eta)} - \frac{y_3^i}{y_3^i + \eta}\right). \tag{12.26}$$

Let us now show that for $\Re\eta = \alpha$ and $\Im\eta = \beta$ equations $P_2(\eta) = 0$ does not have solutions such that $\alpha \geq 0$. We consider the following expression:

$$\frac{y_1^i y_2^i}{(y_1^i + \eta)(y_2^i + \eta)} - \frac{y_3^i}{y_3^i + \eta}. \tag{12.27}$$

Let us introduce new functions:

$$z_1^i(\alpha,\beta) = \frac{y_1^i}{(y_1^i+\alpha)+\beta j} = y_1^i\left(\frac{y_1^i+\alpha}{(y_1^i+\alpha)^2+\beta^2} - \frac{\beta}{(y_1^i+\alpha)+\beta^2}j\right), \tag{12.28}$$

$$z_2^i(\alpha,\beta) = \frac{y_2^i}{(y_2^i+\alpha)+\beta j} = y_2^i\left(\frac{y_2^i+\alpha}{(y_2^i+\alpha)^2+\beta^2} - \frac{\beta}{(y_2^i+\alpha)+\beta^2}j\right), \tag{12.29}$$

$$z_3^i(\alpha,\beta) = \frac{y_3^i}{(y_3^i+\alpha)+\beta j} = y_2^i\left(\frac{y_3^i+\alpha}{(y_3^i+\alpha)^2+\beta^2} - \frac{\beta}{(y_3^i+\alpha)+\beta^2}j\right), \tag{12.30}$$

Substitution (12.28)-(12.30) into (12.27) gives

$$\varphi_i(\alpha,\beta) = \Re\left(z_1^i(\alpha,\beta)z_2^i(\alpha,\beta) - z_3^i(\alpha,\beta)\right) = \tag{12.31}$$

$$= y_1^i y_2^i\left(\frac{(y_1^i+\alpha)(y_2^i+\alpha)}{((y_1^i+\alpha)^2+\beta^2)\left((y_2^i+\alpha)^2+\beta^2\right)} - \frac{\beta^2}{((y_1^i+\alpha)^2+\beta^2)\left((y_2^i+\alpha)^2+\beta^2\right)}\right) - \tag{12.32}$$

$$-\frac{y_3^i(y_3^i+\alpha)}{(y_3^i+\alpha)^2+\beta^2}. \tag{12.33}$$

For $\beta = 0$:

$$\varphi_i(\alpha,0) = y_1^i y_2^i\left(\frac{1}{(y_1^i+\alpha)(y_2^i+\alpha)}\right) - \frac{y_3^i}{y_3^i+\alpha} = z_1^i(\alpha,0)z_1^i(\alpha,0) - z_3^i(\alpha,0). \tag{12.34}$$

From (12.28)

$$\alpha = \frac{y_1^i}{z_1^i(\alpha,0)} - y_1^i. \tag{12.35}$$

Then, from (12.29), (12.30) and (12.35)

$$z_2^i(\alpha,0) = \frac{z_1^i(\alpha,0)y_2^i}{z_1^i(\alpha,0)(y_2^i-y_1^i)+y_1^i},\ z_3^i(\alpha,0) = \frac{z_1^i(\alpha,0)y_3^i}{z_1^i(\alpha,0)(y_3^i-y_1^i)+y_1^i}. \tag{12.36}$$

We introduce auxiliary variables:

$$u_1^i = z_1^i(\alpha,0) = \frac{y_1^i}{y_1^i+\alpha},\ u_2^i = z_2^i(\alpha,0) = \frac{y_2^i}{y_2^i+\alpha},\ u_3^i = z_3^i(\alpha,0) = \frac{y_3^i}{y_3^i+\alpha}. \tag{12.37}$$

For $\alpha \geqslant 0$ auxiliary variables $0 < u_k^i \leqslant 1$, $k = 1,2,3$. Using (12.36), we get

$$\varphi_i(\alpha,0) = u_1^i u_2^i - u_3^i = u_1^i\left(\frac{u_1^i y_2^i}{u_1^i(y_2^i-y_1^i)+y_1^i} - \frac{y_3^i}{u_1^i(y_3^i-y_1^i)+y_1^i}\right) = u_1^i\psi_i(u_1^i). \tag{12.38}$$

Derivative of ψ:

$$\psi_i'(u_1^i) = \frac{y_2^i}{u_1^i(y_2^i-y_1^i)+y_1^i} - \frac{u_1^i y_2^i(y_2^i-y_1^i)}{\left(u_1^i(y_2^i-y_1^i)+y_1^i\right)^2} + \frac{y_3^i(y_3^i-y_1^i)}{\left(u_1^i(y_3^i-y_1^i)+y_1^i\right)^2} = \tag{12.39}$$

$$= \frac{y_2^i}{u_1^i(y_2^i - y_1^i) + y_1^i}\left(1 - \frac{u_1^i(y_2^i - y_1^i)}{u_1^i(y_2^i - y_1^i) + y_1^i}\right) + \frac{y_3^i(y_3^i - y_1^i)}{\left(u_1^i(y_3^i - y_1^i) + y_1^i\right)^2} = \tag{12.40}$$

$$= \frac{y_2^i}{u_1^i(y_2^i - y_1^i) + y_1^i} \cdot \frac{y_1^i}{u_1^i(y_2^i - y_1^i) + y_1^i} + \frac{y_3^i(y_3^i - y_1^i)}{\left(u_1^i(y_3^i - y_1^i) + y_1^i\right)^2}. \tag{12.41}$$

If $y_3^i - y_1^i \geqslant 0$, then $\psi_i'(u_1^i) > 0$ and ψ_i is monotonously increasing. From $\psi_i(1) = 0$ we have $\psi_i(u_1^i) \leqslant 0, u_1^i \in (0, 1]$. Therefore, $\varphi(\alpha, 0) \leqslant 0, \alpha \geqslant 0$. Additionally, $u_1^i = 1$ if and only if $\alpha = 0$, thus, $\varphi(\alpha, 0) < 0$ for $\alpha > 0$. From (12.29)

$$\alpha = \frac{y_2^i}{z_2^i(\alpha, 0)} - y_2^i. \tag{12.42}$$

Same derivation gives $\varphi(\alpha, 0) < 0$ for $\alpha > 0$ and $y_3^i - y_2^i \geqslant 0$.

Let us introduce new variables:

$$k_1^i = y_1^i y_2^i (y_1^i + \alpha)(y_2^i + \alpha),\ c_1^i = (y_1^i + \alpha)^2,\ c_2^i = (y_2^i + \alpha)^2,\ c_3^i = (y_3^i + \alpha)^2. \tag{12.43}$$

Then

$$\varphi_i(\alpha, \beta) = \frac{k_1^i - \beta}{(c_1^i + \beta)(c_2^i + \beta)} - \frac{k_2^i}{c_3^i + \beta} = \tag{12.44}$$

$$= \frac{-(1 + k_2^i)\beta^2 + (k_1^i - c_3^i - k_2^i(c_1^i + c_2^i))\beta + c_3^i k_1^i - k_2^i c_1^i c_2^i}{(c_1^i + \beta)(c_2^i + \beta)(c_3^i + \beta)} = \frac{f_i(\beta)}{(c_1^i + \beta)(c_2^i + \beta)(c_3^i + \beta)}. \tag{12.45}$$

From $f_i(0) = \varphi_i(\alpha, 0) \leqslant 0$ we have $c_3^i k_1^i - k_2^i c_1^i c_2^i \leqslant 0$. Furthermore

$$y_3^i > y_1^i \ \Rightarrow\ c_3^i > c_1^i \ \Rightarrow\ k_1^i c_3^i > k_1^i c_1^i \ \Rightarrow\ k_1^i c_1^i - k_2^i c_1^i c_2^i < k_1^i c_3^i - k_2^i c_1^i c_2^i < 0 \ \Rightarrow \tag{12.46}$$

$$\Rightarrow\ k_1^i - c_3^i - k_2^i c_1^i - k_2^i c_2^i < -c_3^i - k_2^i c_1^i < 0. \tag{12.47}$$

Thus, all second-order coefficients of f_i are negative and from $f_i(0) \leqslant 0$ we have $f_i(\beta) \leqslant 0$. Then $\varphi_i(\alpha, \beta) \leqslant 0$ and

$$P_2(0) = -\sum_{i=1}^{n} \frac{1}{w_i} < 0. \tag{12.48}$$

Therefore, equation $P_2(\eta) = 0$ has solution only if $\alpha < 0$, thus, all real parts of eigenvalues of A are negative and system (12.19) is globally asymptotically stable if $y_3^i - y_1^i \geqslant 0$ or $y_3^i - y_2^i \geqslant 0$ or in original variables $\tilde{t}_i \leq \max\{t_i^m, t_i^v\},\ i \in G$. □

Theorem 12.4 (Control applicability)**.** *Formulas*

$$F(y, W) = W^{-1} \boldsymbol{1}_n y, \tag{12.49}$$

$$G(\mathring{r}, u, y) = -\mathbf{1}_n^\top (u + \mathring{r}) \tag{12.50}$$

define controller functions for the Problem 1 with $s = 1$.

Proof. Substitution of F and G into (12.3) gives system (12.16) with $y = \lambda$, thus item 1 of the Problem 1 is satisfied. From the Theorem 12.3 control u is global asymptotically stable and converges to a constant control, thus item 2 of the Problem 1 is satisfied. From the Lemma 12.2 u converges to $\hat{u}^*$, thus from Lemma 12.1, system (9.13) with the control u converges to the optimal type 1 steady-state. □

12.2 Problem 2. Frequency control with control present on some buses.

Here, similarly to the previous section, no control limits or line limits are present and communication is centralized. However, now control is present only on a subset of buses $N_u \subseteq N$, $n_u = |N_u|$. Without loss of generality it is assumed that $u_i(t) \equiv 0$ on all other buses $i \in N \setminus N_u$. Further the indicator vector will be used: $\kappa^u = (\kappa_1^u, \ldots, \kappa_N^u)^T$,

$$\kappa_i^u = \begin{cases} 1, & \text{if } i \in N_u, \\ 0, & \text{if } i \notin N_u. \end{cases} \tag{12.51}$$

This problem is intermediate between the one considered in the section 12.1, when no control limits are present and problem with control limits considered in the section 12.3.

12.2.1 Problem statement

Problem statement is similar to the one in the previous section. Main difference is in the presence of the vector κ^u.

Definition 12.2. Optimal type 2 steady-state (OS2) is a point $(\hat{u}^*, \hat{\theta}^*, \hat{\omega}^*, \hat{p}^{m*}, \hat{v}^*, \hat{p}^*, \hat{p}^{e*})$ that delivers a solution of the following optimization problem:

$$\min_{\hat{u}, \hat{\theta}, \hat{\omega}, \hat{p}^m, \hat{v}, \hat{p}, \hat{p}^e} f(\hat{u}), \tag{12.52a}$$

$$(\hat{\theta}, \hat{\omega}, \hat{p}^m, \hat{v}, \hat{p}, \hat{p}^e) \in \Psi, \tag{12.52b}$$

$$\hat{u}_i = 0, \ i \in N_u. \tag{12.52c}$$

Problem 2 (Frequency control with control present on some buses). *Let s be the size of auxiliary variables vector y. Then, it is required to find Lipschitz continuous controller functions*

$$F : \mathbb{R}^s \times \mathbb{R}^{n\times n} \times \{0,1\}^n \to \mathbb{R}^n, \tag{12.53a}$$

$$G : \mathbb{R}^n \times \mathbb{R}^n \times \mathbb{R}^s \to \mathbb{R}^s, \tag{12.53b}$$

such that

1. *Control u is defined by a system of integral-algebraic equations*

$$u(t) = F(y(t), W, \kappa^u), \tag{12.54a}$$

$$y(t) = \int_0^t G(\mathring{r}(\tau), u(\tau), y(\tau))d\tau + y^0, \tag{12.54b}$$

2. *Control u must be globally asymptotically stable.*

3. $u_i(t) = 0,\ i \in N_u,\ y \geq 0.$

4. *System (9.13) with control u must converge to OS2.*

12.2.2 Optimal steady-state and control equations

In order to obtain control, optimization problem similar to (12.4) is introduced with an additional constraint of control values being equal to zero on the buses not belonging to the set N_u:

$$\min_{\hat{\theta},\hat{\omega},\hat{p}^m,\hat{v},\hat{p},\hat{p}^e,\hat{u}} f(\hat{u}), \tag{12.55a}$$

$$0 = \hat{\omega}, \tag{12.55b}$$

$$0 = -D_{G,G}\hat{\omega}_G - \hat{p}^e_G + \hat{p}^m + r_G, \tag{12.55c}$$

$$0 = -\hat{p}^m + \hat{v}, \tag{12.55d}$$

$$0 = -\hat{v} + \hat{u}_G, \tag{12.55e}$$

$$0 = -D_{L_1,L_1}\hat{\omega}_{L_1} - \hat{p}^e_{L_1} + \hat{u}_{L_1} + r_{L_1}, \tag{12.55f}$$

$$0 = -D_{L_0,L_0}\hat{\omega}_{L_0} - \hat{p}^e_{L_0} + \hat{u}_{L_0} + r_{L_0}, \tag{12.55g}$$

$$\hat{p} = BC^T\hat{\theta}, \tag{12.55h}$$

$$\hat{p}^e = C\hat{p}, \tag{12.55i}$$

$$\hat{u}_i = 0,\ i \in N_u, \tag{12.55j}$$

or after simplification

$$\min_{\hat{u}} \frac{1}{2}\hat{u}^T_{N_u} W_{N_u,N_u}\hat{u}_{N_u}, \tag{12.56a}$$

$$\mathbf{1}^T_{n_u}\hat{u} + \mathbf{1}_n r = 0. \tag{12.56b}$$

Stationary point of Lagrange function corresponding to (12.56) is defined by the following system of equations:

$$\hat{u}_i = \begin{cases} w_i^{-1}\hat{\lambda}, & \text{if } i \in N_u, \\ 0, & \text{if } i \notin N_u, \end{cases} \tag{12.57a}$$

$$\mathbf{1}^T_{n_u} W^{-1}_{N_u,N_u}\mathbf{1}_{n_u}\hat{\lambda} + \mathbf{1}^T_n r = 0. \tag{12.57b}$$

Lemma 12.5. *Let $u(t) \to \hat{u}^*$, then system (9.13) converges to the optimal type 2 steady-state.*

Proof. Variables $\hat{u}_i$ for $i \in N_u$ are excluded from the optimization problem (12.56). Taking them equal 0 makes the further proof equivalent to the proof of the Lemma 12.1. □

Transition from algebraic to control equations is presented:

$$u_i(t) = \begin{cases} w_i^{-1}\lambda(t), & \text{if } i \in N_u, \\ 0, & \text{if } i \notin N_u, \end{cases} \tag{12.58a}$$

$$\lambda(t) = -\int_0^t \mathbf{1}^T_n(u(\tau) + \mathring{r}(\tau))d\tau + \lambda_0. \tag{12.58b}$$

Block-diagram corresponding to the control equations is shown in Figure 12.2.

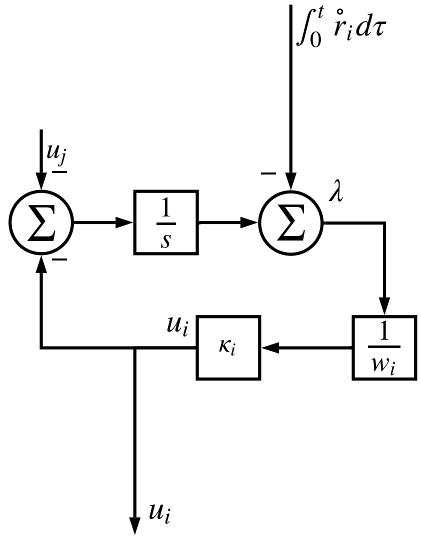

Figure 12.2: Control block diagram for the Problem 2.

12.2.3 Control stability and applicability

Similarly to the Problem 1, in order to prove control stability we need to analyze system

$$\dot{\lambda} = -\,\mathbf{1}_{n_u}^T W_{N_u,N_u}^{-1} \mathbf{1}_{n_u} \lambda - \mathbf{1}_n r + (\kappa_G^u)^T \operatorname{diag}(r_G^I)(p^m - \tilde{p}^m), \tag{12.59a}$$

$$\dot{p}^m = -\,(T^m)^{-1} p^m + (T^m)^{-1} v, \tag{12.59b}$$

$$\dot{v} = -\,(T^v)^{-1} v + (T^v)^{-1} W_{G,G}^{-1} \kappa_G^u \lambda, \tag{12.59c}$$

$$\dot{\tilde{p}}^m = -\,\tilde{T}^{-1} \tilde{p} + \tilde{T}^{-1} W_{G,G}^{-1} \kappa_G^u \lambda. \tag{12.59d}$$

Lemma 12.6. *In stationary point $(\lambda *, p^{m*}, v^*, \tilde{p}^{m*})$ of the system (12.59) λ^* coincides with $\hat{\lambda}^*$ in the solution of (12.56).*

Proof. It can be seen that in stationary point $(p^m)^* = (\tilde{p}^m)^*$. Thus, equation (12.59a) is equivalent to (12.57b) if $\dot{\lambda} = 0$. □

Theorem 12.7 (Control stability)**.** *Let*

$$\tilde{t}_i \leq \max\{t_i^m, t_i^v\},\ i \in G. \tag{12.60}$$

Then, system (12.19) is globally asymptotically stable.

Proof. The proof is equivalent to the proof of 12.3 with replacement of N with N_u and G with $G \cap N_u$. $\square$

Theorem 12.8 (Control applicability)**.** *Formulas*

$$F(y, W, \kappa^u) = W^{-1} \operatorname{diag}(\kappa^u) y, \tag{12.61}$$

$$G(\mathring{r}, u, y) = -\boldsymbol{1}_n^\top (u + \mathring{r}) \tag{12.62}$$

define controller functions for the Problem 2 with $s = 1$.

Proof. The proof is equivalent of the proof of the Theorem 12.4. Substitution of F and G into (12.54) gives system (12.58) with $y = \lambda$, thus item 1 of the Problem 2 is satisfied. From the Theorem 12.7 control u is global asymptotically stable and converges to a constant control, thus item 2 of the Problem 2 is satisfied. From the Lemma 12.6 u converges to $\hat{u}^*$ thus from Lemma 12.5, system (9.13) with the control u converges to the optimal type 2 steady-state. $\square$

12.3 Problem 3. Frequency control.

Here frequency control problem with control limits (9.5) is considered. It is assumed that the problem is feasible (control reserve is sufficient to restore power balance after the disturbance appearance):

$$\mathbf{1}_n^T \underline{u} \leq \mathbf{1}_n^T r \leq \mathbf{1}_n^T \overline{u}, \tag{12.63}$$

where $\underline{u}$ and $\overline{u}$ are lower and upper control limits respectively. As before control derivation is based on the formulation of optimization problem followed by introduction of integral equations. Main difference here is presence of the inequality constraints (9.5) that leads to appearance of complementary slackness equations and positiveness of some dual variables. Thus, a combination of approaches shown in sections 12.1 and 12.2 is used.

12.3.1 Problem statement

Definition 12.3. Optimal type 3 steady-state (OS3) is a point $(\hat{u}^*, \hat{\theta}^*, \hat{\omega}^*, \hat{p}^{m*}, \hat{v}^*, \hat{p}^*, \hat{p}^{e*})$ that delivers a solution of the following optimization problem:

$$\min_{\hat{u}, \hat{\theta}, \hat{\omega}, \hat{p}^m, \hat{v}, \hat{p}, \hat{p}^e} f(\hat{u}), \tag{12.64a}$$

$$(\hat{\theta}, \hat{\omega}, \hat{p}^m, \hat{v}, \hat{p}, \hat{p}^e) \in \Psi, \tag{12.64b}$$

$$\hat{u}_i \in [\underline{u}_i, \overline{u}_i],\ i \in N. \tag{12.64c}$$

Problem 3 (Frequency control)**.** *Let s be the size of auxiliary variables vector y. Then, it is required to find Lipschitz continuous controller functions*

$$F : \mathbb{R}^s \times \mathbb{R}^{n\times n} \times \mathbb{R}^n \times \mathbb{R}^n \to \mathbb{R}^n, \tag{12.65a}$$

$$G : \mathbb{R}^n \times \mathbb{R}^n \times \mathbb{R}^s \to \mathbb{R}^s, \tag{12.65b}$$

such that

1. *Control u is defined by a system of integral-algebraic equations*

$$u(t) = F(y(t), W, \underline{u}, \overline{u}), \tag{12.66a}$$

$$y(t) = \int_0^t G(\mathring{r}(\tau), u(\tau), y(\tau))d\tau + y^0. \tag{12.66b}$$

2. *Control u must be globally asymptotically stable.*

3. $u_i(t) \in [\underline{u}_i, \overline{u}_i],\ i \in N,\ t \geq 0.$

4. *System (9.13) with control u must converge to OS3.*

12.3.2 Optimal steady-state and control equations

Let us introduce the following control participation minimization problem:

$$\min_{\hat{\theta},\hat{\omega},\hat{p}^m,\hat{v},\hat{p},\hat{p}^e,\hat{u}} f(\hat{u}), \tag{12.67a}$$

$$0 = \hat{\omega}, \tag{12.67b}$$

$$0 = -D_{G,G}\hat{\omega}_G - \hat{p}^e_G + \hat{p}^m + r_G, \tag{12.67c}$$

$$0 = -\hat{p}^m + \hat{v}, \tag{12.67d}$$

$$0 = -\hat{v} + \hat{u}_G, \tag{12.67e}$$

$$0 = -D_{L_1,L_1}\hat{\omega}_{L_1} - \hat{p}^e_{L_1} + \hat{u}_{L_1} + r_{L_1}, \tag{12.67f}$$

$$0 = -D_{L_0,L_0}\hat{\omega}_{L_0} - \hat{p}^e_{L_0} + \hat{u}_{L_0} + r_{L_0}, \tag{12.67g}$$

$$\hat{p} = BC^T\hat{\theta}, \tag{12.67h}$$

$$\hat{p}^e = C\hat{p}, \tag{12.67i}$$

$$\underline{u} \leq \hat{u} \leq \overline{u}, \tag{12.67j}$$

or after simplification

$$\min_{\hat{u}} \frac{1}{2}\hat{u}^T W \hat{u}, \tag{12.68a}$$

$$\mathbf{1}_n^T(\hat{u} + r) = 0, \tag{12.68b}$$

$$\underline{u} \leq \hat{u} \leq \overline{u}. \tag{12.68c}$$

Lagrange function, corresponding to the optimization problem (12.68):

$$L(\hat{u}, \hat{\lambda}, \hat{\underline{\chi}}, \hat{\overline{\chi}}) = \frac{1}{2}\hat{u}^T W \hat{u} - \hat{\lambda}\mathbf{1}_n^T(\hat{u} + r) + \hat{\underline{\chi}}^T(\underline{u} - \hat{u}) + \hat{\overline{\chi}}^T(\hat{u} - \overline{u}). \tag{12.69}$$

According to the Karush–Kuhn–Tucker condition [14] solution of (12.68) is given by the following system of equations:

$$\hat{u} = W^{-1}\left(\mathbf{1}_n\hat{\lambda} + \hat{\underline{\chi}} - \hat{\overline{\chi}}\right), \tag{12.70a}$$

$$\mathbf{1}_n^T(\hat{u} + r) = 0, \tag{12.70b}$$

$$\hat{\underline{\chi}}_i(\underline{u}_i - \hat{u}_i) = 0,\ \hat{\underline{\chi}}_i \geq 0,\ i \in N, \tag{12.70c}$$

$$\hat{\overline{\chi}}_i(\hat{u}_i - \overline{u}_i) = 0,\ \hat{\overline{\chi}}_i \geq 0,\ i \in N. \tag{12.70d}$$

As complementary slackness is represented by nonlinear equations transition to integral equations must be done differently from the previous sections. Derivation of integral equations is based on the following idea. Let us assume that at some moment $t_0 \geq 0$ all components of the vectors $u(t_0)$ are within their limits. Then, control within some neighbourhood of t_0 can be defined by the system (12.16). Let $t_1 > t_0$ be the first time at least one component of control vector reaches its limit. Then, at the moment t_1 control switches to form (12.58) where N_u is a set of control components at upper or lower limit with new disturbance vector

$$\mathring{r}_i^{new}(u_i(t)) = \begin{cases} \mathring{r}_i + u_i(t), & \text{if } i \in N_u, \\ \mathring{r}_i, & \text{if } i \notin N_u. \end{cases} \tag{12.71}$$

Thus, control component that reached its limit is interpreted as a part of disturbance vector. As a result, we replace KKT conditions with the following.

$$\hat{u} = \nu^n(W^{-1}\mathbf{1}_n\hat{\lambda}, \underline{u}, \overline{u}), \tag{12.72a}$$

$$0 = -\mathbf{1}_n^T(\hat{u} + r), \tag{12.72b}$$

where function $\nu^n : \mathbb{R}^n \times \mathbb{R}^n \times \mathbb{R}^n \to \mathbb{R}^n$,

$$\nu_i^n(x, y, z) = \max\{\min\{x_i, y_i\}, z_i\},\ i \in \{1, \dots, n\}. \tag{12.73}$$

As a result,control has the following form:

$$u(t) = \nu^n(W^{-1}\mathbf{1}_n\lambda(t), \underline{u}, \overline{u}), \tag{12.74a}$$

$$\lambda(t) = \int_0^t -\mathbf{1}_n^T \left(u(\tau) - \mathring{r}(\tau)\right) d\tau + \lambda_0, \tag{12.74b}$$

Corresponding control diagram is given in the Figure 12.3.

Lemma 12.9. *Solutions of the systems (12.70) and (12.72) are same in $\hat{u}$ and $\hat{\lambda}$.*

Proof. Let us consider one of the control components $\hat{u}_i$. If control limits are not active, then from (12.70a), $\hat{\underline{\chi}}_i = \hat{\overline{\chi}}_i = 0$ and $\hat{u}_i = w_i^{-1}\hat{\lambda}$. If control reaches its upper limit, then dual variable corresponding to the lower limit is equal to zero: $\hat{\underline{\chi}}_i = 0$. Additionally, $\hat{u}_i + \hat{\overline{\chi}}_i = w_i^{-1}\hat{\lambda}$; therefore, $\hat{u}_i \le w_i^{-1}\hat{\lambda}$. Similarly, if lower limit is active, $\hat{u}_i \ge w_i^{-1}\hat{\lambda}$, thus,

$$\hat{u} = \nu^n(W^{-1}\mathbf{1}_n\hat{\lambda}, \underline{u}, \overline{u}), \tag{12.75a}$$

$$\hat{\overline{\chi}}_i = \begin{cases} w_i^{-1}\hat{\lambda} - u, & \text{if } w_i^{-1}\hat{\lambda} \ge \hat{u}, \\ 0, & \text{if } w_i^{-1}\hat{\lambda} < \hat{u}, \end{cases} \tag{12.75b}$$

$$\hat{\underline{\chi}}_i = \begin{cases} \hat{u} - w_i^{-1}\hat{\lambda}, & \text{if } \hat{u} \ge w_i^{-1}\hat{\lambda}, \\ 0 & \text{if } \hat{u} < w_i^{-1}\hat{\lambda}. \end{cases} \tag{12.75c}$$

Substitution of (12.75a) into the first two equations of (12.70) gives

$$\hat{u} = \nu^n(W^{-1}\mathbf{1}_n\hat{\lambda}, \underline{u}, \overline{u}), \tag{12.76a}$$

$$0 = -\mathbf{1}_n^T(\hat{u} + r). \tag{12.76b}$$

Equations (12.75b) and (12.75c) ensure execution of complementary slackness conditions (12.70c) and (12.70d). Therefore, solutions of (12.70) and (12.76) have equivalent u and λ. However, system (12.76) delivers stationary point of (12.77). Thus, stationary point is unique and delivers solution of the optimization problem (12.68). □

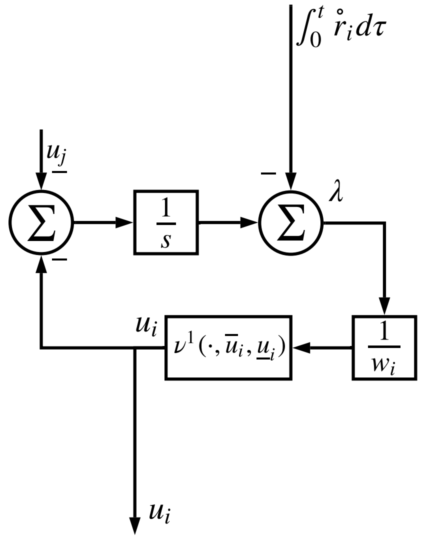

Figure 12.3: Control block diagram for the Problem 3.

Lemma 12.10. *Let $u(t) \to \hat{u}^*$, then system (9.13) converges to the optimal type 3 steady-state.*

Proof. Constraints (12.68c) ensure control to be remain within the acceptable limits. Otherwise optimal type 1 steady-state is similar to the optimal type 3 steady-state and further proof of this lemma coincides with the proof of Lemma 12.1. □

12.3.3 Control properties

Let us reduce equations (12.74), (9.13c), (9.13d) to a system of algebraic differential equations:

$$u = \nu^n(W^{-1}\mathbf{1}_n\lambda, \underline{u}, \overline{u}), \tag{12.77a}$$

$$\dot{\lambda} = -\mathbf{1}_n^T(u + \mathring{r}), \tag{12.77b}$$

$$\dot{p}^m = -(T^m)^{-1}p^m + (T^m)^{-1}v, \tag{12.77c}$$

$$\dot{v} = -(T^v)^{-1}v + (T^v)^{-1}u_G, \tag{12.77d}$$

$$\dot{\tilde{p}}^m = -\tilde{T}^{-1}\tilde{p}^m + \tilde{T}^{-1}u_G. \tag{12.77e}$$

System (12.77) is a piecewise linear system, thus we use the following matrix form:

$$\dot{x} = A(x)x + R, \tag{12.78}$$

where $A(x)$ is a piecewise constant function. The following lemmas are applicable for this system:

Lemma 12.11. *Stationary point $(u^*, \lambda^*, p^{m*}, v^*, \tilde{p}^{m*})$ of the system (12.77) delivers solution $(\hat{u}^*, \hat{\lambda}^*)$ of the optimization problem (12.68).*

Proof. The proof is similar to the proof of Lemma (12.2). □

Lemma 12.12. *Let*

$$\tilde{t}_i \leq \max\{t_i^m, t_i^v\}, \; i \in G. \tag{12.79}$$

Then, matrix $A(x)$ of the system (12.78) for any $x = (u, \lambda, p^m, v, \tilde{p}^m)$ is negative definite.

Proof. For a fixed x let us define vector $\kappa^u(x) \in \mathbb{R}^n$ in the following way:

$$\kappa_i^u(x) = \begin{cases} 0, & u_i > \overline{u}_i \text{ or } u_i < \underline{u}_i, \\ 1, & \text{otherwise.} \end{cases} \tag{12.80}$$

Then result of the Theorem 12.7 gives negative definiteness of the matrix $A(x)$. □

Here we cannot prove global asymptotic stability as negative-definiteness of the system matrix at any point is not a sufficient condition (counterexamples can be found in [100]). Thus, in the further section we adjust disturbance approximation algorithm.

12.3.4 Disturbance estimation approach

Control scheme in the previous section requires knowledge of frequency deviations and electrical powers on each bus. However, according to generating unit structure described in section (6.2), each generation unit can measure ω and p^e. This generating unity can always be represented as a separate bus. As generating unit consumption (e.g. for excitation unit) is known, thus, r_i is also a known value. According to formulas (11.5c), (11.5c) value of $\int_0^t r_i d\tau$ can be measured exactly, $\int_0^t r_i d\tau = \int_0^t \mathring{r}_i d\tau$ (Figure 12.4). Hence further results are obtained after the following model modification:

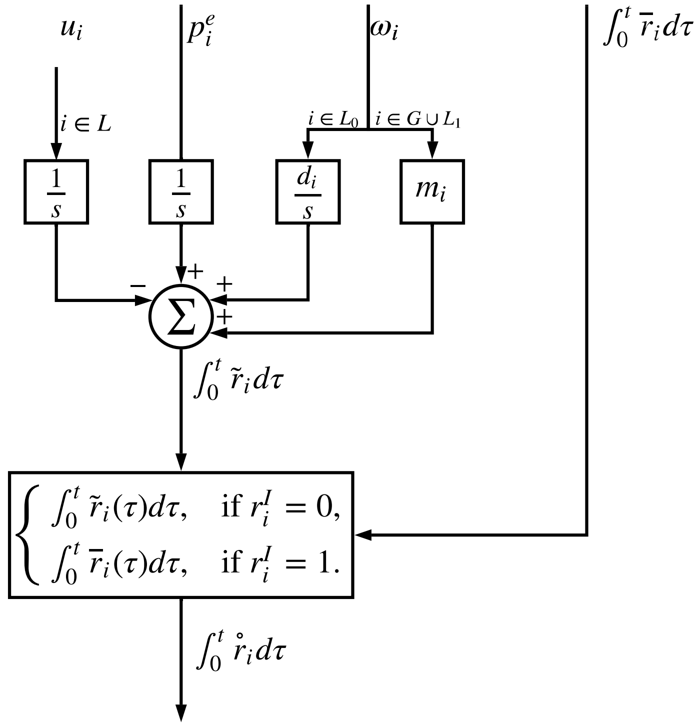

Figure 12.4: Updated disturbance approximation block diagram.

- System graph Γ is constructed so generating buses from G consist only of generating units;
- Values r_i are known ($i \in G$) for generator buses;
- Values $\int_0^t r_i d\tau$ are known for load buses.

12.3.5 Control stability and applicability

Due to the exclusion of the disturbances on the generator buses we analyse stability of the system

$$u = \nu^n(W^{-1}\mathbf{1}_n\lambda, \underline{u}, \overline{u}), \tag{12.81a}$$

$$\dot{\lambda} = -\mathbf{1}_n^T(u + \mathring{r}). \tag{12.81b}$$

Proof of the system (12.81) stability requires the following lemma:

Lemma 12.13. *Let* $Y_1 = \nu^1(x_1, \underline{x}, \overline{x}) - \nu^1(x_2, \underline{x}, \overline{x})$, $Y_2 = x_1 - x_2$. *Then,* $Y_1 Y_2 \geq 0$. *If* $x_1 \neq x_2$ *and* $\underline{x} < x_2 < \overline{x}$, *then* $Y_1 Y_2 > 0$.

Proof. If $x_1 = x_2$, then $Y_1 = Y_2 = 0$ and lemma's statement holds. If $x_1 > x_2$, then $Y_2 > 0$ and there exist 3 cases:

1. $x_1 \leq \underline{x}$, then $Y_1 = 0$;

2. $\underline{x} \leq x_2 < \overline{x}$, then $Y_1 > 0$;

3. $x_2 > \overline{x}$, then $Y_1 = 0$.

In all this cases lemma's statement holds. Let $x_1 < x_2$ and $Y_2 < 0$, then similarly to the previous case there exist 3 cases:

1. $x_1 \geq \overline{x}$, then $Y_1 = 0$;

2. $\underline{x} < x_2 \leq \overline{x}$, then $Y_1 < 0$;

3. $x_2 < \underline{x}$, then $Y_1 = 0$.

In all this cases lemma's statement holds. □

Theorem 12.14 (Control stability)**.** *System (12.77) is globally asymptotically stable.*

Proof. Let u^*, λ^* be stationary point of the system (12.81). Then, system (12.81) is equivalent to the following:

$$\dot{\lambda} = -\mathbf{1}_n^T \left(\nu^n(W^{-1}\mathbf{1}_n\lambda, \underline{u}, \overline{u}) - \nu^n(W^{-1}\mathbf{1}_n\lambda^*, \underline{u}, \overline{u}) \right). \tag{12.82}$$

Thus, the following Lyapunov function can be used for the stability proof:

$$V(\lambda) = \frac{1}{2}(\lambda - \lambda^*)^2. \tag{12.83}$$

It derivative:

$$\begin{aligned} \dot{V}(\lambda) &= -\mathbf{1}_n^T \left(\nu^n(W^{-1}\mathbf{1}_n\lambda, \underline{u}, \overline{u}) - \nu^n(W^{-1}\mathbf{1}_n\lambda^*, \underline{u}, \overline{u}) \right)(\lambda - \lambda^*) = \\ &= -\sum_{i \in N} \frac{1}{w_i} \left(\nu^1(\lambda_i, w_i\underline{u}_i, w_i\overline{u}_i) - \nu^1(\lambda_i^*, w_i\underline{u}_i, w_i\overline{u}_i) \right)(\lambda - \lambda^*). \end{aligned} \tag{12.84}$$

According to the lemma 12.13 derivative of the Lyapunov function is negative if there exists at least one index i_0 such that $\underline{u}_{i_0} < \frac{1}{w_{i_0}}\lambda^* < \overline{u}_{i_0}$. In this case function λ and consequently function u are asymptotically stable. Otherwise set N can be divided into 2 subsets $\underline{N}$ and $\overline{N}$ such that $\frac{1}{w_i}\lambda^* = \underline{u}_i$ for $i \in \underline{N}$ and $\frac{1}{w_i}\lambda^* = \overline{u}_i$ for $i \in \overline{N}$ (if for some i_0 $\underline{u}_{i_0} = \overline{u}_{i_0}$, then i_0 belongs to both sets). Then,

$$\ker \dot{V} = \left\{ \lambda : \frac{1}{w_i}\lambda \le \underline{u}_i, i \in \underline{N} \setminus \overline{N} \text{ and } \frac{1}{w_i}\lambda \ge \overline{u}_i, i \in \overline{N} \setminus \underline{N} \right\}. \tag{12.85}$$

According to Barbashin-Krasovsky theorem any solution of the system (12.82) converges to trajectory fully belonging to $\ker \dot{V}$. Thus,

$$u(t) = \nu^n(W^{-1}\mathbf{1}_n\lambda, \underline{u}, \overline{u}) \to \nu^n(W^{-1}\mathbf{1}_n\lambda^*, \underline{u}, \overline{u}) = u^*, \tag{12.86}$$

which proves global asymptotic stability of the control u. □

Theorem 12.15 (Control applicability)**.** *Formulas*

$$F(y, W, \overline{u}, \underline{u}) = \nu^n(W^{-1}\boldsymbol{1}_n y, \overline{u}, \underline{u}), \tag{12.87}$$

$$G(\mathring{r}, u, y) = -\boldsymbol{1}_n^\top(u + \mathring{r}). \tag{12.88}$$

define controller functions for the Problem 2 with $s = 1$.

Proof. The proof is equivalent of the proof of the Theorem 12.4. Substitution of F and G into (12.66) gives system (12.74) with $y = \lambda$, thus item 1 of the Problem 3 is satisfied. From the Theorem 12.14 control u is global asymptotically stable and converges to a constant control, thus item 2 of the Problem 3 is satisfied. From the Lemma 12.11 u converges to $\hat{u}^*$ thus from Lemma 12.10, system (9.13) with the control u converges to the optimal type 3 steady-state. □

12.4 Numerical experiment

New England System is used for the numerical experiments [8]. Parameters of the system are given in the tables 7.1 and 7.2. Turbine and governor constants are taken from [90]. Partial outage of 100 MW appears on the generator 10. As a consequence of the outage, generator G10 does not participate in the further control actions. It is assumed that only

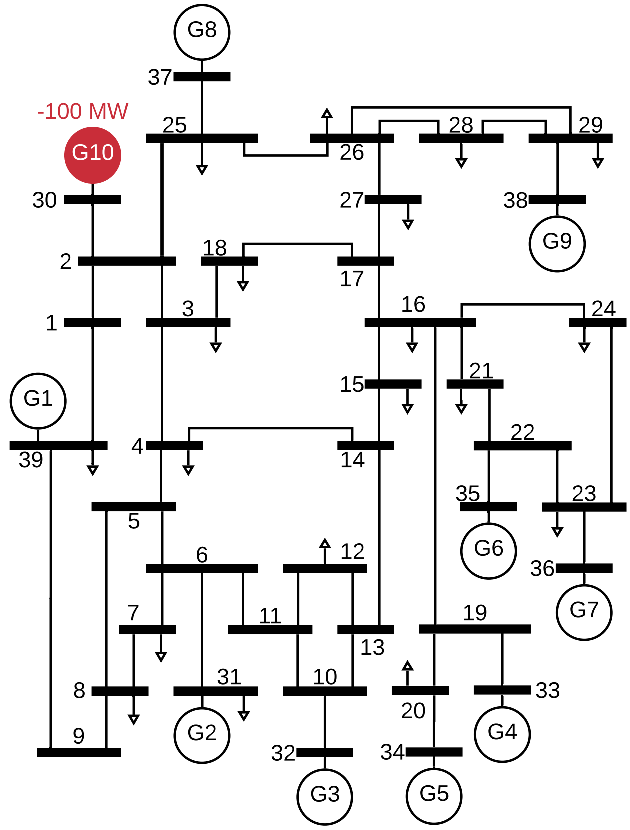

Figure 12.5: New England network

generators participate in the control and participation factors w_i for every generator are equal 1, thus, after transient each generator should increase its output by 11.1 MW. Three control types are considered: (1) traditional primary and secondary frequency controls $(u^I + u^{II})$, (2) developed control (u), (3) developed control summed with primary frequency control $(u + u^I)$. Figure (12.7) has control signals graphs for all three types of control, corresponding frequency responses are show in the Figure (12.6). It can be seen that control u provides fast convergence speed; however, it does not reduce nadir in comparison to the traditional control. Numerical experiments show that the best frequency response can be obtained by adding primary frequency control to the developed one. Such modification does not improve convergence speed; however, reduces nadir. Primary frequency control is represented by the proportional controller and its signal converges to 0, thus, such modification does not change post-transient state of the system.

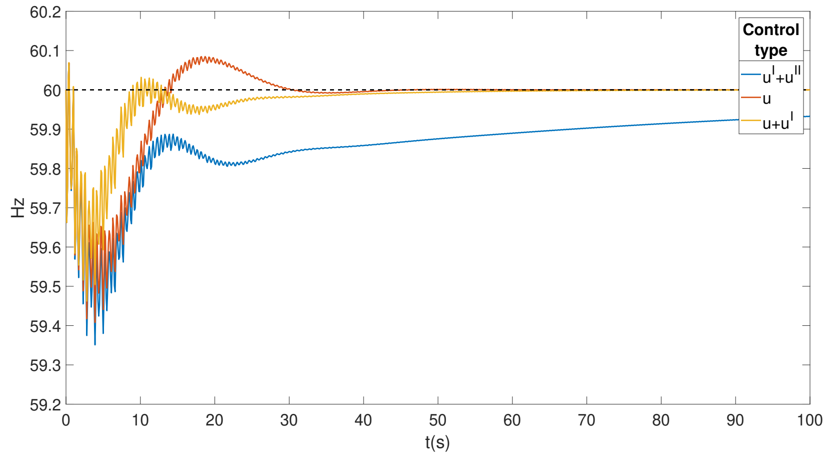

Figure 12.6: System frequencies for different control types.

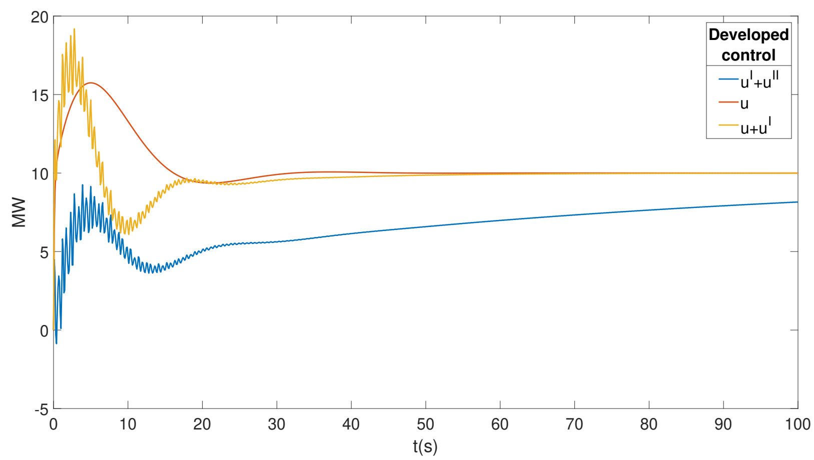

Figure 12.7: Control signals.

12.5 Conclusion

The presented approach separates disturbance approximation step and control calculation steps. Frequency in power system is restored if and only if sum of the control values is equal to the sum of elements of the disturbance vector; thus, every single frequency control approximates the disturbance size in some way. Here we explicitly separate disturbance approximation into a specific stage. Although the derived approximation depends on the state of the physical system, it converges to a vector that does not depend on it (disturbance vector). Compared to traditional control scheme, where only frequency deviations are used, such approach provides significantly more reliable input to the control calculation stage. Thus control can provide faster response without stability loss. Moreover, the second stage can take as input values of some or all disturbance vector components, if the latter are available by some other measurements. As a result, the derived approach provides fast frequency restoration using only frequency and electrical power, disturbance measurements or combinations of them. Moreover, based on the type of the input it can operate as feedback, feedforward or mixed type control. Currently the control is centralized.

The control is derived as a system of piece wise linear integral algebraic equations:

$$u(t) = \nu^n(W^{-1}\mathbf{1}_n\lambda(t), \underline{u}, \overline{u}), \tag{12.89a}$$

$$\lambda(t) = \int_0^t -\mathbf{1}_n^T \left(u(\tau) - \mathring{r}(\tau)\right) d\tau + \lambda_0. \tag{12.89b}$$

Here equation (12.89b) is corresponding to the power balance in the system, while (12.89a) is used to cut $W^{-1}\mathbf{1}_n\lambda$ and keep values of u within the control limits.

13 Decentralized control

13.1 Problem 4. Distributed frequency control without control limits.

Section 7.4 describes limitation of secondary frequency control response speed due to centralization requirement. If load side control implemented in addition to generators control, this problem becomes even more significant due to increased amount of controllable buses. Thus, we derive control that requires only communication between adjacent buses for its operation. Thus, control on each bus can observe only local measurements of frequency deviations ω_i and electrical power p_i^e, local values of system parameters $m_i,\ d_i,\ w_i$, and line parameters b_{ij} of adjacent lines. Thus, each regulator has only local information and does not need any information about the rest of the system. As a result, overall number of controllable buses does not affect amount of local communications.

13.1.1 Problem statement

Let us denote

$$n_\Gamma = \max_{i \in N} |\operatorname{Adj}(i)|. \tag{13.1}$$

Within this section distributed control is derived. Therefore, instead of functions F and G that cover all control variables we introduce functions F and G^h that would operate on each bus separately from each other. Nevertheless, communication between neighbors is allowed. Arguments of the function G include information from the other buses. The type of information is discussed further. However, dimension of the input parameters for G^h depends on the number of the neighboring buses. Therefore, instead of introducing one function G here a set of functions G^h is introduced for buses that have h neighbors. Thus, h is taken from the set $\{1, \ldots, n_\Gamma\}$.

Problem 4 (Distributed frequency control without control limits)**.** *Let s be the size of auxiliary variables vector y. Then, it is required to find Lipschitz continuous controller functions*

$$F : \mathbb{R}^s \times \mathbb{R} \to \mathbb{R}, \tag{13.2a}$$

$$G^h : \mathbb{R} \times \mathbb{R} \times \mathbb{R}^s \times \mathbb{R}^{h \times s} \to \mathbb{R}^s, \tag{13.2b}$$

such that

1. *Control u is defined by a system of integral-algebraic equations*

$$u_i(t) = F(y^i(t), w_i), \; i \in N, \tag{13.3a}$$

$$y^i(t) = \int_0^t G^{|\operatorname{Adj}(i)|}(\mathring{r}_i(\tau), u_i(\tau), y^i(\tau), Y^i(\tau))d\tau + y^{i0}, \; i \in N, \tag{13.3b}$$

   where Y^i is a matrix that consists of columns y^i, $i \in \operatorname{Adj}(i)$.

2. *Control u must be globally asymptotically stable.*

3. *System (9.13) with control u must converge to OS1.*

Here the form of the control equations (13.3) is used to introduce decentralization requirement. Here each vector y^i, $i \in N$ is vector of local auxiliary variables. In order to calculate control functions u_i in (13.3a) only local y^i and participation factor w_i are used. Communication between neighbors is implemented in (13.3b) through the usage of the second argument which consists of the neighboring buses auxiliary variables. It can be seen, that only $\int_0^t r d\tau$ is the parameter from the physical system (9.13). Calculation of these integrals is discussed in section 12.3.4. In order to calculate scalar $\int_0^t r_i d\tau$ for some $i \in N$ only information from bus i is needed. Thus, vectors y^i are the only ones use by neighboring buses.

It can be seen that unlike in previous sections function F defines local control values u_i using only local and adjacent auxiliary variables y^i and all measurements are only used locally.

13.1.2 Optimal steady-state and control equations

Problem (12.4) is taken as initial optimization problem; however, now instead of reducing it to (12.3) it is reduced to

$$\min_{\hat{u},\hat{\theta}} f(\hat{u}), \tag{13.4a}$$

$$-CBC^T\hat{\theta} + \hat{u} + r = 0. \tag{13.4b}$$

Here line parameters B are used. It is possible to exclude them and transition to the following optimization problem

$$\min_{\hat{\eta},\hat{u}} f(\hat{u}), \tag{13.5a}$$

$$CC^{\top}\hat{\eta} - \hat{u} - r = 0. \tag{13.5b}$$

For this problem we proof the following lemma.

Lemma 13.1. *Let $(\hat{\theta}^{\#}, \hat{u}^{\#1})$ and $(\hat{\eta}^{\#}, \hat{u}^{\#2})$ be solutions (13.4) and (13.5) respectively. Then, $\hat{u}^{\#1} = \hat{u}^{\#2}$.*

Proof. According to the Fredholm theorem [101] solutions of (13.4b) has a solution if and only if

$$\begin{gathered}\hat{u} \in \{\hat{u} \in \mathbb{R}^n \mid \exists \hat{\theta} : CBC^{\top}\hat{\theta} = \hat{u} + r\} = \{\hat{u} \in \mathbb{R}^n \mid (\hat{u}+r)^T z = 0 \; \forall z \in \ker CBC^T\} = \\ \{\hat{u} \in \mathbb{R}^n \mid (\hat{u}+r)^T z = 0 \; \forall z \in \ker CC^T\} = \{\hat{u} \in \mathbb{R}^n \mid \exists \hat{\eta} : CC^{\top}\hat{\eta} = \hat{u} + r\}.\end{gathered} \tag{13.6}$$

The derived statement proves the lemma. □

Definition 13.1. Variable $\hat{\eta}$ is used as a replacement for the phase angles, therefore everywhere further we will refer to it as to the vector of virtual phase angles.

Definition 13.2. Similarly to virtual phase angles we denote $\hat{\pi} = C^T\hat{\eta}$ virtual power flows.

Then, equation (13.5b) in the optimization problem (13.5) can be interpreted as following: it is a power balance equations; however, power exchange between buses is described via virtual variables linearly dependent on real power flows.

Lagrange function is given by

$$\mathcal{L}(\hat{u}, \hat{\eta}, \hat{\lambda}) = \frac{1}{2}\hat{u}^T W \hat{u} - \hat{\lambda}^T(-CC^T\hat{\eta} + \hat{u} + r). \tag{13.7}$$

Corresponding stationary point:

$$W\hat{u} = \hat{\lambda}, \tag{13.8a}$$

$$CC^T\hat{\lambda} = 0, \tag{13.8b}$$

$$-CC^T\hat{\eta} + \hat{u} + r = 0. \tag{13.8c}$$

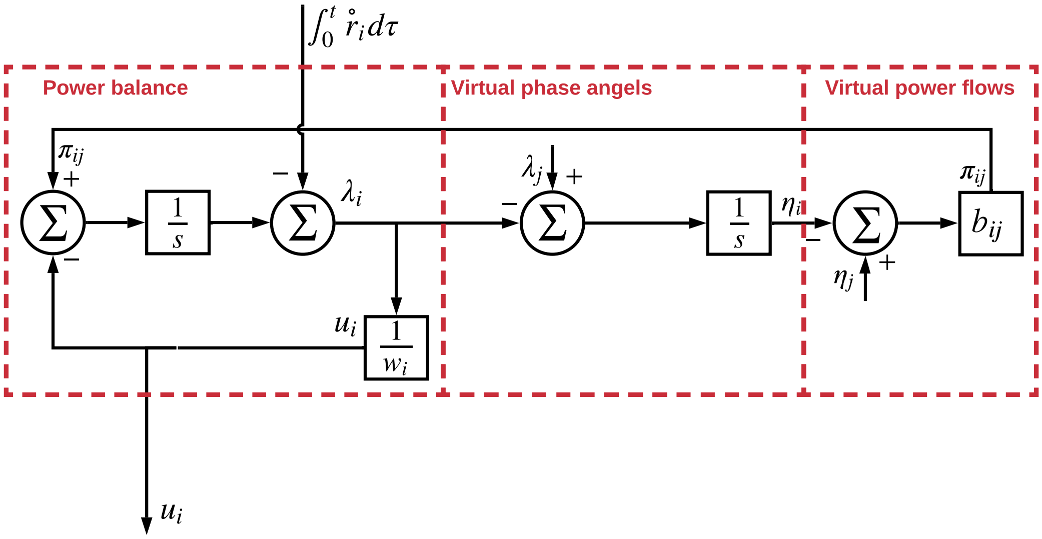

Figure 13.1: Control block diagram for the Problem 4.

Lemma 13.2. *Let $u(t) \to \hat{u}^*$, then system (9.13) converges to the optimal type 1 steady-state.*

Proof. Proof of this lemma coincides with the proof of Lemma 12.1. □

Transition to control equations:

$$u(t) = W^{-1}\lambda(t), \tag{13.9a}$$

$$\eta(t) = -\int_0^t CC^T\lambda(\tau)d\tau + \eta^0, \tag{13.9b}$$

$$\lambda(t) = \int_0^t CC^T\eta(\tau) - u(\tau) - \mathring{r}d\tau + \lambda^0. \tag{13.9c}$$

Block-diagram corresponding to the control equations are shown in Figure 13.1.

13.1.3 Control stability and applicability

As before system (13.9) is reduced to a system of differential equations:

$$u = W^{-1}\lambda, \tag{13.10a}$$

$$\dot{\eta} = -CC^T\lambda, \tag{13.10b}$$

$$\dot{\lambda} = CC^T\eta - W^{-1}\lambda - \mathring{r}. \tag{13.10c}$$

Lemma 13.3. *Stationary points of the system (13.10) coincide with the solutions of (13.4).*

Proof. It can be seen that if $\dot{\eta} = 0$ and $\dot{\lambda} = 0$ then the system (13.10) is the same as the equations of stationary point for the Lagrange function (13.8), thus, the lemma statement holds. □

Theorem 13.4 (Control stability). *In the system (13.10) solutions u and λ are globally asymptotically stable.*

Proof. Let u^*, λ^*, η^* be stationary point of (13.10). Let us introduce Lyapunov function:

$$V(\lambda, \eta) = \frac{1}{2}\left((\lambda - \lambda^*)^T(\lambda - \lambda^*) + (\eta - \eta^*)^T(\eta - \eta^*)\right). \tag{13.11}$$

Then,

$$\begin{aligned} \dot{V}(\lambda, \eta) = (\lambda - \lambda^*)^T(CC^T(\eta - \eta^*) - W^{-1}(\lambda - \lambda^*)) + (\eta - \eta^*)^T CC^T(\lambda - \lambda^*) = \\ = (\lambda - \lambda^*)^T W^{-1}(\lambda - \lambda^*) \leq 0. \end{aligned} \tag{13.12}$$

Lyapunov function derivative is negative definite over λ. Thus, system (13.10) is globally asymptotically stable over λ and u. □

Theorem 13.5 (Control applicability). *Formulas*

$$F(y^i, w_i) = \frac{y_2^i}{w_i}, \tag{13.13}$$

$$G_1^h(\mathring{r}_i, u_i, y^i, Y^i) = -hy_2^i + \mathbf{1}_h^\top (Y_2^i)^T, \tag{13.14}$$

$$G_2^h(\mathring{r}_i, u_i, y^i, Y^i) = hy_1^i - \mathbf{1}_h^\top (Y_1^i)^\top - u_i - \mathring{r}_i. \tag{13.15}$$

define controller functions for the Problem 4 with $s = 2$.

Proof. We take

$$y^i = \begin{pmatrix} \eta_i \\ \lambda_i \end{pmatrix}, \ i \in N. \tag{13.16}$$

Element-wise form of the equation (13.9a) is given by:

$$u_i = \frac{\lambda_i}{\omega_i}, \tag{13.17}$$

thus

$$F(y^i, w_i) = \frac{y_2^i}{w_i}. \tag{13.18}$$

In the equations (13.9b) and (13.9c) matrix CC^T is Laplace matrix of the graph Γ. Thus, its elements are given by

$$(CC^T)_{ii} = |Adj(i)|, \ i \in N, \tag{13.19}$$

$$(CC^T)_{ij} = \begin{cases} -k, & \text{if } k \text{ is number of the line } ij, \\ 0, & \text{if there is no line between} i \text{ and } j. \end{cases} \tag{13.20}$$

Thus, equation (13.9b) has the following element-wise representation:

$$\eta_i(t) = \int_0^t \sum_{j \in Adj(i)} (\lambda_j(\tau) - \lambda_i(\tau)) d\tau + \eta_i^0. \tag{13.21}$$

Thus, the first component of G is given by

$$G_1^h(\mathring{r}_i, u_i, y^i, Y^i) = -hy_2^i + \mathbf{1}_h^\top (Y_2^i)^T. \tag{13.22}$$

Similarly equation (13.9c) can be represented as:

$$\lambda(t) = \int_0^t \sum_{j \in Adj(i)} (\eta_i(\tau) - \eta_j(\tau)) - u_i(\tau) - \mathring{r}(\tau) d\tau + \lambda_i^0. \tag{13.23}$$

From the equations (11.10) component Y_2 has the following form:

$$G_2^h(\mathring{r}_i, u_i, y^i, Y^i) = hy_1^i - \mathbf{1}_h^\top (Y_1^i)^\top - u_i - \mathring{r}_i. \tag{13.24}$$

From the Theorem 13.4 control u is global asymptotically stable and converges to a constant control, thus item 2 of the Problem 4 is satisfied. From the Lemma 13.3 u converges to $\hat{u}^*$ thus from Lemma 13.2, system (9.13) with the control u converges to the optimal type 3 steady-state. □

13.2 Problem 5. Distributed frequency control.

Here we add control limits (9.5). As before the control scheme must be distributed. Here control limits will be introduced similarly to the way they were introduced into the Problem 3.

13.2.1 Problem statement

Problem 5 (Distributed frequency control)**.** *Let s be the size of auxiliary variables vector y. Then, it is required to find Lipschitz continuous controller functions*

$$F : \mathbb{R}^s \times \mathbb{R} \times \mathbb{R} \times \mathbb{R} \to \mathbb{R}, \tag{13.25a}$$

$$G^h : \mathbb{R} \times \mathbb{R} \times \mathbb{R}^s \times \mathbb{R}^{h\times s} \to \mathbb{R}^s, \tag{13.25b}$$

such that

1. *Control u is defined by a system of integral-algebraic equations*

$$u_i(t) = F(y^i(t), w_i, \underline{u}_i, \overline{u}_i),\ i \in N, \tag{13.26a}$$

$$y^i(t) = \int_0^t G^{|\operatorname{Adj}(i)|}(\mathring{r}_i(\tau), u_i(\tau), y^i(\tau), Y^i(\tau))d\tau + y^{i0},\ i \in N. \tag{13.26b}$$

2. *Control u must be globally asymptotically stable.*

3. $u_i(t) \in [\underline{u}_i, \overline{u}_i],\ i \in N,\ t \geq 0.$

4. *System (9.13) with control u must converge to OS3.*

13.2.2 Optimal steady-state and control equations

Problem (13.5) is taken as initial and substituted with control limits:

$$\min_{\hat{u},\hat{\eta}} f(\hat{u}), \tag{13.27a}$$

$$-CC^T\hat{\eta} + \hat{u} + r = 0, \tag{13.27b}$$

$$\underline{u} \leq \hat{u} \leq \overline{u}. \tag{13.27c}$$

Lagrange function is given by

$$\mathcal{L}(\hat{u}, \hat{\eta}, \hat{\lambda}, \hat{\overline{\chi}}, \hat{\underline{\chi}}) = \frac{1}{2}\hat{u}^T W\hat{u} - \hat{\lambda}^T(-CC^T\hat{\eta} + \hat{u} + r) + \hat{\overline{\chi}}^T(\hat{u} - \overline{u}) + \hat{\underline{\chi}}^T(\underline{u} - \hat{u}). \tag{13.28}$$

Corresponding Karush–Kuhn–Tucker conditions with complementary slackness replacement introduced in (13.30):

$$W\hat{u} - \hat{\lambda} + \hat{\overline{\chi}} - \hat{\underline{\chi}} = 0, \tag{13.29a}$$

$$CC^T\hat{\lambda} = 0, \tag{13.29b}$$

$$-CC^T\hat{\eta} + \hat{u} + r = 0, \tag{13.29c}$$

$$\hat{\overline{\chi}}_i(\hat{u}_i - \overline{u}_i) = 0,\ \hat{\overline{\chi}}_i \geq 0,\ i \in N, \tag{13.29d}$$

$$\hat{\underline{\chi}}_i(\underline{u}_i - \hat{u}_i) = 0,\ \hat{\underline{\chi}}_i \geq 0,\ i \in N. \tag{13.29e}$$

The following substitution is used:

$$\hat{u} = \nu^n(W^{-1}\hat{\lambda}, \overline{u}, \underline{u}). \tag{13.30}$$

As a result optimal point is defined by a system of piece-wise linear system of equations:

$$CC^T\hat{\lambda} = 0, \tag{13.31a}$$

$$-CC^T\hat{\eta} + \hat{u} + r = 0, \tag{13.31b}$$

$$\hat{u} = \nu^n(W^{-1}\hat{\lambda}, \overline{u}, \underline{u}). \tag{13.31c}$$

Lemma 13.6. *Let $u(t) \to \hat{u}^*$, then system (9.13) converges to the optimal type 3 steady-state.*

Proof. Proof of this lemma coincides with the proof of Lemma 12.10. □

Transition to control equations:

$$\begin{aligned} u(t) =& \nu^n(W^{-1}\lambda(t), \overline{u}, \underline{u}), & (13.32a)\\ \eta(t) =& -\int_0^t CC^T\lambda(\tau)d\tau + \eta^0, & (13.32b)\\ \lambda(t) =& \int_0^t CC^T\eta(\tau) - u(\tau) - \mathring{r}d\tau + \lambda^0. & (13.32c) \end{aligned}$$

Block-diagram corresponding to the control equations are shown in Figure 13.2.

13.2.3 Control stability and applicability

Reduction of (13.32) to a system of algebraic differential equations:

$$\begin{aligned} u =& \nu^n(W^{-1}\lambda, \overline{u}, \underline{u}), & (13.33a)\\ \dot{\eta} =& -CC^T\lambda, & (13.33b)\\ \dot{\lambda} =& CC^T\eta - \nu^n(W^{-1}\lambda, \overline{u}, \underline{u}) - \mathring{r}. & (13.33c) \end{aligned}$$

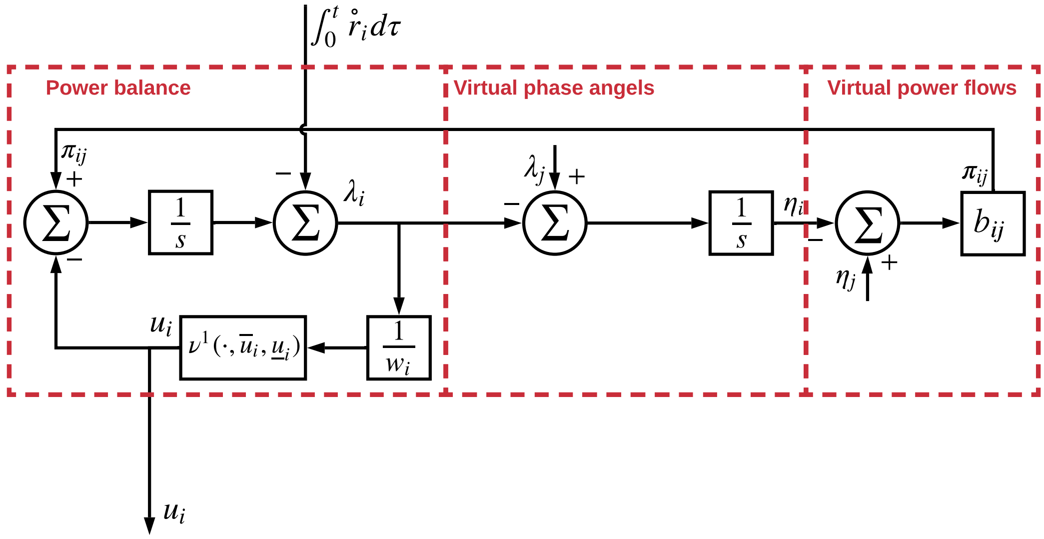

Figure 13.2: Control block diagram for the Problem 5.

Lemma 13.7. *System (13.33) has unique stationary point that delivers solution of (13.27).*

Proof. Proof has the same structure as the proof of lemma 12.11. Variables $\underline{\chi}$ and $\overline{\chi}$ are equivalent to $\max\{\lambda - u, 0\}$ and $\max\{u - \lambda, 0\}$ respectively, this together with equation (13.33a)gives complementary slackness conditions (13.29d) and (13.29e). Equations (13.33b) and (13.33c) with $\eta = 0$ and $\lambda = 0$ give (13.29a) and (13.29c). Thus, stationary point of the system (13.33) is equal to the one given by Karush–Kuhn–Tucker conditions. □

Theorem 13.8 (Control stability)**.** *System (13.33) is globally asymptotically stable over u.*

Proof. Let u^*, λ^*, η^* be stationary point of (13.33). Let us introduce Lyapunov function:

$$V(\lambda, \eta) = \frac{1}{2}\left((\lambda - \lambda^*)^T(\lambda - \lambda^*) + (\eta - \eta^*)^T(\eta - \eta^*)\right). \tag{13.34}$$

Then,

$$\begin{aligned} \dot{V}(\lambda, \eta) &= (\lambda - \lambda^*)^T(CC^T(\eta - \eta^*) - W^{-1}(\lambda - \lambda^*)) + (\eta - \eta^*)^T CBC^T(\lambda - \lambda^*) = \\ &= (\lambda - \lambda^*)(\nu^n(W^{-1}\lambda, \overline{u}, \underline{u}) - \nu^n(W^{-1}\lambda^*, \overline{u}, \underline{u})) = \\ &= (\lambda - \lambda^*)W^{-1}(\nu^n(\lambda, W\overline{u}, W\underline{u}) - \nu^n(\lambda^*, W\overline{u}, W\underline{u})) \leq 0. \end{aligned} \tag{13.35}$$

According to the lemma

$$\ker \dot{V} = \left\{\lambda : \frac{1}{w_i}\lambda < \underline{u}_i, i \in \underline{N} \setminus \overline{N} \text{ and } \frac{1}{w_i}\lambda > \overline{u}_i, i \in \overline{N} \setminus \underline{N}\right\}. \tag{13.36}$$

According to Barbashin-Krasovsky-LaSalle theorem any solution of the system (13.33) converges to trajectory fully belonging to $\ker \dot{V}$. Thus,

$$u(t) = \nu^n(W^{-1}\lambda, \underline{u}, \overline{u}) \to \nu^n(W^{-1}\lambda^*, \underline{u}, \overline{u}) = u^*, \tag{13.37}$$

which proves global asymptotic stability of the control u. □

Theorem 13.9 (Control applicability)**.** *Formulas*

$$F(y^i, w_i, \underline{u}_i, \overline{u}_i) = \nu^1\left(\frac{y_2^i}{w_i}, \underline{u}_i, \overline{u}_i\right), \tag{13.38}$$

$$G_1^h(\mathring{r}_i, u_i, y^i, Y^i) = -hy_2^i + \boldsymbol{1}_h^\top (Y_2^i)^T, \tag{13.39}$$

$$G_2^h(\mathring{r}_i, u_i, y^i, Y^i) = hy_1^i - \boldsymbol{1}_h^\top (Y_1^i)^\top - u_i - \mathring{r}_i. \tag{13.40}$$

define controller functions for the Problem 4 with $s = 2$.

Proof. The proof is equivalent of the proof of the Theorem 13.5. Substitution of F and G into (13.26) gives system (13.32) with $y = \lambda$, thus item 1 of the Problem 4 is satisfied. From the Theorem 13.8 control u is global asymptotically stable and converges to a constant control, thus item 2 of the Problem 1 is satisfied. From the Lemma 13.7 u converges to $\hat{u}^*$ thus from Lemma 13.6, system (9.13) with the control u converges to the optimal type 3 steady-state. □

13.3 Problem 6. Distributed frequency control and congestion management.

Here we expand the previous problem with introduction of upper and lower line constraints

$$\underline{p} \le p \le \overline{p}. \tag{13.41}$$

Reasons of their presence are described in section (7.6). Line flows cannot be controlled directly. They must be adjusted using the same control functions u on buses. Thus, limits not possible to use approach from the Problems 3 and 6 applied to implement control limits. Instead special integral equations that correspond to the complementary slackness equations are added.

13.3.1 Problem statement

Definition 13.3. Optimal type 4 steady-state (OS4) is a point $(\hat{u}, \hat{\theta}, \hat{\omega}, \hat{p}^m, \hat{v}, \hat{p}, \hat{p}^e)$ that delivers a solution of the following optimization problem:

$$\min_{\hat{u}, \hat{\theta}, \hat{\omega}, \hat{p}^m, \hat{v}, \hat{p}, \hat{p}^e} f(\hat{u}), \tag{13.42a}$$

$$(\hat{\theta}, \hat{\omega}, \hat{p}^m, \hat{v}, \hat{p}, \hat{p}^e) \in \Psi, \tag{13.42b}$$

$$\hat{u}_i \in [\underline{u}_i, \overline{u}_i],\ i \in N_u, \tag{13.42c}$$

$$p_j \in [\underline{p}_j, \overline{p}_j],\ j \in \{1, \dots, q\}. \tag{13.42d}$$

Problem 6 (Distributed frequency control and congestion management)**.** *Let s be the size of auxiliary variables vector y. Then, it is required to find Lipschitz continuous controller functions*

$$F : \mathbb{R}^s \times \mathbb{R} \times \mathbb{R} \times \mathbb{R} \to \mathbb{R}, \tag{13.43a}$$

$$G^h : \mathbb{R} \times \mathbb{R} \times \mathbb{R}^s \times \mathbb{R}^{h \times s} \times \mathbb{R}^{h \times h} \times \mathbb{R}^{1 \times h} \to \mathbb{R}^s, \tag{13.43b}$$

such that

1. *Control u is defined by a system of integral-algebraic equations*

$$u_i(t) = F(y^i(t), w_i, \underline{u}_i, \overline{u}_i),\ i \in N, \tag{13.44a}$$

$$y^i(t) = \int_0^t G^{|\operatorname{Adj}(i)|}(\mathring{r}_i(\tau), u_i(\tau), y^i(\tau), Y^i(\tau), B^i, C^i) d\tau + y^{i0},\ i \in N, \tag{13.44b}$$

where $B^i = B_{\overline{\operatorname{Adj}(i)}, \overline{\operatorname{Adj}(i)}}$ and $C^i = C_{i, \overline{\operatorname{Adj}(i)}}$.

2. *Control u must be globally asymptotically stable.*

3. $u_i(t) \in [\underline{u}_i, \overline{u}_i],\ i \in N,\ t \geq 0.$

4. *System (9.13) with control u must converge to OS4.*

13.3.2 Optimal steady-state and control equations

Problem (12.67) with addition of line constraints (13.41) is taken as initial:

$$\min_{\hat{\theta},\hat{\omega},\hat{p}^m,\hat{v},\hat{p},\hat{p}^e,\hat{u}} f(\hat{u}), \tag{13.45a}$$

$$
\begin{aligned}
0 =&\hat{\omega}, && (13.45\text{b})\\
0 =&-D_{G,G}\hat{\omega}_G - \hat{p}^e_G + \hat{p}^m + r_G, && (13.45\text{c})\\
0 =&-\hat{p}^m + \hat{v}, && (13.45\text{d})\\
0 =&-\hat{v} + \hat{u}_G, && (13.45\text{e})\\
0 =&-D_{L_1,L_1}\hat{\omega}_{L_1} - \hat{p}^e_{L_1} + \hat{u}_{L_1} + r_{L_1}, && (13.45\text{f})\\
0 =&-D_{L_0,L_0}\hat{\omega}_{L_0} - \hat{p}^e_{L_0} + \hat{u}_{L_0} + r_{L_0}, && (13.45\text{g})\\
\hat{p} =&BC^T\hat{\theta}, && (13.45\text{h})\\
\hat{p}^e =&C\hat{p}, && (13.45\text{i})
\end{aligned}
$$

$$\underline{u} \leq \hat{u} \leq \overline{u}, \tag{13.45j}$$

$$\underline{p} \leq \hat{p} \leq \overline{p}. \tag{13.45k}$$

simplification gives the following optimization problem:

$$\min_{\hat{u},\hat{\theta}} f(\hat{u}), \tag{13.46a}$$

$$-CBC^T\hat{\theta} + \hat{u} + r = 0, \tag{13.46b}$$

$$\underline{u} \leq \hat{u} \leq \overline{u}, \tag{13.46c}$$

$$\underline{p} \leq BC^T\hat{\theta} \leq \overline{p}. \tag{13.46d}$$

This problem is convex and its unique solution is given by the corresponding Karush–Kuhn–Tucker conditions. Lagrange function:

$$
\begin{gathered}
\mathcal{L}(\hat{u},\hat{\theta},\hat{\lambda},\hat{\overline{\chi}},\hat{\underline{\chi}},\hat{\overline{\delta}},\hat{\underline{\delta}}) = \frac{1}{2}\hat{u}^T W\hat{u} - \hat{\lambda}^T(-CBC^T\hat{\theta} + \hat{u} + r) + \\
+\hat{\overline{\chi}}^T(\hat{u} - \overline{u}) + \hat{\underline{\chi}}^T(\underline{u} - \hat{u}) + \hat{\overline{\delta}}^T(BC^T\hat{\theta} - \overline{p}) + \hat{\underline{\delta}}^T(\underline{p} - BC^T\hat{\theta}).
\end{gathered}
\tag{13.47}
$$

Karush–Kuhn–Tucker conditions with replaced complementary slackness for the control limits:

$$CB(C^T u - \hat{\overline{\delta}} + \hat{\underline{\delta}}) = 0, \tag{13.48a}$$

$$-CBC^T\hat{\theta} + \hat{u} + r = 0, \tag{13.48b}$$

$$\hat{u} = \nu^n(W^{-1}\hat{\lambda}, \overline{u}, \underline{u}), \tag{13.48c}$$

$$\hat{\overline{\delta}}_i((BC^T\hat{\theta})_i - \overline{p}_i) = 0,\ \hat{\overline{\delta}}_i \geq 0,\ i \in \{1, \ldots, q\}, \tag{13.48d}$$

$$\hat{\underline{\delta}}_i(\underline{p}_i - (BC^T\hat{\theta})_i) = 0,\ \hat{\underline{\delta}}_i \geq 0,\ i \in \{1, \ldots, q\}. \tag{13.48e}$$

Complementary slackness conditions corresponding to the control limits are excluded via function (13.30). It is not possible to use the same approach for the line limits, since line flows are not controlled directly and are defined by the physical system of differential algebraic equations (9.13), while control is defined by the function F. Thus, equations (13.48d) and (13.48e) are replaced with

$$\phi^q(BC^T\hat{\eta} - \overline{p}, \hat{\overline{\delta}}),\ \hat{\overline{\delta}} \geq 0, \tag{13.49}$$

$$\phi^q(\underline{p} - BC^T\hat{\eta}, \hat{\underline{\delta}}),\ \hat{\underline{\delta}} \geq 0, \tag{13.50}$$

where function $\phi^n : \mathbb{R}^n \times \mathbb{R}^n \to \mathbb{R}^n$,

$$\phi_i^n(x, y) = \begin{cases} x_i, & \text{if } x_i \geq 0 \text{ or } y_i \geq 0, \\ 0 & \text{otherwise.} \end{cases},\ i \in \{1, \ldots, n\}. \tag{13.51}$$

As a result, the following lemma holds.

Lemma 13.10. *Let $u(t) \to \hat{u}^*$, then system (9.13) converges to the optimal type 4 steady-state.*

Proof. Proof of this lemma coincides with the proof of Lemma 12.10. □

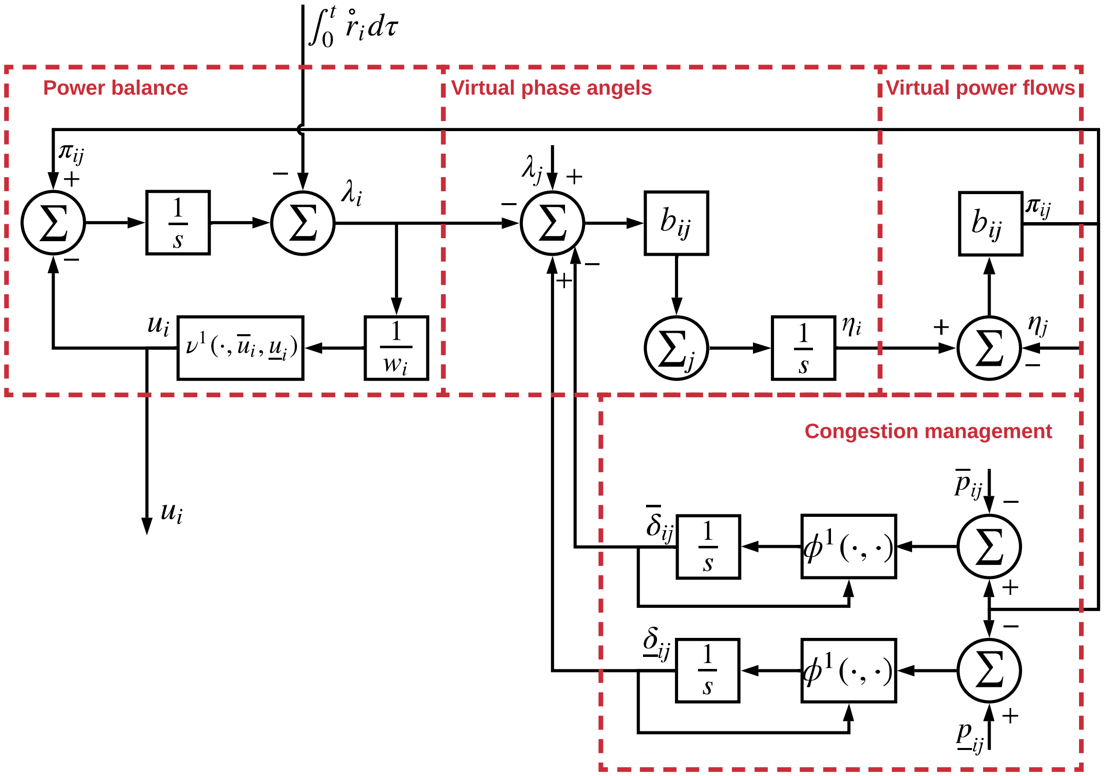

Figure 13.3: Control block diagram for the Problem 6.

This method allows us transition to the following system of control equations:

$$u(t) = \nu^n(W^{-1}\lambda(t), \overline{u}, \underline{u}), \tag{13.52a}$$

$$\eta(t) = \int_0^t CB(-C^T\lambda(\tau) - \overline{\delta}(\tau) + \underline{\delta}(\tau))d\tau + \eta^0, \tag{13.52b}$$

$$\lambda(t) = \int_0^t CBC^T\eta(\tau) - u(\tau)d\tau - \int_0^t \mathring{r}(\tau)d\tau + \lambda^0, \tag{13.52c}$$

$$\overline{\delta}(t) = \int_0^t \phi^q(BC^T\eta(\tau) - \overline{p}, \overline{\delta}(\tau))d\tau + \overline{\delta}^0, \tag{13.52d}$$

$$\underline{\delta}(t) = \int_0^t \phi^q(\underline{p} - BC^T\eta(\tau), \underline{\delta}(\tau))d\tau + \underline{\delta}^0. \tag{13.52e}$$

Block-diagram corresponding to the control equations are shown in Figure 13.3.

13.3.3 Control stability and applicability

Differential equations equivalent to (13.52):

$$\dot{\eta} = CB(-C^T\lambda - \overline{\delta} + \underline{\delta}), \tag{13.53a}$$

$$\dot{\lambda} = CBC^T\eta - u - \mathring{r}, \tag{13.53b}$$

$$u = \nu^n(W^{-1}\lambda, \overline{u}, \underline{u}), \tag{13.53c}$$

$$\dot{\overline{\delta}} = \phi^q(BC^T\eta - \overline{p}, \overline{\delta}), \tag{13.53d}$$

$$\dot{\underline{\delta}} = \phi^q(\underline{p} - BC^T\eta, \underline{\delta}). \tag{13.53e}$$

Lemma 13.11. *System (13.53) has unique stationary point that delivers solution of (13.46).*

Proof. Proof has the same structure as the proof of lemma 13.7. In additions to the results of lemma 13.7 equations (13.53d) and (13.53e) with $\overline{\delta} = 0$ and $\underline{\delta} = 0$ give (13.49) and (13.50). Thus, stationary point of the system (13.53) is equal to the one given by Karush–Kuhn–Tucker conditions. □

Theorem 13.12 (Control stability)**.** *In the system (13.53) solutions u are globally asymptotically stable.*

Proof. Let us introduce the following Lyapunov function

$$\begin{aligned} V(\eta, \lambda, \overline{\delta}, \underline{\delta}) = \frac{1}{2}((\eta - \eta^*)^T(\eta - \eta^*) + (\lambda - \lambda^*)^T(\lambda - \lambda^*) + \\ +(\overline{\delta} - \overline{\delta}^*)^T(\overline{\delta} - \overline{\delta}^*) + (\underline{\delta} - \underline{\delta}^*)^T(\underline{\delta} - \underline{\delta}^*). \end{aligned} \tag{13.54}$$

Its derivative is given by

$$\begin{aligned} \dot{V}(\eta, \lambda, \overline{\delta}, \underline{\delta}) = (\eta - \eta^*)^T CB(-C^T(\lambda - \lambda^*) - (\overline{\delta} - \overline{\delta}^*) + (\underline{\delta} - \underline{\delta})^*) + \\ +(\lambda - \lambda^*)^T(CBC^T(\eta - \eta^*) - (\nu^n(W^{-1}\lambda, \overline{u}, \underline{u}) - \nu^n(W^{-1}\lambda^*, \overline{u}, \underline{u}))) + \\ +(\overline{\delta} - \overline{\delta}^*)^T\phi^q(BC^T\eta - \overline{p}, \overline{\delta}) + (\underline{\delta} - \underline{\delta}^*)^T\phi^q(\underline{p} - BC^T\eta, \underline{\delta}) = \\ = (\lambda - \lambda^*)^T(\nu^n(W^{-1}\lambda, \overline{u}, \underline{u}) - \nu^n(W^{-1}\lambda^*, \overline{u}, \underline{u})) + \\ +(\eta - \eta^*)^T CB(-(\overline{\delta} - \overline{\delta}^*) + (\underline{\delta} - \underline{\delta}^*)) + \\ +(\overline{\delta} - \overline{\delta}^*)^T\phi^q(BC^T\eta - \overline{p}, \overline{\delta}) + (\underline{\delta} - \underline{\delta}^*)^T\phi^q(\underline{p} - BC^T\eta, \underline{\delta}). \end{aligned} \tag{13.55}$$

Let us introduce the following notations

$$\pi = BC^T\eta, \tag{13.56a}$$

$$\pi^* = BC^T\eta^*. \tag{13.56b}$$

Then, derivative $\dot{V}$ can be represented as a sum of 3 expressions:

$$\begin{aligned}\dot{V}^0(\eta,\lambda,\overline{\delta},\underline{\delta}) = \Upsilon_1(\eta,\lambda,\overline{\delta},\underline{\delta})+ \\ +\overline{\Upsilon}_2(\eta,\lambda,\overline{\delta},\underline{\delta}) + \underline{\Upsilon}_2(\eta,\lambda,\overline{\delta},\underline{\delta}),\end{aligned} \tag{13.57}$$

where

$$\Upsilon_1(\eta,\lambda,\overline{\delta},\underline{\delta}) = -(\lambda-\lambda^*)^T(\nu^n(W^{-1}\lambda,\overline{u},\underline{u}) - \nu^n(W^{-1}\lambda^*,\overline{u},\underline{u})), \tag{13.58}$$

$$\overline{\Upsilon}_2(\eta,\lambda,\overline{\delta},\underline{\delta}) = (\overline{\delta}-\overline{\delta}^*)^T(\phi^q(\pi-\overline{p},\overline{\delta}) - (\pi-\pi^*)), \tag{13.59}$$

$$\underline{\Upsilon}_2(\eta,\lambda,\overline{\delta},\underline{\delta}) = (\underline{\delta}-\underline{\delta}^*)^T(\phi^q(\underline{p}-\pi,\underline{\delta}) + (\pi-\pi^*)). \tag{13.60}$$

From the lemma 12.13

$$\Upsilon_1(\eta,\lambda,\overline{\delta},\underline{\delta}) \le 0. \tag{13.61}$$

Let us now show that $\overline{\Upsilon}_2(\eta,\lambda,\overline{\delta},\underline{\delta}) \le 0$. Three cases are possible here:

1. $\pi^* = \overline{p}$. Then, $\overline{\Upsilon}_2(\eta,\lambda,\overline{\delta},\underline{\delta}) = (\overline{\delta}-\overline{\delta}^*)^T(\phi^q(\pi-\pi^*,\overline{\delta}) - (\pi-\pi^*))$,
   (a) $\pi \ge \overline{p}$. Then, $\phi^q(\pi-\overline{p},\underline{\delta}) = \pi-\pi^*$ and $\overline{\Upsilon}_2(\eta,\lambda,\overline{\delta},\underline{\delta}) = (\overline{\delta}-\overline{\delta}^*)^T(\phi^q(\pi-\pi,\overline{\delta}) - (\pi-\pi)) = 0$;
   (b) $\pi < \overline{p}$. Then,
      i. $\overline{\delta} > 0$. Then, $\phi^q(\pi-\pi^*,\underline{\delta}) = \pi-\pi^*$, thus, $\overline{\Upsilon}_2(\eta,\lambda,\overline{\delta},\underline{\delta}) = (\overline{\delta}-\overline{\delta}^*)^T((\pi-\pi^*) - (\pi-\pi^*)) = 0$;
      ii. $\overline{\delta} = 0$ and $\phi^q(\pi-\pi^*,\underline{\delta}) = 0$, thus, $\overline{\Upsilon}_2(\eta,\lambda,\overline{\delta},\underline{\delta}) = (\overline{\delta}^*)^T(\pi-\pi^*) \le 0$ since $\overline{\delta}^* \ge 0$ as a dual variable and $\pi^* = \overline{p} > \pi$;
2. $\pi^* < \overline{p}$. Then, $\overline{\delta}^* = 0$ as a dual variable and $\overline{\Upsilon}_2(\eta,\lambda,\overline{\delta},\underline{\delta}) = \overline{\delta}^T(\phi^q(\pi-\overline{p},\overline{\delta}) - (\pi-\pi^*))$,
   (a) $\pi \ge \overline{p}$. Then, $\phi^q(\pi-\overline{p},\overline{\delta}) = \pi-\overline{p}$ and $\overline{\Upsilon}_2(\eta,\lambda,\overline{\delta},\underline{\delta}) = (\overline{\delta}-\overline{\delta}^*)^T(\phi^q(\pi-\pi,\overline{\delta}) - (\pi-\pi)) = 0$;
   (b) $\pi < \overline{p}$. Then,

i. $\overline{\delta} < 0$. Then, $\phi^q(\pi - \overline{p}, \underline{\delta}) = \pi - \overline{p}$, thus, $\overline{\Upsilon}_2(\eta, \lambda, \overline{\delta}, \underline{\delta}) = \overline{\delta}^T((\pi - \overline{p}, \overline{\delta}) - (\pi - \pi^*)) = \overline{\delta}^T(\pi^* - \overline{p}) \leq 0$;

ii. $\overline{\delta} = 0$. Then, $\phi^q(\pi - \overline{p}, \overline{\delta}) = 0$ and $\overline{\Upsilon}_2(\eta, \lambda, \overline{\delta}, \underline{\delta}) = -\overline{\delta}^T(\pi - \pi^*) \leq 0$.

Similarly inequality $\overline{\Upsilon}_2(\eta, \lambda, \overline{\delta}, \underline{\delta}) \leq 0$ is proven. Thus, $\dot{V}(\eta, \lambda, \overline{\delta}, \underline{\delta}) \leq 0$ and system (13.53) is stable. From the form of $\Upsilon_1(\eta, \lambda, \overline{\delta}, \underline{\delta})$ we have

$$\ker \dot{V} \subseteq \left\{(\eta, \lambda, \overline{\delta}, \underline{\delta}, \phi) : \frac{1}{w_i}\lambda < \underline{u}_i, i \in \underline{N} \setminus \overline{N} \text{ and } \frac{1}{w_i}\lambda > \overline{u}_i, i \in \overline{N} \setminus \underline{N}\right\}. \tag{13.62}$$

According to Barbashin-Krasovsky theorem any solution of the system (13.53) converges to trajectory fully belonging to $\ker \dot{V}$. Thus,

$$u(t) = \nu^n(W^{-1}\mathbf{1}_n\lambda, \underline{u}, \overline{u}) \to \nu^n(W^{-1}\mathbf{1}_n\lambda^*, \underline{u}, \overline{u}) = u^*, \tag{13.63}$$

which proves global asymptotic stability of the control u. □

Theorem 13.13 (Control applicability)**.** *Formulas*

$$F(y^i, w_i, \overline{u}_i, \underline{u}_i) = \nu^1\left(\frac{y_1^i}{w_i}, \overline{u}_i, \underline{u}_i\right). \tag{13.64}$$

$$G_1^h(\tilde{r}_i, u_i, y^i, Y^i, B^i, C^i, \overline{p}^i, \underline{p}^i) = C^iB^i\left((C^i)^\top((Y_2^i)^\top - \boldsymbol{1}_h y_2^i) - y^i_{3,\dots,h+2} + y^i_{3+h,\dots,2h+2}\right), \tag{13.65a}$$

$$G_2^h(\tilde{r}_i, u_i, y^i, Y^i, B^i, C^i, \overline{p}^i, \underline{p}^i) = C^iB^i(C^i)^\top(\boldsymbol{1}_h y_1^i - (Y_1^i)^\top) - u_i - \tilde{r}_i, \tag{13.65b}$$

$$G_{2+j}^h(\tilde{r}_i, u_i, y^i, Y^i, B^i, C^i, \overline{p}^i, \underline{p}^i) = \phi^1(B^i_{jj}C^i_j(y_1^i - Y^i_{1j}) - \overline{p}_j, y^i_{2+j}),\ j \in \{1, \dots, q\}, \tag{13.65c}$$

$$G_{2+h+j}^h(\tilde{r}_i, u_i, y^i, Y^i, B^i, C^i, \overline{p}^i, \underline{p}^i) = \phi^1(\underline{p}_j - B^i_{jj}C^i_j(y_1^i - Y^i_{1j}), y^i_{2+h+j}),\ j \in \{1, \dots, q\}. \tag{13.65d}$$

define controller functions for the Problem 6 with $s = 2(1 + |\operatorname{Adj}(i)|)$.

Proof. We take

$$y^i(t) = \begin{pmatrix} \eta_i \\ \lambda_i \\ \overline{\delta}_{\overline{\operatorname{Adj}(i)}} \\ \underline{\delta}_{\overline{\operatorname{Adj}(i)}} \end{pmatrix},\ i \in N. \tag{13.66}$$

Equation (13.52a) gives form of the function F: Equations (13.52) give form of the functions $G_i^h,\ i \in \{1,\dots,s\}$. From the Theorem 13.12 control u is global asymptotically stable and converges to a constant control, thus item 2 of the Problem 4 is satisfied. From the Lemma 13.11 u converges to $\hat{u}^*$ thus from Lemma 13.10, system (9.13) with the control u converges to the optimal type 4 steady-state. □

13.4 Problem 7. Distributed frequency control, congestion management and inter-area flows control.

A case when power system is divided into areas is considered here. Inter-area flows must be kept equal to the nominal values. It is assumed that power system contains n^{area} disjoint areas defined by sets of buses $\alpha(k) \subseteq N,\ k \in \{1,\dots,n^{area}\}$. Nominal value of Inter-area flow for each area k is denoted by κ_k. Decentralization requirement is relaxed in this section. It is assumed that border buses (that have connections outside their areas) can communicate between each other despite their topological locations. Therefore, it can be said, that inter-area control is done in a centralized way for each area. Usually, area is connected to the rest of the system by only few lines; therefore, communication between border buses is technically easy to implement.

13.4.1 Problem statement

Definition 13.4. For each area $\alpha(k)$, $k \in \{1,\dots,n^{area}\}$ buses that are connected to buses not from the same area are called border buses. Set of this buses are denoted by

$$\tilde{\alpha}(k) = \{i \in \alpha(k) \mid \exists j \in \mathrm{Adj}(i) : j \notin \alpha(k)\}. \tag{13.67}$$

Definition 13.5. Set$\beta(k)$ is a set of buses from areas $\hat{k} \neq k$ adjacent to buses from $\alpha(k)$.

Definition 13.6. Set $\gamma(k)$ is a set of lines connecting border buses with other areas.

Definition 13.7. Matrix $S \in \mathbb{R}^{n^{area} \times q}$ consists of vectors $s^i \in \mathbb{R}^q$, with elements

$$s_j^i = \begin{cases} 1, & \text{if line } j \text{ enters area } i, \\ -1, & \text{if line } j \text{ exits area } i, \quad i \in \{1,\dots,q\}. \\ 0 & \text{otherwise,} \end{cases} \tag{13.68}$$

Definition 13.8. Optimal type 5 steady-state is a point $(\hat{u}, \hat{\theta}, \hat{\omega}, \hat{p}^m, \hat{v}, \hat{p}, \hat{p}^e)$ that delivers a solution of the following optimization problem:

$$\min_{\hat{u},\hat{\theta},\hat{\omega},\hat{p}^m,\hat{v},\hat{p},\hat{p}^e} f(\hat{u}), \tag{13.69a}$$

$$(\hat{\theta}, \hat{\omega}, \hat{p}^m, \hat{v}, \hat{p}, \hat{p}^e) \in \Psi, \tag{13.69b}$$

$$\hat{u}_i \in [\underline{u}_i, \overline{u}_i],\ i \in N, \tag{13.69c}$$

$$\hat{p}_j \in [\underline{p}_j, \overline{p}_j],\ j \in \{1, \ldots, q\}, \tag{13.69d}$$

$$S\hat{p} = \delta. \tag{13.69e}$$

Problem 7 (Distributed frequency control, congestion management, and inter-area flows control)**.** *Let s be the size of auxiliary variables vector y. Then, it is required to find Lipschitz continuous controller functions*

$$F : \mathbb{R}^s \times \mathbb{R} \times \mathbb{R} \times \mathbb{R} \to \mathbb{R}, \tag{13.70a}$$

$$G^h : \mathbb{R} \times \mathbb{R} \times \mathbb{R}^s \times \mathbb{R}^{h\times s} \times \mathbb{R}^{h\times h} \times \mathbb{R}^{1\times h} \to \mathbb{R}^s, \tag{13.70b}$$

$$Q^h : \mathbb{R} \times \mathbb{R}^{h\times h} \times \mathbb{R}^{1\times h_3} \times \mathbb{R}^{1\times h} \times \mathbb{R} \to \mathbb{R}, \tag{13.70c}$$

$$\overline{Q}^{h_1,h_2,h_3} : \mathbb{R}^{h_1\times s} \times \mathbb{R}^{h_2\times s} \times \mathbb{R}^{h_3\times h_3} \times \mathbb{R}^{h_1\times h_3} \times \mathbb{R}^{1\times h_3} \times \mathbb{R} \to \mathbb{R}, \tag{13.70d}$$

such that

1. *Control u is defined by a system of integral-algebraic equations*

$$u_i(t) = F(y^i(t), w_i, \underline{u}_i, \overline{u}_i),\ i \in N, \tag{13.71a}$$

$$y^i(t) = \int_0^t G^{|\operatorname{Adj}(i)|}(\mathring{r}_i(\tau), u_i(\tau), y^i(\tau), Y^i(\tau), B^i, C^i)d\tau,\ i \in N \setminus \left(\bigcup_{k=1}^{n^{area}} \tilde{\alpha}(k)\right) + y^{i0}, \tag{13.71b}$$

$$\begin{aligned} y^i(t) = &\int_0^t G^{|\operatorname{Adj}(i)|}(\mathring{r}_i(\tau), u_i(\tau), y^i(\tau), Y^i(\tau), B^i, C^i)d\tau + \\ + &\int_0^t Q^{|\operatorname{Adj}(i)|}(z_k, B^i, C^i, S_{ki})d\tau + y^{i0},\ i \in \tilde{\alpha}(k),\ k = \{1, \ldots, n^{area}\}, \end{aligned} \tag{13.71c}$$

$$z_k(t) = \int_0^t Q^{|\tilde{\alpha}(k)|,|\beta(k)|,|\gamma(k)|}(Y^{\tilde{\alpha}(k)}, Y^{\beta(k)}, B^{\gamma(k)}, C^{\gamma(k)}, S^{\gamma(k)}, \zeta_k)d\tau + z_k^0,\ k = \{1, \ldots, n^{area}\}, \tag{13.71d}$$

where $Y^{\tilde{\alpha}(k)} \in \mathbb{R}^{|\tilde{\alpha}(k)| \times s}$ *is a matrix of auxiliary vectors* $y^i,\ i \in \tilde{\alpha}(k)$*. Similarly* $Y^{\beta(k)} \in \mathbb{R}^{|\beta(k)| \times s}$ *is matrix of columns* $y^i,\ i \in \beta(k)$*. Additionally* $B^{\gamma(k)} = B_{\gamma(k),\gamma(k)}$*,* $C^{\gamma(k)} = C_{\tilde{\alpha}(k),\gamma(k)}$*, and* $S^{\gamma(k)} = S_{k,\gamma(k)}$*.*

2. *Control* u *must be globally asymptotically stable.*

3. $u_i(t) \in [\underline{u}_i, \overline{u}_i],\ i \in N,\ t \geq 0.$

4. *System (9.13) with control* u *must converge to OS5.*

13.4.2 Optimal steady-state and control equations

Problem (13.45) with addition of line constraints (13.69e) is taken as initial:

$$\min_{\hat{\theta},\hat{\omega},\hat{p}^m,\hat{v},\hat{p},\hat{p}^e,\hat{u}} f(\hat{u}), \tag{13.72a}$$

$$0 = \hat{\omega}, \tag{13.72b}$$

$$0 = -D_{G,G}\hat{\omega}_G - \hat{p}^e_G + \hat{p}^m + r_G, \tag{13.72c}$$

$$0 = -\hat{p}^m + \hat{v}, \tag{13.72d}$$

$$0 = -\hat{v} + \hat{u}_G, \tag{13.72e}$$

$$0 = -D_{L_1,L_1}\hat{\omega}_{L_1} - \hat{p}^e_{L_1} + \hat{u}_{L_1} + r_{L_1}, \tag{13.72f}$$

$$0 = -D_{L_0,L_0}\hat{\omega}_{L_0} - \hat{p}^e_{L_0} + \hat{u}_{L_0} + r_{L_0}, \tag{13.72g}$$

$$\hat{p} = BC^T\hat{\theta}, \tag{13.72h}$$

$$\hat{p}^e = C\hat{p}, \tag{13.72i}$$

$$\underline{u} \leq \hat{u} \leq \overline{u}, \tag{13.72j}$$

$$\underline{p} \leq \hat{p} \leq \overline{p}, \tag{13.72k}$$

$$Sp = \delta. \tag{13.72l}$$

simplification gives the following optimization problem:

$$\min_{\hat{u},\hat{\theta}} f(\hat{u}), \tag{13.73a}$$

$$-CBC^T\hat{\theta} + \hat{u} + r = 0. \tag{13.73b}$$

$$\underline{u} \le \hat{u} \le \overline{u}, \tag{13.73c}$$

$$\underline{p} \le BC^T\hat{\theta} \le \overline{p}, \tag{13.73d}$$

$$SBC^T\hat{\theta} = \zeta. \tag{13.73e}$$

This problem is convex and its unique solution is given by the corresponding Karush–Kuhn–Tucker conditions. Lagrange function:

$$\begin{gathered}\mathcal{L}(\hat{u}, \hat{\theta}, \hat{\lambda}, \hat{\overline{\chi}}, \hat{\underline{\chi}}, \hat{\overline{\delta}}, \hat{\underline{\delta}}) = \frac{1}{2}\hat{u}^T W \hat{u} + \hat{\lambda}^T(-CBC^T\hat{\theta} + \hat{u} + r) + \\ +\hat{\overline{\chi}}^T(\hat{u} - \overline{u}) + \hat{\underline{\chi}}^T(\underline{u} - \hat{u}) + \hat{\overline{\delta}}^T(BC^T\hat{\theta} - \overline{p}) + \hat{\underline{\delta}}^T(\underline{p} - BC^T\hat{\theta}) + \\ +\hat{\xi}^T(SBC^T\theta - \zeta).\end{gathered} \tag{13.74}$$

Modified Karush–Kuhn–Tucker conditions:

$$CB(C^T\hat{u} - \hat{\overline{\delta}} + \hat{\underline{\delta}} - S^T\xi) = 0, \tag{13.75a}$$

$$-C\hat{p} + \hat{u} + r = 0, \tag{13.75b}$$

$$\hat{u} = \nu^n(W^{-1}\hat{\lambda}, \overline{u}, \underline{u}), \tag{13.75c}$$

$$\hat{\overline{\delta}}_i((BC^T\hat{\theta})_i - \overline{p}_i) = 0,\ \hat{\overline{\delta}}_i \ge 0,\ i \in \{1, \dots, q\}, \tag{13.75d}$$

$$\hat{\underline{\delta}}_i(\underline{p}_i - (BC^T\hat{\theta})_i) = 0,\ \hat{\underline{\delta}}_i \ge 0,\ i \in \{1, \dots, q\}, \tag{13.75e}$$

$$SBC^T\hat{\theta} - \zeta = 0. \tag{13.75f}$$

Lemma 13.14. *Let $u(t) \to \hat{u}^*$, then system (9.13) converges to the optimal type 5 steady-state.*

Proof. Proof of this lemma coincides with the proof of Lemma 12.10. □

Transition to integral algebraic control equations:

$$u(t) = \nu^n(W^{-1}\lambda(t), \overline{u}, \underline{u}), \tag{13.76a}$$

$$\eta(t) = \int_0^t CB(-C^T\lambda(\tau) - \overline{\delta}(\tau) + \underline{\delta}(\tau) - S^T\xi(\tau))d\tau + \eta^0, \tag{13.76b}$$

$$\lambda(t) = \int_0^t CBC^T\eta(\tau) - u(\tau)d\tau - \int_0^t \mathring{r}(\tau)d\tau + \lambda^0, \tag{13.76c}$$

$$\overline{\delta}(t) = \int_0^t \phi^q(BC^T\eta(\tau) - \overline{p}, \overline{\delta}(\tau))d\tau + \overline{\delta}^0, \tag{13.76d}$$

$$\underline{\delta}(t) = \int_0^t \phi^q(\underline{p} - BC^T\eta(\tau), \underline{\delta}(\tau))d\tau + \underline{\delta}^0, \tag{13.76e}$$

$$\xi(t) = \int_0^t SBC^T\eta(\tau) - \zeta d\tau + \xi^0. \tag{13.76f}$$

Block-diagram corresponding to the control equations are shown in Figure 13.1.

13.4.3 Control stability and applicability

Differential algebraic equations equivalent to (13.52):

$$\dot{\eta} = CB(-C^T\lambda - \overline{\delta} + \underline{\delta}), \tag{13.77a}$$

$$\dot{\lambda} = CBC^T\eta - u - r, \tag{13.77b}$$

$$u = \nu^n(W^{-1}\lambda, \overline{u}, \underline{u}), \tag{13.77c}$$

$$\dot{\overline{\delta}} = \phi^q(BC^T\eta - \overline{p}, \overline{\delta}), \tag{13.77d}$$

$$\dot{\underline{\delta}} = \phi^q(\underline{p} - BC^T\eta, \underline{\delta}), \tag{13.77e}$$

$$\dot{\xi} = SBC^T\eta - \zeta. \tag{13.77f}$$

Lemma 13.15. *System (13.77) has unique stationary point that delivers solution of (13.73).*

Proof. Proof has the same structure as the proof of lemma 13.15 with addition of equation (13.77f) corresponding to the constraint (13.75f). □

Theorem 13.16 (System stability)**.** *In the system (13.77) solutions u are globally asymptotically stable.*

Proof. Let us introduce the following Lyapunov function:

$$\begin{aligned} V(\eta, \lambda, \overline{\delta}, \underline{\delta}) = \frac{1}{2}((\eta - \eta^*)^T(\eta - \eta^*) + (\lambda - \lambda^*)^T(\lambda - \lambda^*) + \\ + (\overline{\delta} - \overline{\delta}^*)^T(\overline{\delta} - \overline{\delta}^*) + (\underline{\delta} - \underline{\delta}^*)^T(\underline{\delta} - \underline{\delta}^*) + (\xi - \xi^*)^T(\xi - \xi^*). \end{aligned} \tag{13.78}$$

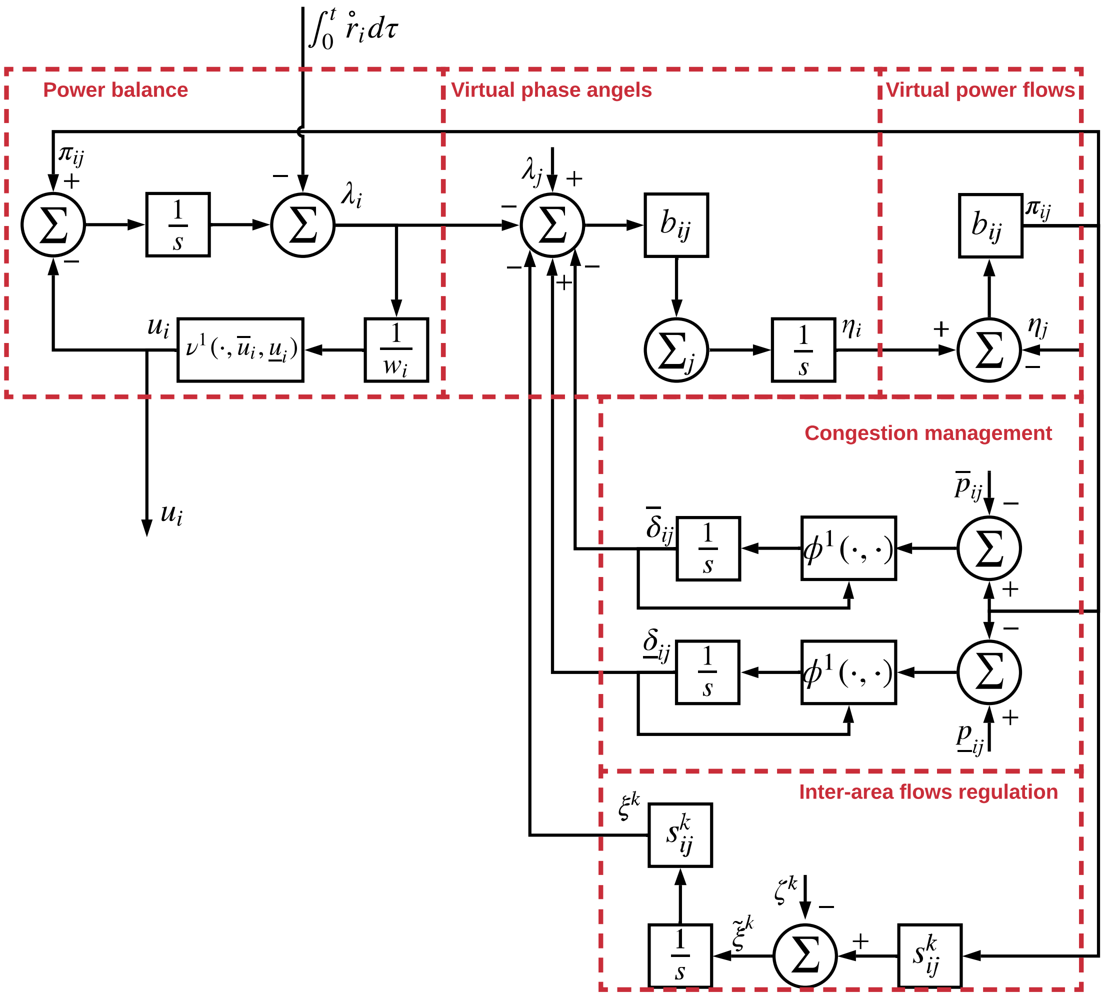

Figure 13.4: Control block diagram for the Problem 7.

Its derivative is equal to the derivative of Lyapunov function from (13.12), thus, the statement of the lemma holds. □

Theorem 13.17 (Control applicability)**.** *Formulas*

$$F(y^i, w_i, \overline{u}_i, \underline{u}_i) = \nu^1\left(\frac{y_1^i}{w_i}, \overline{u}_i, \underline{u}_i\right), \tag{13.79}$$

$$G_1^h(\tilde{r}_i, u_i, y^i, Y^i, B^i, C^i, \overline{p}^i, \underline{p}^i) = C^iB^i\left((C^i)^\top((Y_2^i)^\top - \boldsymbol{1}_h y_2^i) - y^i_{3,\dots,h+2} + y^i_{3+h,\dots,2h+2}\right), \tag{13.80a}$$

$$G_2^h(\tilde{r}_i, u_i, y^i, Y^i, B^i, C^i, \overline{p}^i, \underline{p}^i) = C^iB^i(C^i)^\top(\boldsymbol{1}_h y_1^i - (Y_1^i)^\top) - u_i - \tilde{r}_i, \tag{13.80b}$$

$$G_{2+j}^h(\tilde{r}_i, u_i, y^i, Y^i, B^i, C^i, \overline{p}^i, \underline{p}^i) = \phi^1(B^i_{jj}C^i_j(y^i_1 - Y^i_{1j}) - \overline{p}_j, y^i_{2+j}),\ j \in \{1, \dots, q\}, \tag{13.80c}$$

$$G_{2+h+j}^h(\tilde{r}_i, u_i, y^i, Y^i, B^i, C^i, \overline{p}^i, \underline{p}^i) = \phi^1(\underline{p}_j - B^i_{jj}C^i_j(y^i_1 - Y^i_{1j}), y^i_{2+h+j}),\ j \in \{1, \dots, q\}, \tag{13.80d}$$

$$\overline{Q}^h(z_k, B^i, C^i, S_{ki}) = C^iB^iS_{ki}z_k, \tag{13.81}$$

$$Q^{h_1,h_2,h_3}(Y^{\tilde{\alpha}(k)}, Y^{\beta(k)}, B^{\gamma(k)}, C^{\gamma(k)}, S^{\gamma(k)}, \zeta_k) = \sum_{i=1}^{h_1} S^{\gamma(k)}B^{\gamma(k)}(C_i^{\gamma(k)})^\top(\boldsymbol{1}_{h_1}Y_{1,i}^{\tilde{\alpha}(k)} - Y_1^{\beta(k)}) \tag{13.82}$$

with $h = 2(1 + |\operatorname{Adj}(i)|),\ h_1 = |\tilde{\alpha}(k)|,\ h_2 = |\beta(k)|,\ h_3 = |\gamma(k)|$.

Proof. We take

$$y^i(t) = \begin{pmatrix} \eta_i \\ \lambda_i \\ \overline{\delta}_{\overline{\operatorname{Adj}(i)}} \\ \underline{\delta}_{\overline{\operatorname{Adj}(i)}} \end{pmatrix},\ i \in N, z_k = \xi_k,\ k \in \{1, \dots, n^{area}\}. \tag{13.83}$$

Equation (13.76a) gives form of the function F: Equations (13.76) give form of the functions $G_i^h,\ i \in \{1, \dots, s\}$. From the Theorem 13.16 control u is global asymptotically stable and converges to a constant control, thus item 2 of the Problem 4 is satisfied. From the Lemma 13.15 u converges to $\hat{u}^*$ thus from Lemma 13.14, system (9.13) with the control u converges to the optimal type 4 steady-state. □

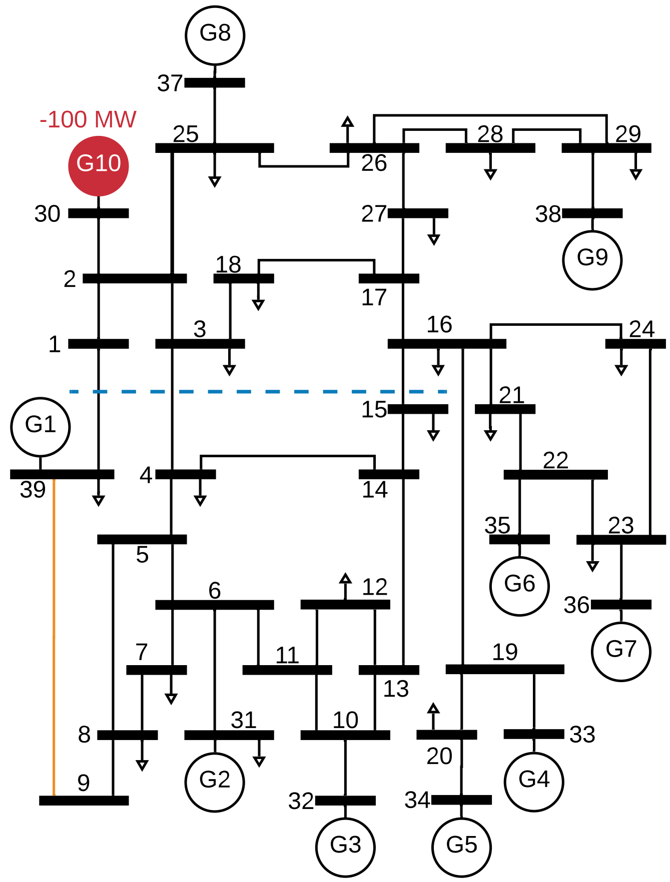

Figure 13.5: New England System. Partial outage on the generator G10. Line (9-39) is operating at its limit. System is divided into two areas by lines (1-39), (3-4) and (15-16).

13.5 Numerical experiment

Let us consider New England IEEE 39 bus system [8]. Parameters of the system are given in the tables 7.1 and 7.2. Turbine and governor constants are taken from [90].

Partial outage of 100 MW appears on the generator 10. As a consequence of the outage, generator G10 does not participate in the further control actions. It is assumed that participation factors w_i for every generator are equal 1. The system is separated into two areas by the lines (1-39), (3-4) and (16-15). Finally, line (9-39) works at its thermal limit and increase of its power flow will lead to overheat (Figure 13.5). Let us firstly consider response of the traditional frequency control. After the transient dynamics, power balance will be restored by the secondary frequency control with usage of only generators of the same area: G5 —

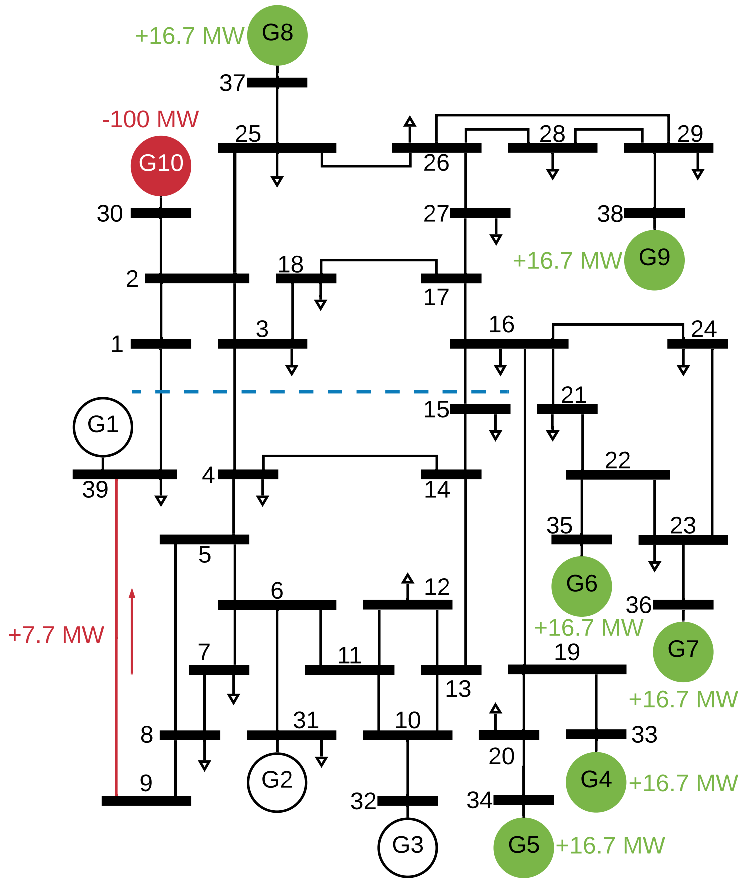

Figure 13.6: Standard frequency control. Power balance is restored by generators of the top area. Line (9-39) is congested.

G9. Since all participation factors are equal they both must increase their output by 15.9 MW. However, such change leads to increased power flow from the right half of the system to the left and from the bottom to the top, thus, line (9-39) becomes overloaded (Figure 13.6). In order to comply with all constraints the developed algorithm delivers system to the state shown in the Figure 13.7. Here generators marked blue reduce their output and generators marked green increase their output. Here generator G1 increases output in order create counterflow on the line (9-39). For the same reason outputs of the generators G8 and G9 are slightly increased. This allows to remove congestion. Generators G2 and G3 decrease their output in order to keep inter-area flow intact. Finally generators G5 — G7 are connected to the rest of the network by a single bus 16. Thus, from the perspective of the rest of the system they are treated as a single aggregated generator. As a result, they increase their

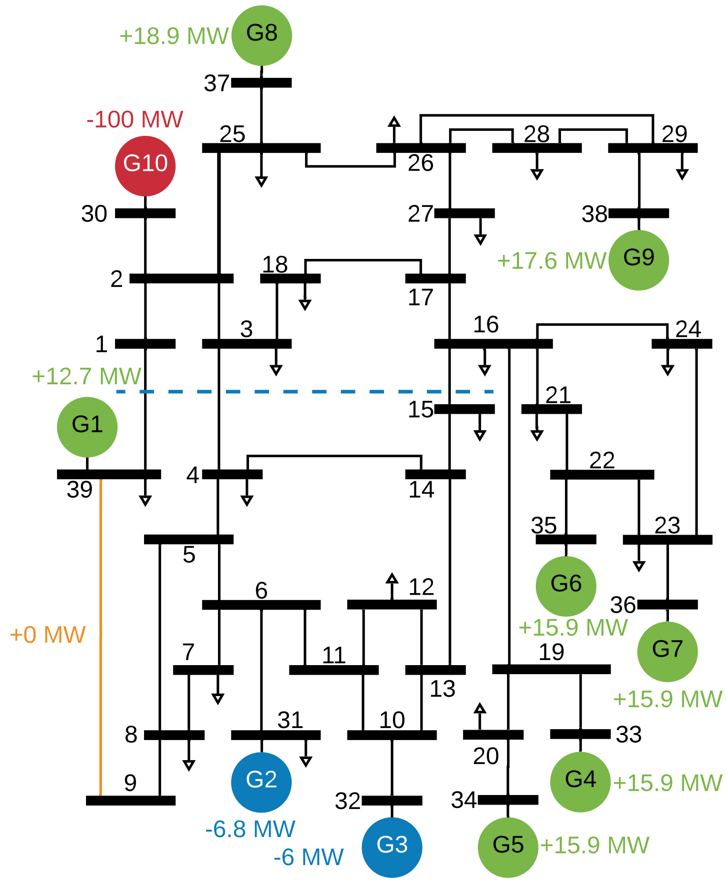

Figure 13.7: Developed control. All generators are controlled individually. All constraints are satisfied at minimal possible effort.

generation equally to each other in order to balance power at minimal cost. This way all constraints are satisfied at minimal control effort. Dynamics of the system for both types of control are shown in the Figures 13.8 — 13.12. Similar to the previous numerical experiment (section 12.4), here developed control is used with addition of primary frequency control in order to improve nadir.

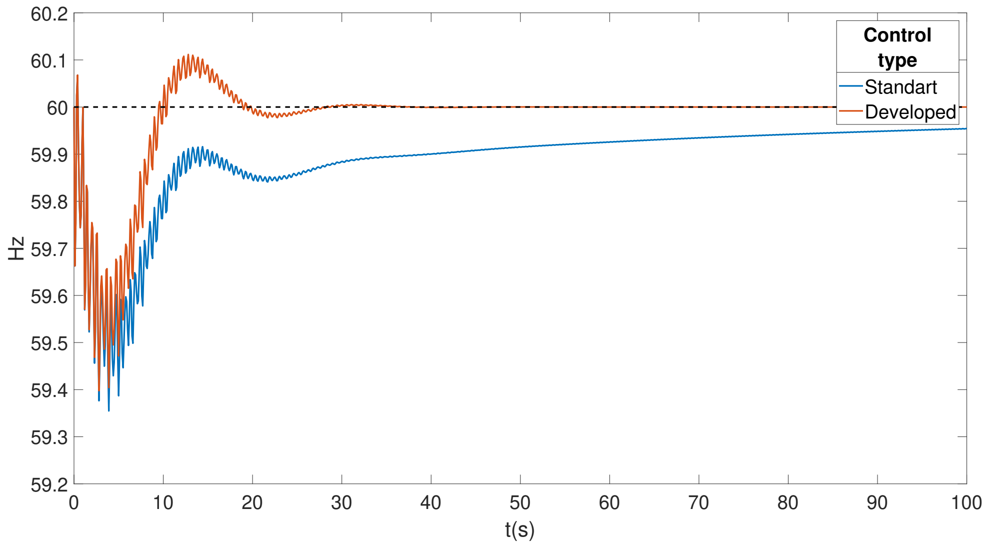

Figure 13.8: Frequency dynamics. Standard and developed control.

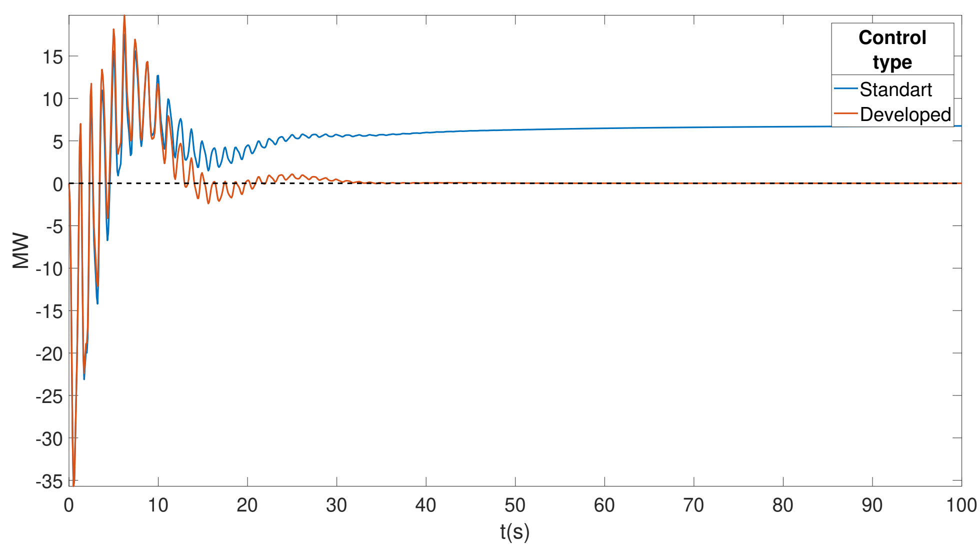

Figure 13.9: Deviation of power flows for the line (9-39). Standard and developed control.

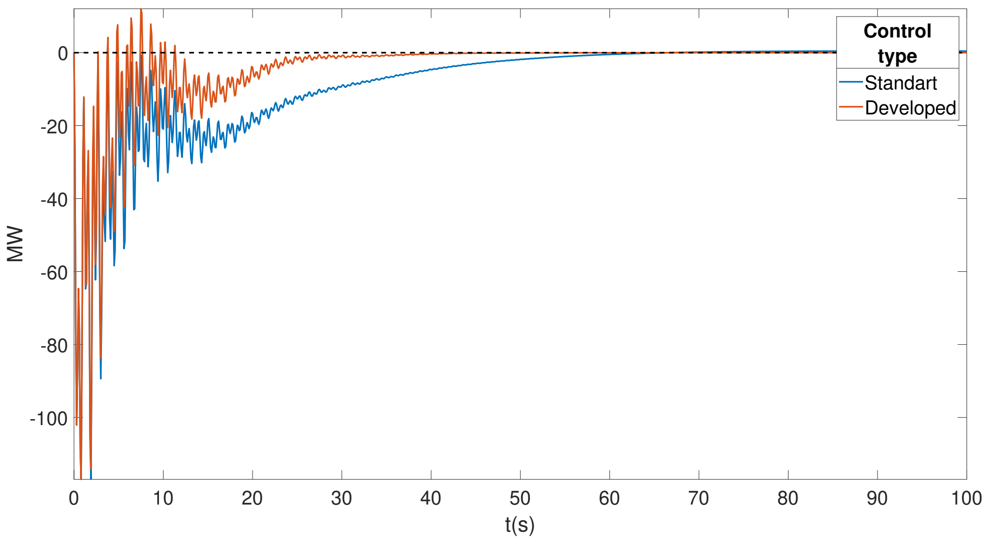

Figure 13.10: Inter-area flow deviation. . Standard and developed control.

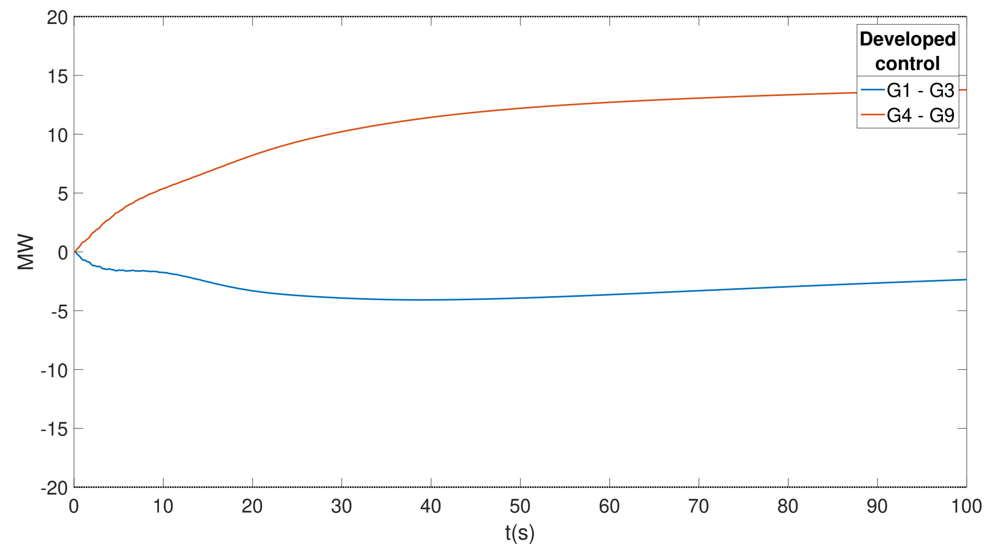

Figure 13.11: Secondary frequency control

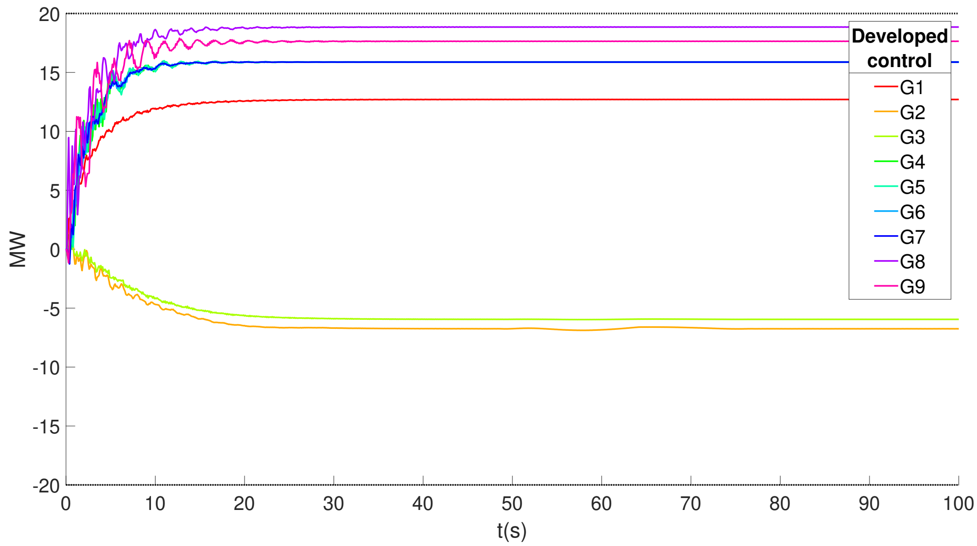

Figure 13.12: Developed control

13.6 Conclusion

Within this section a distributed frequency control with no control limits is developed. It is by a system of integral algebraic equations:

$$u(t) = \nu^n(W^{-1}\lambda(t), \overline{u}, \underline{u}), \tag{13.84a}$$

$$\eta(t) = \int_0^t CB(-C^T\lambda(\tau) - \overline{\delta}(\tau) + \underline{\delta}(\tau) - S^T\xi(\tau))d\tau + \eta^0, \tag{13.84b}$$

$$\lambda(t) = \int_0^t CBC^T\eta(\tau) - u(\tau)d\tau - \int_0^t \mathring{r}(\tau)d\tau + \lambda^0, \tag{13.84c}$$

$$\overline{\delta}(t) = \int_0^t \phi^q(BC^T\eta(\tau) - \overline{p}, \overline{\delta}(\tau))d\tau + \overline{\delta}^0, \tag{13.84d}$$

$$\underline{\delta}(t) = \int_0^t \phi^q(\underline{p} - BC^T\eta(\tau), \underline{\delta}(\tau))d\tau + \underline{\delta}^0, \tag{13.84e}$$

$$\xi(t) = \int_0^t SBC^T\eta(t) - \zeta d\tau + \xi^0. \tag{13.84f}$$

Here equations (13.84a) are used to enforce control limits, equations (13.84c) correspond to bus power balance, equations (13.84d) and (13.84e) represent complementary slackness conditions for the line constraints and (13.84f) correspond to the inter-area flows constraints.

14 Numerical Experiment

Let us illustrate our feedback control by the following example. We consider New England IEEE 39 bus system [8]. Parameters of the system are given in the tables 7.1 and 7.2. Turbine and governor constants are taken from [90]. Here we use model, described in section 9.2 with $G^s = \{1,2\},\ G^h = \{3,5\},\ G^g = G \setminus (G^s \cup G^h)$. Control limits for generators are set to $[-20\ MW, 20\ MW]$. Initially, loads do not participate in control (upper and lower limits for the load buses are set to 0). The following set of events happens:

1. At $t = 1\ sec$ partial power outage of 50 MW happens on generator G10. This generator does not participate in further control.

2. At $t = 10\ sec$ additional outage of 50 MW happens on generator G10.

3. At $t = 30\ sec$ generator control limits start reducing at speed of 400 kW/sec and $-400\ kW/sec$ for lower and upper limits respectively. Generators usually are obliged to provide spinning reserves for only limited amount of time sufficient for the system operator to make regulating actions. Therefore the generators reduce their control limits 29 seconds after the initial disturbance. This reduction will eventually lead to the deficit of power. Therefore system operator decides to enable load-sides control to complement for the reduction of the generator control limits. Lower and upper control limits change at the rate of $-100\ kW/sec$ and 100 kW/sec respectively for the load buses 3,4,7,8,12,15,16,18,20,21, and 23-29.

4. At $t = 40\ sec$ generator control limits stop at $[-16\ MW, 16\ MW]$, load control limits stop at $[-1\ MW, 1\ MW]$. As a result, all loads of the top area reduce their power consumption by 1 MW and loads of the bottom area increase their power consumption by $-1\ MW$.

5. At $t = 50\ sec$ line (4-5) trips. This event reduces flow on the line (4-3) and increases flow on the line (9-39). However, due to load-side control the case remains feasible and the system converges to the optimal state (Figure 14.1).

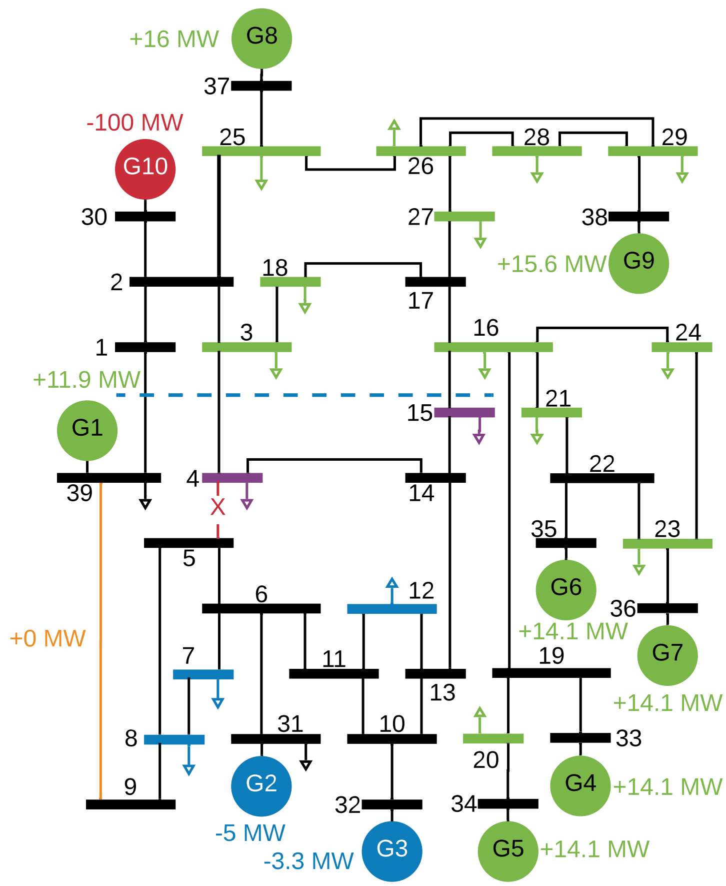

Figure 14.1: New England Power System. Partial outage on the generator G10. Line (9-39) operates at its limit. Line (4-5) is tripped. Control for load buses marked green equals $+1\ MW$, control for load buses marked blue equals $-1\ MW$, control for buses 4 and 15 equals $-320\ kW$ and $-150\ kW$ respectively. All constraints are satisfied at minimal effort.

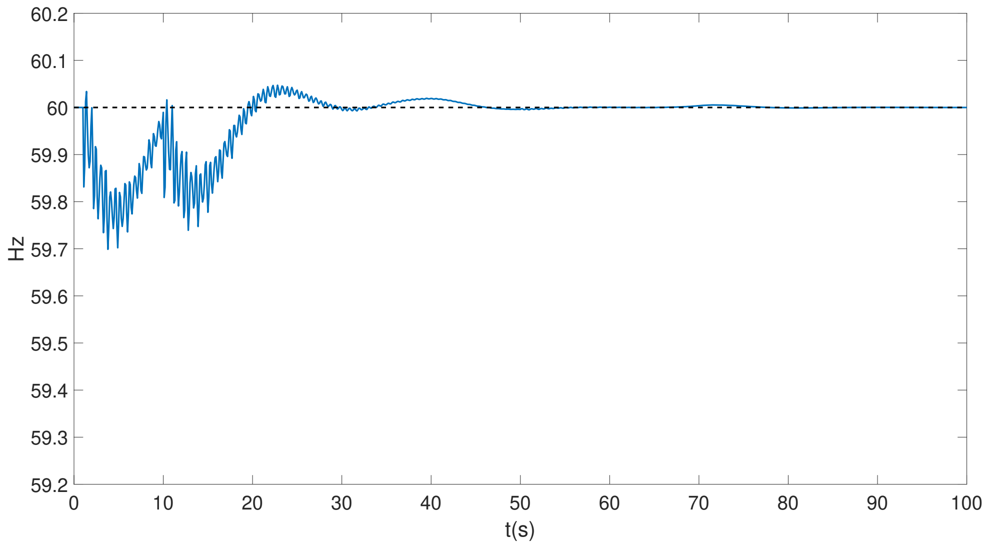

Figure 14.2: Frequency dynamics.

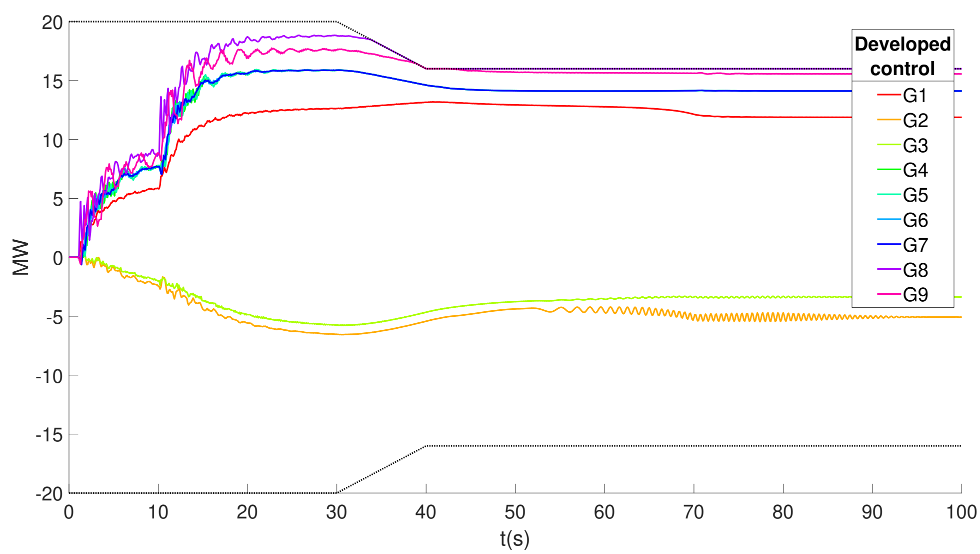

Figure 14.3: Generators control values with reduction of control limits.

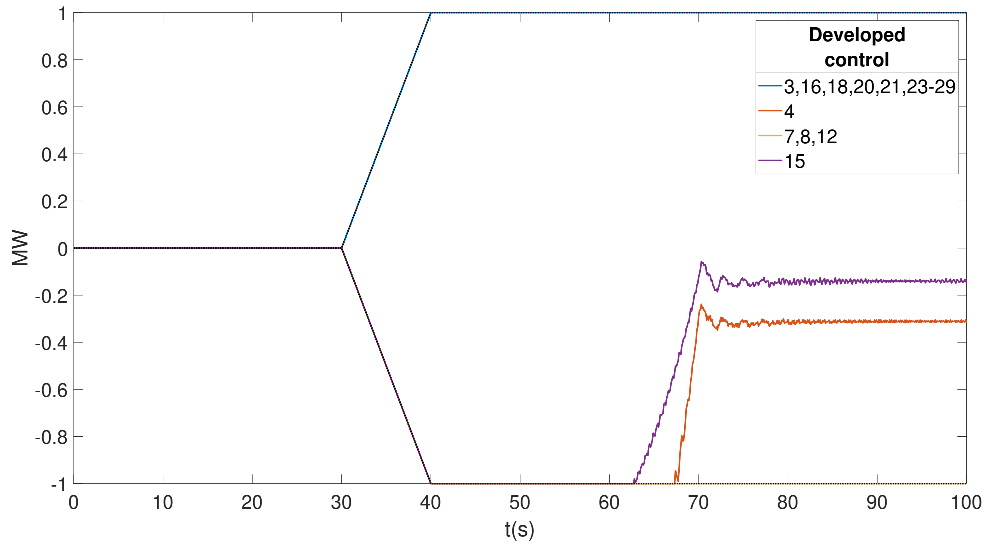

Figure 14.4: Loads control values with initial values of 0.

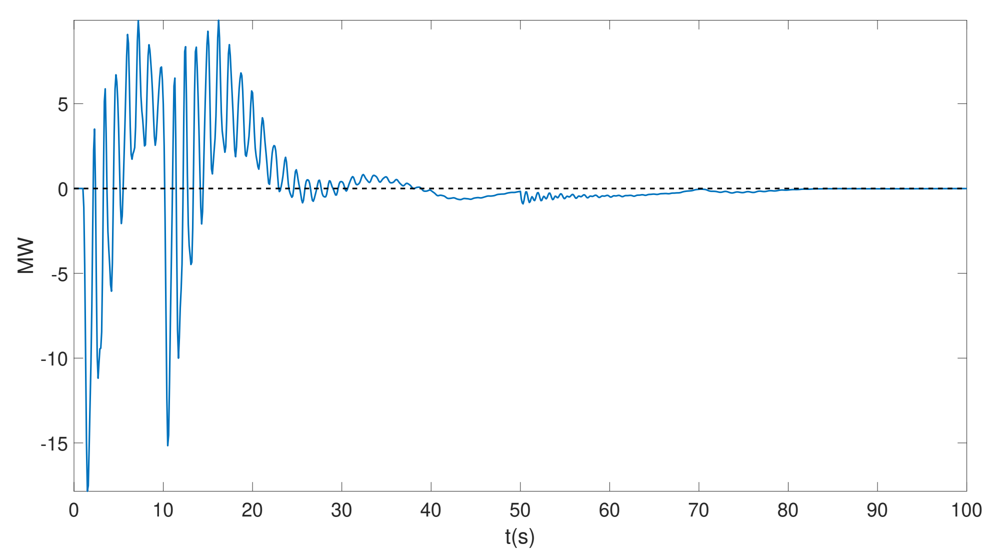

Figure 14.5: Deviations of power flow on the line (9-39).

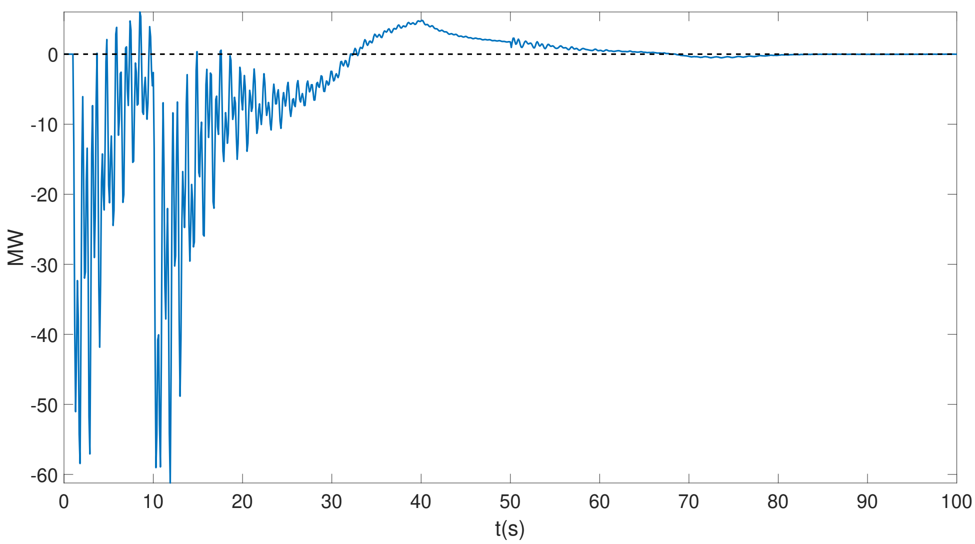

Figure 14.6: Inter-area flow deviation.

Figure 14.2 represents frequency response to the changes in the system state. It can be seen that the developed control arrests both frequency drops caused by power outage and suppresses frequency oscillations caused by changes in the control limits. Figure 14.3 represents generator control signals. Despite the distributed structure of the control, each generator acts in order to minimize overall deviation from the initial generation. Dashed lines demonstrate changes in control limits. Figure 14.4 represents load control signals. It is important to outline that loads not only change the control limits buts also switch from non-working state to controlled state simultaneously without any oscillations in physical or control systems. Figures 14.5 and 14.6 represent power flow on the congested line (9-39) and inter-area power flow respectively. It can be seen that all deviations are suppressed quickly despite the changes in the system's state. The developed algorithm performs frequency control, congestion management, and inter-area flows regulation despite non-constant disturbance and non-constant control limits.

15 Suggestions for the further work

In this thesis we consider linear power system model with second order generator equations, second order turbine and governor equations and DC power flows. For the numerical experiments the model is expanded to nonlinear power flows and turbine and governor equations for hydro and steam turbine of 4-th and 5-th orders respectively. We do not consider control discretization, communication delays, and bandwidth. Further work is planned to be done in the following three directions:

1. Implementation of a more realistic model. The usage of the two stage approach allows to reduce the effect of the physical system dynamics on the control values calculations in the stage two. This allows us to bypass issues with the cascade form of the turbine governor dynamics. It is possible, that such approach remains valid for other complications of the system dynamics, namely full AC network model, including non-constant voltages, reactive power flows and higher order generator model.

2. Analysis of the control robustness:

   (a) All measurements go through low-pass filter, which normally improves control reliability. It would be useful to ensure this statement with some analytical results.

   (b) In order to calculate disturbance size the control uses system inertia and damping. Errors in the measurements of this parameters will add some unwanted PI control actions. Such problem must be analyzed. Gains of a traditional PI controller are chosen with some margin of safety, i.e. small PI actions on top of the traditional controller would not destabilize the system. The controller, presented in this work, demonstrates better transient performance than the traditional one. Therefore, it seems likely, that the developed control will remain stable after introduction of additional unwanted PI actions.

   (c) Errors in measurements of line parameters may result in power flows exceeding corresponding limits. In general, small violations of thermal limits do not have a negative impact on the system. However, whiting this work we do not use power flows measurements. It might be possible to adjust line parameters within the control algorithm using the comparison between this measurements and virtual power flows.

3. Analysis of control implementation issues:

   (a) Discretization of the algorithm. Within this work we prove global asymptotic stability of the developed control. That gives optimistic expectations for the control implementation. However, explicit analysis of the control scheme discretization will provide clear requirements to the communication network and measurements frequency.

   (b) Analysis of the communication delays. While it is always possible to increase discretization step in order to mitigate negative effect of delays, it is necessary to analyse limits of the control effectiveness in realistic communication network models.

   (c) Analysis of the communication bandwidth. The presented control is distributed, therefore it requires only communications between neighbours in order to work. However, volume of the exchanged information might be too big even between two buses. Thus, inclusion of the communication bandwidth into control analysis is necessary.

4. Introduction of algorithms capable to work in infeasible case. In practice it might not be possible to restore frequency after a contingency subject to all line constraints. In this case control must remain stable and prioritize frequency restoration over congestion management. The control must identify presence of infeasibility in real time and perform corresponding actions.

5. Optimization of transient dynamics. At the current state control is obtained via transition from system of algebraic equations into a system of integral algebraic ones. It is possible to multiply right-hand side of the integral equations by a set of positive constants. Such multiplication would not affect stability of the system and stationary point, but will change control system dynamics. As a result, it is possible to adjust

control behavior in order to achieve various goals i.e. increase convergence of power flows to the feasible set.

6. Expanded numerical experiments. The items above require more detailed numerical experiments that would allow to ensure proper tests of all control properties. Numerical experiments must use more detailed model and larger networks in order to test scalability of the distributed control.

While the items above are not included in the current work, numerical experiments demonstrate stable dynamics and lack of oscillations in both control and physical system for the cases with nonconstant disturbances and control limits. This together with the proof of global asymptotic stability of the control allows to assume that control dynamics would remain acceptable even in the case of more complicated dynamics, inaccurate measurements and communication delays. Purpose of the control derivation approach, designed in this work, is to reduce effect of the physical system dynamics on the control. In order to do so we use information of the system state only to approximate disturbance, which is an independent parameter.

16 Conclusion

There exist multiple reasons for creating a new frequency control scheme: increased amount of renewable energy, possibility to control loads, distributed generation and communication limitations. In order to reduce impact of negative effects and utilize the new opportunities a control scheme that performs frequency control, congestion management and inter-area flows control in a distributed way is derived in this thesis. It is based on two main parts: approximation of the disturbance and convergence of the power system to a state called optimal under the developed control. For convenience the thesis is divided into 7 major consequent problems:

1. Frequency control with no control limits: control is centralized. It is assumed, that disturbances are too small for the control values to reach limits on any of the system's buses;

2. Frequency control with control present on some buses: intermediate step between control without and with limits;

3. Frequency control: centralized control with control limits. Modification of disturbance approximation algorithm is introduced allowing us to prove global asymptotic stability;

4. Distributed frequency control without control limits;

5. Distributed frequency control;

6. Distributed frequency control and congestion management;

7. Distributed frequency control, congestion management and inter-area flows control.

For each problem a control scheme is developed and its global asymptotic stability is proven. Numerical experiments show that the developed approach, while operating in a distributed way, provides better transient dynamics and delivers physical system to an optimal state. The obtained results are published in [23, 83, 98, 99].

The control schemes derived in this work are based on the fact that any frequency control method approximates the disturbance size, because frequency is restored if and only if power balance is restored and sum of control signals is equal to the sum of the disturbances. We utilize this fact and divided our controller into two stages. First stage is aimed to approximate the size of the disturbance using system's state, namely bus frequencies and electrical powers. While we use systems measurements,we approximate parameter that does not depend on the system's state. Such approach allows the control to remain stable and fast even for the second-order cascade type turbine-governor equations. This control stage is decentralized and provides disturbance approximation to the second stage. The latter is distributed, so that communication is done only between adjacent buses or border buses of each one area. Its control calculation algorithm is based on transition from Karush-Khunn-Takker condition of the control cost minimization problem to integral algebraic ones. This approach allows distributed implementation and provides low-pass filtering of all measurements inputs as well as control signals from the adjacent buses. Additionally, the second control stage can use as inputs disturbance measurements directly instead of approximations of the stage one, if these disturbance are available. Separation of the control algorithm into to methodologically different stages allows to implement the developed algorithm as feedback control using stage one, as feedforward control using direct disturbance measurements or as any combinations of these approaches.

We consider network model that includes second order turbine-governor dynamics and two different types of loads in order to provide accurate frequency behavior of the frequency band power flows in the network. Additional detalization of the model (e.g. inclusion of nonlinear power flows, hydro generation model with transient droop), as well as analysis of the impact of control discretization at implementation stage and communication delays are the aim of the future work.

The results of numerical experiments suggest that control stability will be present in more realistic models, since current dynamics of the control lack oscillations even if during transient some of the control limits are changing, or control on some buses is getting turned on/off.

Here we use system model with second order turbine governor dynamics. This is a necessity, as simpler models provide unrealistic dynamics of the power system (i.e. system with primary frequency control is stable regardless of the control gain). This approach ensures realistic behavior of the control and physical system. However, second order turbine governor dynamics introduce cascade type structure to the power system equations. Usually it means that corresponding Lyapunov function strongly depends on the system parameters and it is difficult to provide its general form. Normally works on frequency control and congestion management use lower order turbine governor dynamics in order to provide stability assessment. However here we prove global asymptotic stability of the control despite the presence of cascade block in the system. It is the key novelty of the work, as it provides strict analytical result about the control dynamics in comparison to the asymptotic stability without convergence radius assessment or lack of cascade block that are present in other works that consider both congestion management and frequency control.

References

[1] S. Trip, *Distributed control of power networks Distributed control of power networks: Passivity, optimality and energy functions.* Rijksuniversiteit Groningen, 2017.

[2] C. Zhao, *Real-Time Load-Side Control of Electric Power Systems.* California Institute of Technology, 2016.

[3] X. Zhang, *Scalable (Re)design Frameworks for Optimal, Distributed Control in Power Networks.* Oxford University, 2015.

[4] M. B. C. Salles, M. J. Aziz, and W. W. Hogan, "Potential arbitrage revenue of energy storage systems in pjm during 2014," in *2016 IEEE Power and Energy Society General Meeting (PESGM)*, July 2016, pp. 1–5.

[5] D. Wu, T. Yang, A. A. Stoorvogel, and J. Stoustrup, "Distributed optimal coordination for distributed energy resources in power systems," *IEEE Transactions on Automation Science and Engineering*, vol. 14, no. 2, pp. 414–424, April 2017.

[6] A. R. Bergen and V. Vittal, *Power Systems Analysis*, 2nd ed. Prentice Hall, 2000.

[7] AEMO Operational Support, "Power system security guidelines," Sep. 2019.

[8] J. Chow and G. Rogers, *Power system toolbox.* Cherry Tree Scientific Software, 2000.

[9] Engrid Soni, "Annual renewable energy constraint and curtailment report 2016," 2017.

[10] A. J. Wood and B. F. Wollenberg, *Power Generation, Operation, and Control*, 2nd ed. John Wiley & Sons, Inc, 1996.

[11] J. Alshahrani and P. Boait, "Reducing high energy demand associated with air-conditioning needs in saudi arabia," *Energies*, vol. 12, no. 1:87, p. 73–79, Dedc. 2018.

[12] Department of the Environment and Energy, "Basics of hvac energy efficiency," Australia, Sep. 2013.

[13] A. Monticelli, M. V. F. Pereira, and S. Granville, "Security-constrained optimal power flow with post-contingency corrective rescheduling," *IEEE Transactions on Power Systems*, vol. 2, no. 1, pp. 175–180, Feb 1987.

[14] S. Boyd and L. Vandenberghe, *Convex optimization.* Cambridge University Press, 2004.

[15] Z. A. Oabid, L. M. Cipciganl, L. Abrahim, and M. T. Muhssin, "Frequency control of

future power systems: reviewing and evaluating challenges and new control methods," *Journal of Modern Power Systems and Clean Energy*, vol. 7, pp. 9–25, 2019.

[16] D. K. Molzahn, F. Dörfler, H. Sandberg, S. H. Low, S. Chakrabarti, R. Baldick, and J. Lavaei, "A survey of distributed optimization and control algorithms for electric power systems," *IEEE Transactions on Smart Grid*, vol. 8, no. 6, pp. 2941–2962, Nov 2017.

[17] S. Huang, Q. Wu, Z. Liu, and A. H. Nielsen, "Review of congestion management methods for distribution networks with high penetration of distributed energy resources," in *IEEE PES Innovative Smart Grid Technologies, Europe*, Oct 2014, pp. 1–6.

[18] Q. Liu and M. D. Ilić, "Enhanced automatic generation control (e-agc) for future electric energy systems," in *2012 IEEE Power and Energy Society General Meeting*, July 2012, pp. 1–8.

[19] D. Apostolopoulou, P. W. Sauer, and A. D. Domínguez-García, "Balancing authority area model and its application to the design of adaptive agc systems," *IEEE Transactions on Power Systems*, vol. 31, no. 5, pp. 3756–3764, Sep. 2016.

[20] J. A. Short, D. G. Infield, and L. L. Freris, "Stabilization of grid frequency through dynamic demand control," *IEEE Transactions on Power Systems*, vol. 22, no. 3, pp. 1284–1293, Aug 2007.

[21] X. Zhang and A. Papachristodoulou, "A real-time control framework for smart power networks: Design methodology and stability," *Automatica*, vol. 58, pp. 43–50, 08 2015.

[22] C. Zhao, E. Mallada, S. Low, and J. Bialek, "A unified framework for frequency control and congestion management," in *2016 Power Systems Computation Conference (PSCC)*, June 2016, pp. 1–7.

[23] O. O. Khamisov, T. Chernova, and J. W. Bialek, "Comparison of two schemes for closed-loop decentralized frequency control and overload alleviation," in *2019 IEEE Milan PowerTech*, June 2019, pp. 1–6.

[24] A. Ghafouri, J. Milimonfared, and G. B. Gharehpetian, "Coordinated control of distributed energy resources and conventional power plants for frequency control of power systems," *IEEE Transactions on Smart Grid*, vol. 6, no. 1, pp. 104–114, Jan 2015.

[25] A. C. Chapman and G. Verbic, "Dynamic distributed energy resource allocation for

load-side emergency reserve provision," in *2016 IEEE Innovative Smart Grid Technologies - Asia (ISGT-Asia)*, Nov 2016, pp. 1189–1194.

[26] M. Andreasson, D. V. Dimarogonas, K. H. Johansson, and H. Sandberg, "Distributed vs. centralized power systems frequency control," in *2013 European Control Conference (ECC)*, July 2013, pp. 3524–3529.

[27] C. Zhao, U. Topcu, N. Li, and S. Low, "Design and stability of load-side primary frequency control in power systems," *IEEE Transactions on Automatic Control*, vol. 59, no. 5, pp. 1177–1189, May 2014.

[28] E. Mallada, C. Zhao, and S. Low, "Optimal load-side control for frequency regulation in smart grids," *IEEE Transactions on Automatic Control*, vol. 62, no. 12, pp. 6294–6309, Dec 2017.

[29] N. Li, C. Zhao, and L. Chen, "Connecting automatic generation control and economic dispatch from an optimization view," *IEEE Transactions on Control of Network Systems*, vol. 3, no. 3, pp. 254–264, Sep. 2016.

[30] Z. Wang, F. Liu, S. H. Low, C. Zhao, and S. Mei, "Distributed frequency control with operational constraints, part i: Per-node power balance," *IEEE Transactions on Smart Grid*, vol. 10, no. 1, pp. 40–52, Jan 2019.

[31] ——, "Distributed frequency control with operational constraints, part ii: Network power balance," *IEEE Transactions on Smart Grid*, vol. 10, no. 1, pp. 53–64, Jan 2019.

[32] E. Mallada, C. Zhao, and S. H. Low, "Fair load-side control for frequency regulation in smart grids," in *Allerton Conf. Commun., Control, Comput., Sept. 2014*, Sept 2014.

[33] X. Zhang and A. Papachristodoulou, "A real-time control framework for smart power networks with star topology," in *2013 American Control Conference*, June 2013, pp. 5062–5067.

[34] ——, "Distributed dynamic feedback control for smart power networks with tree topology," in *2014 American Control Conference*, June 2014, pp. 1156–1161.

[35] M. D. Ilic, "From hierarchical to open access electric power systems," *Proceedings of the IEEE*, vol. 95, no. 5, pp. 1060–1084, May 2007.

[36] T. Stegink, C. De Persis, and A. van der Schaft, "A unifying energy-based approach

to stability of power grids with market dynamics," *IEEE Transactions on Automatic Control*, vol. 62, no. 6, pp. 2612–2622, June 2017.

[37] X. Zhang, N. Li, and A. Papachristodoulou, "Achieving real-time economic dispatch in power networks via a saddle point design approach," in *2015 IEEE Power Energy Society General Meeting*, July 2015, pp. 1–5.

[38] L. Chen and S. You, "Reverse and forward engineering of frequency control in power networks," *IEEE Transactions on Automatic Control*, vol. 62, no. 9, pp. 4631–4638, Sep. 2017.

[39] S. Trip, M. Bürger, and C. De Persis, "An internal model approach to frequency regulation in inverter-based microgrids with time-varying voltages," in *53rd IEEE Conference on Decision and Control*, Dec 2014, pp. 223–228.

[40] M. Andreasson, D. V. Dimarogonas, H. Sandberg, and K. H. Johansson, "Distributed control of networked dynamical systems: Static feedback, integral action and consensus," *IEEE Transactions on Automatic Control*, vol. 59, no. 7, pp. 1750–1764, July 2014.

[41] ——, "Distributed pi-control with applications to power systems frequency control," in *2014 American Control Conference*, June 2014, pp. 3183–3188.

[42] T. Kose, "Solutions of saddle value problems by differential equations," *Econometrica*, vol. 24, no. 1, pp. 59–70, Jan. 1956.

[43] K. J. Arrow, L. Hurwicz, H. Uzawa, , and H. B. Chenery, "Studies in linear and nonlinear programming," *Stanford Mathematical Studies in the Social Sciences*, vol. 2, 1958.

[44] G. W. Brown and J. Von Neumann, "Solutions of games by differential equations," *Contributions to the Theory of Games (Annals of Math. Studies 24, Princeton University Press)*, vol. 141, no. VI.14, p. 73–79, 1950.

[45] S. Balaraman and N. Kamaraj, "Application of differential evolution for congestion management in power system," *Modern Applied Science*, vol. 4, 07 2010.

[46] L. Gan and S. H. Low, "An online gradient algorithm for optimal power flow on radial networks," *IEEE Journal on Selected Areas in Communications*, vol. 34, no. 3, pp. 625–638, March 2016.

[47] D. B. Arnold, M. Negrete-Pincetic, M. D. Sankur, D. M. Auslander, and D. S. Callaway, "Model-free optimal control of var resources in distribution systems: An extremum seeking approach," *IEEE Transactions on Power Systems*, vol. 31, no. 5, pp. 3583–3593, Sep. 2016.

[48] T. Erseghe, "Distributed optimal power flow using admm," *IEEE Transactions on Power Systems*, vol. 29, no. 5, pp. 2370–2380, Sep. 2014.

[49] E. Dall'Anese, "Optimal power flow pursuit," in *2016 American Control Conference (ACC)*, July 2016, pp. 1767–1767.

[50] F. J. Christophersen, *Optimal Control of Constrained Piecewise Affine Systems*, ser. Lecture Notes in Control and Information Sciences. Springer, 2007.

[51] A. Saberi, A. A. Stoorvogel, and P. Sannuti, *Internal and External Stabilization of Linear Systems with Constraints*, ser. Systems & Control: Foundations & Applications. Springer, 2012.

[52] A. A. Martynyuk, *Stability Theory for Dynamic Equations on Time Scales*, ser. Systems & Control: Foundations & Applications. Birkhäuser Base, 2016.

[53] V. Lakshmikantham, S. Leela, and A. A. Martynyuk, *Stability Analysis of Nonlinear Systems*, ser. Systems & Control: Foundations & Applications. Birkhäuser Base, 2017.

[54] I. Karafyllis and Z.-P. Jiang, *Stability and Stabilization of Nonlinear Systems*, ser. Communications and Control Engineering. Birkhäuser Base, 2011.

[55] M. Malisoff and F. Mazenc, *Constructions of Strict Lyapunov Functions*, ser. Communications and Control Engineering. Springer, 2009.

[56] J. Lunz, *Feedback control of large scale systems*, ser. Systems and Control Engineering. Prentice Hall, 1992.

[57] D. D. Šiljak, *Decentralized control of complex systems*, ser. Mathematics in Science and engineering. Academic Press, 1991, vol. 184.

[58] J. B. Rawlings and D. Q. Mayne, *Model predictive control: theory and design*, ser. Mathematics in Science and engineering. Nob Hill Publications, 2009.

[59] L. Bakule, "Decentralized control: An overview," *Annual Reviews in Control*, vol. 32, no. 1, pp. 87 – 98, 2008.

[60] S.-H. Wang and E. J. Davison, "On the stabilization of decentralized control systems,"

IEEE Transactions on Automatic Control, vol. AC-18, no. 5, pp. 473 – 478, 1973.

[61] N. Sandell, P. Varaiya, M. Athans, and M. Safonov, "Survey of decentralized control methods for large scale systems," *IEEE Transactions on Automatic Control*, vol. 23, no. 2, pp. 108–128, April 1978.

[62] P. D. Christofides, J. Liu, and D. Muñoz de la Peña, *Networked and Distributed Predictive Control. Methods and Nonlinear Process Network Applications*, ser. Advances in Industrial Control. Springer, 2011.

[63] U. Häger, C. Rehtanz, and N. Voropai, *Monitoring, Control and Protection of Interconnected Power Systems.* Springer, 2014.

[64] O. Vahamaki, A. Allen, and J. Gaff, "High speed peer-to-peer communication system for integrated protection and control in distribution networks," in *Proceedings of Developments in power system protection, sixth international conference on (Conf. Publ. No. 434)*, vol. 19, 03 1997, pp. 243 – 246.

[65] Cisco Systems, "Pmu networking with ip multicast—white paper." [Online]. Available: http://www.cisco.com/en/US/prod/collateral/routers/ps10967/ps10977/whitepaper_c11-697665.html

[66] P. Vorobev, D. M. Greenwood, J. H. Bell, J. W. Bialek, P. C. Taylor, and K. Turitsyn, "Deadbands, droop, and inertia impact on power system frequency distribution," *IEEE Transactions on Power Systems*, vol. 34, no. 4, pp. 3098–3108, July 2019.

[67] N. W. Miller, K. Clark, and M. Shao, "Frequency responsive wind plant controls: Impacts on grid performance," in *2011 IEEE Power and Energy Society General Meeting*, July 2011, pp. 1–8.

[68] F. Wilches-Bernal, J. H. Chow, and J. J. Sanchez-Gasca, "A fundamental study of applying wind turbines for power system frequency control," *IEEE Transactions on Power Systems*, vol. 31, no. 2, pp. 1496–1505, March 2016.

[69] J. Ekanayake and N. Jenkins, "Comparison of the response of doubly fed and fixed-speed induction generator wind turbines to changes in network frequency," *IEEE Transactions on Energy Conversion*, vol. 19, no. 4, pp. 800–802, Dec 2004.

[70] G. Lalor, A. Mullane, and M. O'Malley, "Frequency control and wind turbine technologies," *IEEE Transactions on Power Systems*, vol. 20, no. 4, pp. 1905–1913, Nov

2005.

[71] J. Morren, S. W. H. de Haan, W. L. Kling, and J. A. Ferreira, "Wind turbines emulating inertia and supporting primary frequency control," *IEEE Transactions on Power Systems*, vol. 21, no. 1, pp. 433–434, Feb 2006.

[72] J. M. Mauricio, A. Marano, A. Gomez-Exposito, and J. L. Martinez Ramos, "Frequency regulation contribution through variable-speed wind energy conversion systems," *IEEE Transactions on Power Systems*, vol. 24, no. 1, pp. 173–180, Feb 2009.

[73] J. W. Ingleson and E. Allen, "Tracking the eastern interconnection frequency governing characteristic," in *IEEE PES General Meeting*, July 2010, pp. 1–6.

[74] Z. Y. Dong, J. H. Zhao, and D. J. Hill, "Numerical simulation for stochastic transient stability assessment," *IEEE Transactions on Power Systems*, vol. 27, no. 4, pp. 1741–1749, Nov 2012.

[75] F. Milano and R. Zárate-Miñano, "A systematic method to model power systems as stochastic differential algebraic equations," *IEEE Transactions on Power Systems*, vol. 28, no. 4, pp. 4537–4544, Nov 2013.

[76] P. N. Papadopoulos and J. V. Milanović, "Probabilistic framework for transient stability assessment of power systems with high penetration of renewable generation," *IEEE Transactions on Power Systems*, vol. 32, no. 4, pp. 3078–3088, July 2017.

[77] D. Lee, L. Aolaritei, T. L. Vu, and K. Turitsyn, "Robustness against disturbances in power systems under frequency constraints," *IEEE Transactions on Control of Network Systems*, vol. 6, no. 3, pp. 971–979, Sep. 2019.

[78] Y. C. Chen and A. D. Dominguez-Garcia, "A method to study the effect of renewable resource variability on power system dynamics," *IEEE Transactions on Power Systems*, vol. 27, no. 4, pp. 1978–1989, Nov 2012.

[79] H. Choi, P. J. Seiler, and S. V. Dhople, "Propagating uncertainty in power-system dae models with semidefinite programming," *IEEE Transactions on Power Systems*, vol. 32, no. 4, pp. 3146–3156, July 2017.

[80] A. Moreira, D. Pozo, A. Street, and E. Sauma, "Reliable renewable generation and transmission expansion planning: Co-optimizing system's resources for meeting renewable targets," in *2018 IEEE Power Energy Society General Meeting (PESGM)*, Aug

2018, pp. 1–1.

[81] D. Pozo and J. Contreras, "A chance-constrained unit commitment with an $n-k$ security criterion and significant wind generation," *IEEE Transactions on Power Systems*, vol. 28, no. 3, pp. 2842–2851, Aug 2013.

[82] A. Jokić, M. Lazar, and P. Bosch, "Real-time control of power systems using nodal prices," *International Journal of Electrical Power & Energy Systems*, vol. 31, pp. 522–530, 01 2008.

[83] O. O. Khamisov, T. S. Chernova, J. W. Bialek, and S. H. Low, "Corrective control: Stability analysis of unified controller combining frequency control and congestion management," in *NEIS 2018; Conference on Sustainable Energy Supply and Energy Storage Systems*, Sep. 2018, pp. 1–6.

[84] A. Gomez-Exposito, A. Conejo, and C. Cañizares, *Electric Energy Systems: Analysis and Operation*. CRC Press, 01 2008.

[85] J. Machowski, J. Bialek, and J. Bumby, *Power System Dynamics: Stability and Control*, 2nd ed. John Wiley & Sons, Inc, 2008.

[86] A. R. Bergen and D. J. Hill, "A structure preserving model for power system stability analysis," *IEEE Transactions on Power Apparatus and Systems*, vol. PAS-100, no. 1, pp. 25–35, Jan 1981.

[87] P. Kundur, J. Paserba, V. Ajjarapu, G. Andersson, A. Bose, C. Canizares, N. Hatziargyriou, D. Hill, A. Stankovic, C. Taylor, T. Van Cutsem, and V. Vittal, "Definition and classification of power system stability ieee/cigre joint task force on stability terms and definitions," *Power Systems, IEEE Transactions on Power Systems*, vol. 19, pp. 1387 – 1401, 09 2004.

[88] N. Voropai, Ed., *A set of intelligent tools for major accidents in power systems prevention*. Novosibirsk: Nauka, 2016 (in Russian).

[89] ——, *Reducing the Risk of Cascading Blackouts in Electrical Power Systems*. Novosibirsk: Publishing House of the SB RAS, 2011 (in Russian).

[90] P. Kundur, *Power System Stability And Control*. McGraw-Hill, 1994.

[91] Q. Wang, J. Watson, and Y. Guan, "Two-stage robust optimization for n-k contingency-constrained unit commitment," *IEEE Transactions on Power Systems*, vol. 28, no. 3,

pp. 2366–2375, Aug 2013.

[92] B. P. Demidovich, *Lectures on the Mathematical Stability Theory.* Moscow: Nauka, 1967 (in Russian).

[93] W. M. Haddad and V. Chellaboina, *Nonlinear Dynamical Systems and Control, A Lyapunov-Based Approach.* Princeton University Press, 2008.

[94] E. A. Barbashin, *Lyapunov Functions.* Moscow: Nauka, 1970 (in Russian).

[95] V. Rumyantsev and A. Oziraner, *Partial Stability and Stabilization of Motion.* Moscow: Nauka, 1987 (in Russian).

[96] G. Merkuriev and G. Meleshkin, *Power system stability.* Novosibirsk: Nauka, 2006 (in Russian).

[97] Y. E. Boyarintsev, *Linear and Nonlinear Algebro-Differential Systems.* Novosibirsk: Nauka, 2000 (in Russian).

[98] O. O. Khamisov, "Direct disturbance based decentralized frequency control for power systems," in *2017 IEEE 56th Annual Conference on Decision and Control (CDC)*, Dec 2017, pp. 3271–3276.

[99] O. O. Khamisov and V. A. Stennikov, "Interior point and newton methods in solving high dimensional flow distribution problems for pipe networks," *Learning and Intelligent Optimization. LION 2017*, vol. 10556, pp. 139–149, Oct 2017.

[100] K. Dekker and J. G. Verver, *Stability of Runge-Kutta Methods for Stiff Nonlinear Differential Equations.* Amsterdam: North-Holland, 1984 (in Russian).

[101] V. V. Voevodin, *Linear Algebra.* Moscow: Nauka, 1974 (in Russian).